Alma Mater Studiorum - Università di Bologna

DOTTORATO DI RICERCA IN

SCIENZE E TECNOLOGIE DELLA SALUTE

Ciclo 35

Settore Concorsuale: 05/E1 - BIOCHIMICA GENERALE

Settore Scientifico Disciplinare: BIO/10 - BIOCHIMICA

PLASMA-ACTIVATED LIQUIDS AS PROMISING TOOLS FOR NON-INVASIVE SELECTIVE TREATMENT OF EPITHELIAL OVARIAN CANCER

Presentata da: Cristiana Bucci

Coordinatore Dottorato

Marco Viceconti

Supervisore

Vittorio Colombo

Co-supervisore

Anna Maria Porcelli

Esame finale anno 2023

Index

Abstract

Plasma is a rapidly growing technology, widely employed in various industrial processes and experimental studies, including water treatment and health care. It has positive results and is a flexible, easy-to-scale, and environmentally friendly alternative to traditional techniques. Plasma medicine is a branch of plasma-promising biomedical applications that uses cold atmospheric plasma (CAP) as a therapeutic agent in treating a wide range of medical conditions including cancer. Cancer is a leading cause of death worldwide, and there is a need for novel and effective treatments to address the limitations of current therapies. Epithelial ovarian cancer (EOC) is a highly malignant and aggressive form of ovarian cancer, and most patients are diagnosed at advanced stages which significantly reduces the chances of successful treatment, with a 5-year survival rate of less than 50%. Treatment resistance is also common, highlighting the need for novel therapies to be developed to treat EOC. Research in Plasma Medicine has revealed that plasma has unique properties suitable for biomedical applications and medical therapies, including responses to hormetic stimuli. However, the exact mechanisms by which CAP works at the molecular level are not yet fully understood. Further research is needed to safely and effectively use CAP in the clinic.

In this regard, the main goal of this thesis is to identify a possible adjuvant therapy for cancer, which could exert a cytotoxic effect, without damaging the surrounding healthy cells. An examination of different plasma-activated liquids (PALs) revealed their potential as effective tools for significantly inhibiting the growth of EOC. The dose-response profile between PALs and their targeted cytotoxic effects on EOC cells without affecting healthy cells was established. Additionally, it was validated that PALs exert distinct effects on different subtypes of EOC, possibly linked to the cells' metabolism. This suggests the potential for developing new, personalized anticancer strategies. Furthermore, it was observed that CAP treatment can alter the chemistry of a biomolecule present in PAL, impacting its cytotoxic activity. The effectiveness of the treatment was also preliminarily evaluated in 3D cultures, opening the door for further investigation of a possible correlation between the tumor microenvironment and PALs' resistance. These findings shed light on the intricate interplay between CAP and the liquid substrate and cell behaviour, providing valuable insights for the

development of a novel and promising CAP-based cancer treatment for clinical application.

CHAPTER 1

Introduction

This chapter is inspired by the book *Plasma Medicine* written by Prof. Alexander Fridman and Prof. Gary Friedman [1]. Their book, very complete, exposes every aspect of plasma medicine.

1.1 What is plasma?

In 1928, the chemist Irving Langmuir first used the term "plasma" as a description of ionized gas [2]:

> "Except near the electrodes, where there are *sheaths* containing very few electrons, the ionized gas contains ions and electrons in about equal numbers so that the resultant space charge is very small. We shall use the name *plasma* to describe this region containing balanced charges of ions and electrons."

A plasma is a partially ionized gas characterized by a blend of free electrons, ions, neutral species (atoms, molecules, and radicals) and electromagnetic radiation [3,4]. Its composition depends on a wide range of parameters such as gas mixture and temperature, especially [5]. Based on its temperature, plasma can be classified as thermal and non-thermal [3,4]. Thus, in nature non-thermal plasmas can be found in the Aurora Borealis while examples of thermal plasmas are lightnings (Figure 1.1-1).

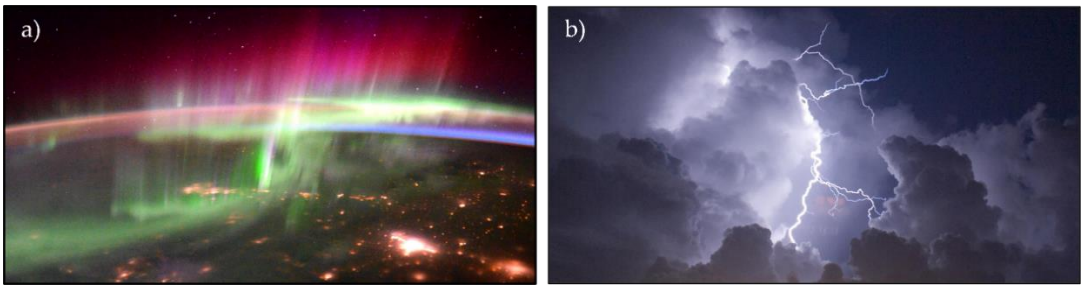

Figure 1.1-1 Plasmas in nature. a) Aurora Borealis and b) lightning. Pictures are taken from nasa.gov.

Plasmas can be distinguished by their energy density and degree of ionization. Indeed, thermal plasmas, due to high ionization degrees, induce a high rate of collisions among the species present in the gas mixture, with temperatures ranging

from about 5000 K to about 100000 K, with all species in thermal equilibrium. On the other hand, non-thermal plasmas have a low ionization degree and a bulk temperature close to room temperature, with only the free electrons in a high energy state. Because of these physical differences, thermal and non-thermal plasmas have different specific applications in both biological and medical fields. The high temperatures and energy densities typical of thermal plasmas are nowadays widely used in clinics for cauterization and ablation of tissues during surgeries. In contrast, non-thermal plasma, by having low bulk temperatures, can be used in various applications, for example in environment and health, as well as tissue engineering and wound healing [6]. Non-thermal plasma can be generated at both low-pressure and atmospheric pressure [1]. Low-pressure plasma is a type of plasma that is generated at a pressure lower than 1 atm, usually in the range of 10^{-2} - 10^{-3} millibars and at higher temperatures [1,7]. Cold atmospheric plasma (CAP) is a type of plasma that is generated at atmospheric pressure and ambient temperature [7]. It has been widely studied for its therapeutic application, due to its body-compatible temperature, atmospheric pressure and ability to generate an extremely high concentration of chemically active species which, in the medical field, can be also useful for the development of new therapies [3,8,9].

1.2 Plasma chemistry as the fundamental basis of plasma medicine

Plasmas are extremely reactive environments in which free electrons and radical ions are produced. These species quickly react to create secondary reactive species or recombine to restore the neutral atoms or molecules.

When a plasma is generated in the proximity of a liquid, it is customary, to study the process, to divide the environment in which the reactions occur into three different regions: gas phase, gas-liquid interface and liquid phase (Figure 1.2-1) [10,11].

In the gas phase, plasma produces a cocktail of reactive oxygen and nitrogen species (RONS), such as ozone (O_3), atomic oxygen (O), singlet oxygen ($^1O_2$), superoxide ($\cdot O_2^-$) and nitrogen oxides (NO, NO_2), strongly influenced by the type of gas (air, argon, helium, etc.) [10,12]. On the other hand, the gas-liquid interface whereby the plasma interacts with liquid substrate, or with the air containing water vapour, transport phenomena are involved which regulate the diffusion of charged particles

and reactive molecules into the underlying liquid phase [10,11]. As a result of solvation, diffusion and interaction with the molecules of the liquid substrate, secondary reactions occur which lead to the formation of reactive oxygen species (ROS) and reactive nitrogen species (RNS) of which the most typical are hydroxyl radicals (·OH), hydrogen peroxide (H_2O_2), nitric and nitrous acids (HNO_2 and HNO_3, that dissociate in water, totally or partially, depending on the pH) [13]. Many RONS are capable of diffusing into the bulk liquid and reacting with the molecules present. In addition, some RONS can be relatively stable, and two types of RONS can be distinguished, accordingly to literature [14,15]: short-lived species (from hundreds of nanoseconds to milliseconds) such as hydrogen atoms, OH radicals, and hydrated (solvated) electrons and long-lived (> 1 s) species such as H_2O_2, NO_2^- and NO_3^-.

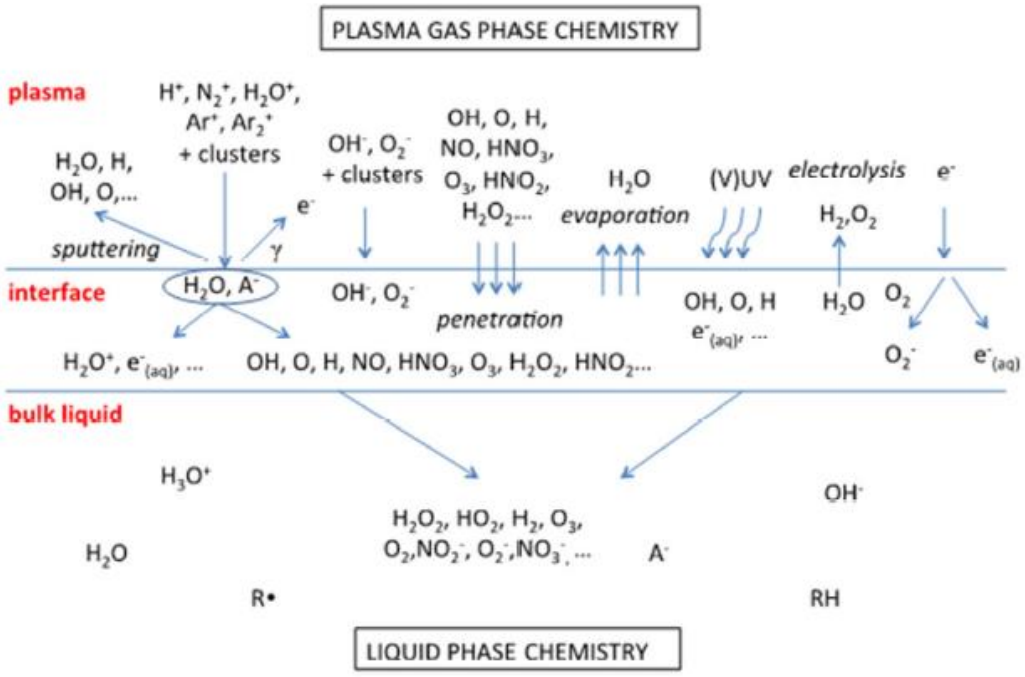

Figure 1.2-1 RONS generated by CAP-liquid interactions [10].

Considering that RONS play important roles in biological responses, the use of CAP for the generation of RONS as a possible anticancer approach is worthwhile to be investigated [16–19].

There are two main types of plasma treatments: direct and indirect plasma treatment (Figure 1.2-2) [20,21]. The direct plasma treatment involves applying plasma directly to the target area, promoting the interaction of all the plasma components (short-lived

species, long-lived species, electric field, UV-radiation) with the specific region of interest [15,22]. The indirect plasma treatment involves applying plasma to a liquid substrate to load it with long-lived reactive species. This plasma-treated liquid, or plasma-activated liquid (PAL), is then put in contact with the target of interest [15,22]. Thus, it is of interest to report the reactions involved in the formation of H_2O_2 and NO_2^- in the treated liquid, to explore the reactions in which occur these two main long-lived species.

Figure 1.2-2 Schematic representation of direct and indirect plasma treatment. Figure adapted from [21].

1.2.1 Peroxides

The concentration of hydrogen peroxide (H_2O_2) strongly depends on the production of hydroxyl radicals (·OH) in the gas phase, and to a lesser extent in the liquid phase and at the gas-liquid interface [23]. Specifically, regarding the gas phase, ·OH radicals are formed as a result of the dissociation of water molecules (H_2O) according to the reaction:

$$H_2O + e^- \rightarrow \cdot H + \cdot OH + e^- \quad \textbf{(1)}$$

The interaction between electrons (e^-) and moisture in the air causes the dissociation of H_2O molecules with the subsequent formation of a hydrogen atom (·H) and an ·OH radical [12,24]. Due to its high reactivity, this radical can react with another ·OH and form H_2O_2 [12,24,25] according to the reaction:

$$\cdot OH + \cdot OH \rightarrow H_2O_2 \quad \textbf{(2)}$$

Being a quite stable molecule, hydrogen peroxide tends not to react with other molecules but diffuses into the underlying liquid. Reactions (**1**) and (**2**), apart from the gas phase, have an even greater weight at the gas-liquid interface where the evaporation rate is high [26].

In the liquid phase, the presence of H_2O_2 is due not only to diffusion but also to the photolysis of H_2O molecules according to the reactions [24–26]:

$$e^- + N_2 \rightarrow e^- + N_2^* \quad (\mathbf{3})$$

$$N_2^* \rightarrow N_2 + h\nu \quad (\mathbf{4})$$

$$H_2O_{(aq)} + h\nu \rightarrow H_{(aq)} + {\cdot}OH_{(aq)} \quad (\mathbf{5})$$

$${\cdot}OH_{(aq)} + {\cdot}OH_{(aq)} \rightarrow H_2O_{2\,(aq)} \quad (\mathbf{6})$$

Closer to the liquid surface, as shown in reaction (**3**), the impact between an electron and a nitrogen molecule can bring the latter into an excited state (N_2^*). From the excited state, the molecule spontaneously tends to return to its fundamental state, resulting in the emission of photons (**4**). The latter can react with H_2O molecules according to reaction (**5**), leading to the formation of ·OH radicals directly in the liquid phase [26]. Being very reactive, these radicals can recombine to the formation of H_2O_2.

1.2.2 Nitrite ions

The concentration of nitrite ions (NO_2^-) in the liquid phase is strongly linked to the formation of nitric oxide (NO) in the gas phase.

In thermal plasma, NO can be produced through the Zeldovich mechanism, which passes through the generation of excited nitrogen molecular species [25,27]. In low-pressure plasmas, NO can be produced through similar mechanisms as in thermal plasmas via the generation of excited oxygen atoms [25].

At atmospheric pressure, oxygen tends to assume a more energetically stable configuration very quickly due to its electronegativity [25]. Hence, NO can be produced through the dissociation of nitrogen molecules following electronic impact [25]. This is the most important mechanism for the synthesis of NO in the gas phase.

$$e^- + N_2 \rightarrow 2N + e^- \quad (\mathbf{7})$$

Following reaction (**7**), nitrogen atoms can react with ·OH radicals and oxygen molecules resulting in the formation of NO, atomic hydrogen and atomic oxygen:

$$N + {\cdot}OH \rightarrow NO + H \quad (\mathbf{8})$$

$$N + O_2 \rightarrow NO + O \quad (\mathbf{9})$$

Once produced, NO molecules can react with water or ·OH radicals to generate nitrous acid (HNO_2; reaction **10** and **11**) and diffuse into the liquid phase or diffuse in the liquid as itself and react there according to the same reactions [28]. Nitrous acid (HNO_2), which can dissociate in water to produce nitrite (NO_2^-) and hydrogen ions (H^+) according to the pH of the solution (reaction **12**) [12,29]:

$$NO + \cdot OH \rightarrow HNO_2 \quad (\mathbf{10})$$

$$4NO + 2H_2O + O_2 \rightarrow 4HNO_2 \quad (\mathbf{11})$$

$$HNO_2 + H_2O \rightleftarrows NO_2^- + H_3O^+ \quad (pK_a = 3.15) \quad (\mathbf{12})$$

In addition, nitric oxide can also react with nitrogen dioxide (NO_2), which is formed in the gas phase (as a result of dissociation reactions of oxygen and nitrogen monoxide molecules) and diffuses into the liquid [29]:

$$NO + \tfrac{1}{2}O_2 \rightarrow NO_2 \quad (\mathbf{13})$$

$$NO_{(aq)} + NO_{2(aq)} + H_2O \rightarrow 2NO_2^- + 2H^+ \quad (\mathbf{14})$$

1.3 Plasma medicine

Plasma medicine is a relatively new field of study, which combines plasma physics with life science to study plasma applications in medicine. Due to its promising biomedical applications, plasma medicine is gaining increasing attention. Figure 1.3-1 summarizes the main milestones in the field.

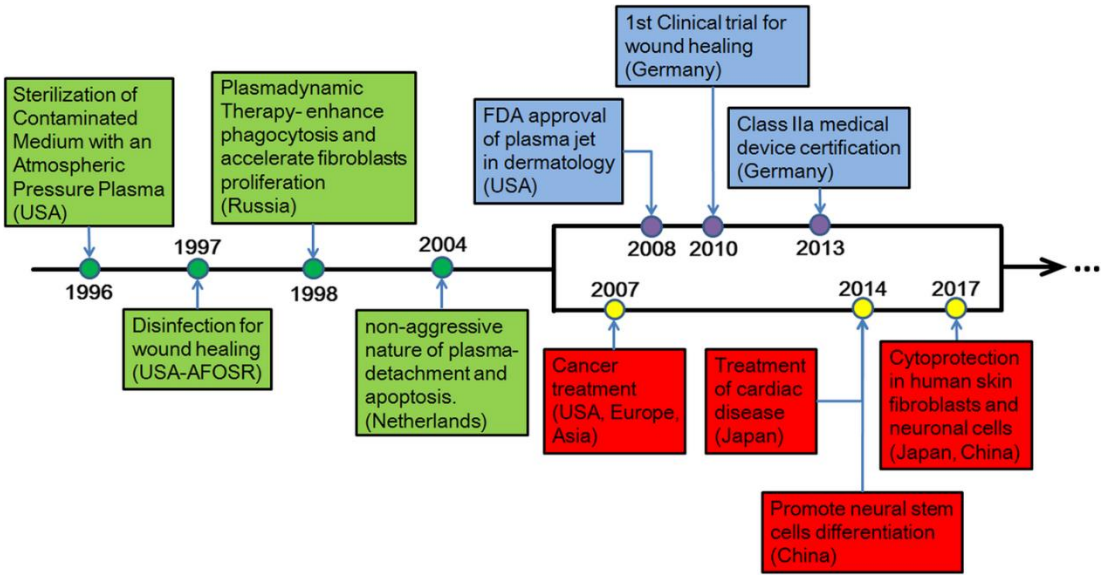

Figure 1.3-1 Timeline of the major milestones of plasma medicine [30]. In green, the first decade of the early foundation of plasma medicine; in blue, plasma medical technology development; in red, medical interventions with plasma in medical therapy.

Over two decades ago, researchers proposed that RONS produced by plasmas could be used for therapeutic purposes [30]. These were originally used to sterilize surfaces and liquids since they possess bactericidal properties [21,30,31]. However, it was later discovered that plasma-derived RONS could also target eukaryotic cells through cell-intrinsic mechanisms [21]. Nowadays, the physical and engineering foundations of plasma medicine have been improved finding applications in wound healing, drug delivery process, and cancer treatment [30,32], since it may result in cell death as well as cell proliferation [21,31]. This is attributed to a phenomenon called hormesis [8]. Hormesis is a term used to describe the phenomenon whereby a substance that is toxic at high doses has beneficial effects at low doses [33]. This biphasic dose response can be seen with a wide range of substances, including toxins, radiation, neurotransmitters, and ROS [8,33]. ROS are highly reactive molecules that are produced as a by-product of normal cellular metabolism [34]. As reported in Figure 1.3-2, at low concentrations ROS can have beneficial effects, such as promoting cell proliferation and helping to stimulate the immune system. At high concentrations, ROS can be harmful and can contribute to the development of various diseases [8,21]. In wound healing and cancer, for instance, low concentrations of ROS can promote cell proliferation, while high concentrations can be damaging [8,21]. In both cases, the signalling pathways that are activated in response to ROS are key in determining the subsequent biological effects.

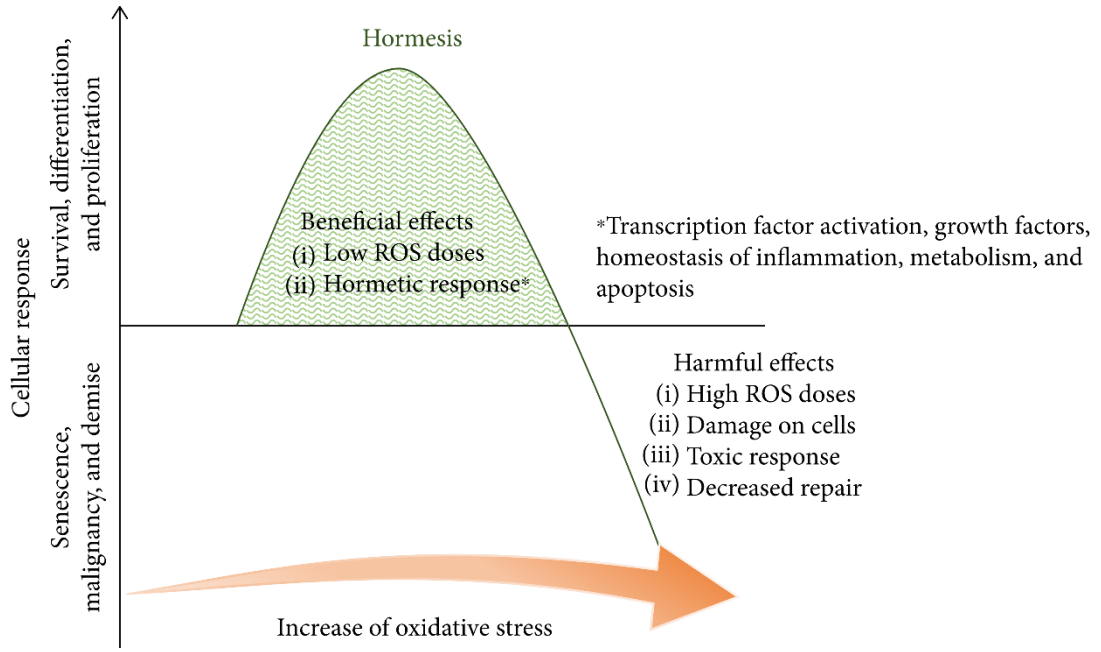

Figure 1.3-2 Responses to hormetic stimuli. A substance or molecule at a low concentration can have opposing effects compared to high concentrations. Figure is adapted from [8].

Since these reactive species often follow hermetic responses in biology [21], the interest in using CAP for cancer treatment has grown as it has been investigated as a possible new therapeutic approach [21]. As a result, two major approaches are used in this context to induce cell death in cancer cells and tissues: direct CAP discharge to the target area, which is an active component of the discharge, or indirect CAP discharge using a gas flow to move active plasma species [32].

1.4 Plasma for cancer treatment

Reactive oxygen and nitrogen species are known to play a key role in maintaining cellular homeostasis, i.e. the ability to regulate the balance between exogenous stimuli (such as increased ROS concentrations induced by chemotherapeutic agents or ionising radiation) and endogenous stimuli (such as metabolic activity and the action of antioxidant enzymes) [8,11,35,36]. The biochemical oxidation-reduction reactions that characterise these reactive species are involved in both cellular and tumorigenic signalling and regulatory mechanisms [8,17,35]. Indeed, increasing experimental evidence suggests their correlation between endogenous levels and biological effects [5,21,32,36].

ROS are highly reactive chemical species that include free radicals, such as $\cdot O_2^-$ and ·OH, and non-radical forms, such as H_2O_2 and O_3. These latter are also highly reactive and can easily be converted into radicals. Of all the reactive oxygen species, hydrogen peroxide plays a key role as a cell signalling molecule [37]. Indeed, at low concentrations, it regulates bio-signalling mechanisms (cell growth, migration and differentiation) while, at high concentrations, it can cause irreversible damage to DNA, lipid peroxidation and protein oxidation (Figure 1.4-1) [8,11,38,39].

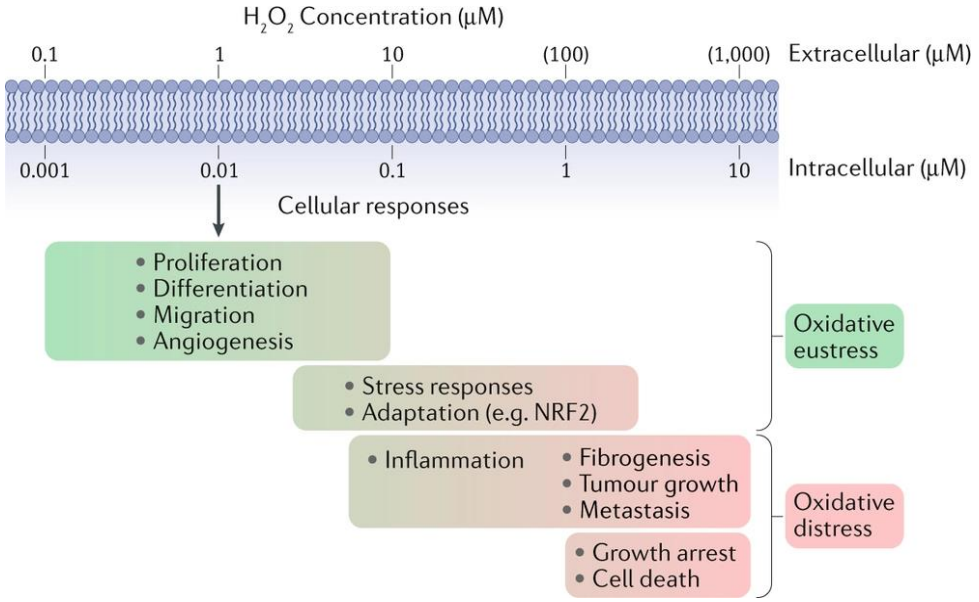

Figure 1.4-1 ROS concentration influences cellular homeostasis [11].

Cellular homeostasis depends on the balance between endogenous ROS generation, as a consequence of metabolic activity, and antioxidant systems such as superoxide dismutase, catalase, or glutathione peroxidase enzymes [38,40,41]. When this balance is no longer respected, cells undergo oxidative stress, often associated with the development of tumors [35,41]. These latter are often characterised by cellular metabolic alterations or mitochondrial dysfunction, which can cause an increase in intracellular ROS levels and impair the functioning of antioxidant enzymes [35,42]. As shown in Figure 1.4-2, unlike healthy cells, cancer cells display a higher intrinsic ROS level than healthy cells, much closer to the threshold of toxicity [35]. Thus, cancer cells are more sensitive to a further increase in ROS induced by exogenous administration by using CAP, for instance.

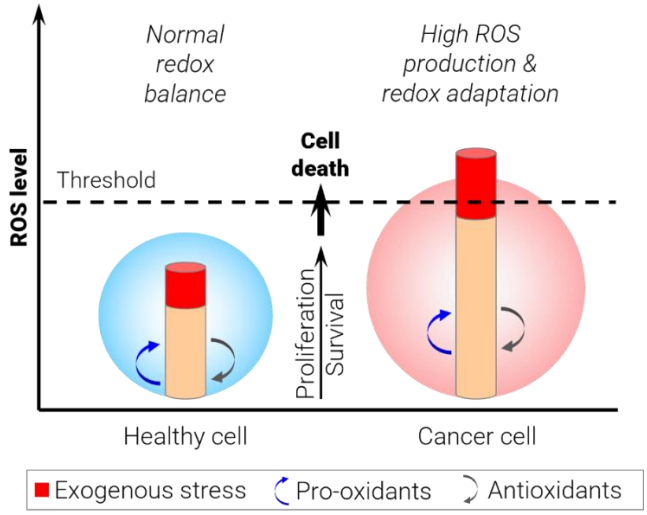

Figure 1.4-2 Redox balance in cancer and non-cancer cells [35].

Reactive nitrogen species are also important in cell signalling mechanisms, especially under hypoxic conditions for which NO_2^- can react with enzymes or proteins by producing NO [43,44]. Depending on its concentration, NO has a dual role in cancer biology as it can both promote and inhibit tumor progression (Figure 1.4-3). Nitric oxide induces tumor progression and metastasis by acting directly on the proliferation and migration of tumor cells and indirectly through the expression of angiogenic and lymphangiogenic factors [45,46]. However, a high concentration of nitric oxide can cause cytotoxic effects that can lead to tumor regression and inhibition of metastasis [46]. This dichotomy mainly depends on the quantity, localization and generation kinetics of nitric oxide [46,47]. In particular, cancer cells are enriched in the nitric oxide synthases (NOS), the enzymes deputed to synthesize NO [46,47]. NOS plays a unique role in the production of NO and the regulation of various physiological processes [46], which in turn can be influenced by various factors, including hormones, neurotransmitters, and signalling pathways [46,48]. At the tumor site, NO combines with other radicals, leading to RNS generation that sustains genomic instability. Basically, it can react with the superoxide anion ($\cdot O_2^-$) and form peroxynitrite ($ONOO^-$). The latter is capable of causing irreparable damage to DNA and mitochondria, inducing apoptosis in cancer cells [16,45,49].

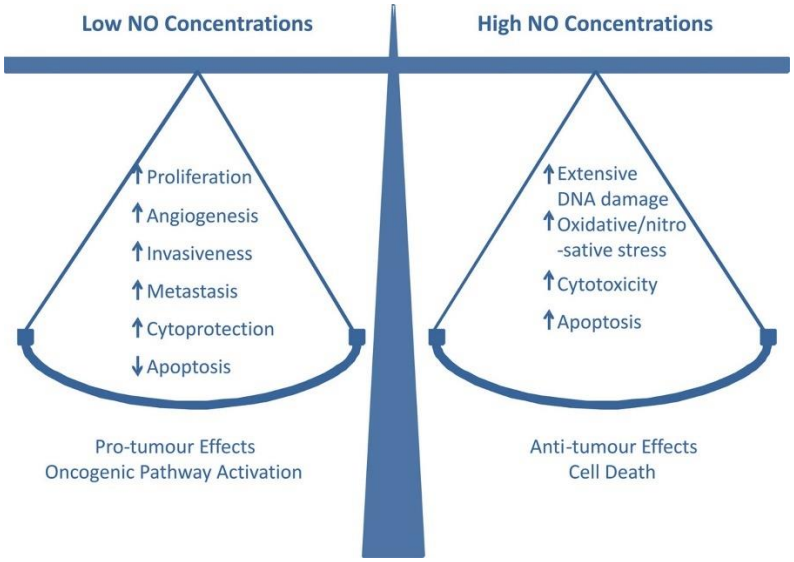

Figure 1.4-3 NO/RNS concentration influences cancer homeostasis [48].

On the whole, RONS are produced by cells as a by-product of normal metabolism [34]. They are highly reactive and can damage cellular structures and DNA if they are not properly regulated [50]. RONS can be either beneficial or harmful, depending on their levels and the context in which they are produced [34,51,52]. In certain circumstances, high levels of RONS can induce apoptotic (cell death) and mutagenic (DNA-damaging) processes in cells [34,36]. This can be a useful property in cancer therapy, as cancer cells are often resistant to cell death and may require additional stimuli to trigger cell death [53,54]. Therefore, an exogenous alteration of RONS levels, capable of inducing cytotoxic effects, may serve as the basis for a promising therapy for the treatment of cancer.

Plasma-generated RONS exert the ability to inhibit and kill cancer cells without affecting healthy cells due to their cytotoxic properties [55].

As reported in section 1.2, CAP can be employed in direct or indirect routes. In the field of cancer therapy (Figure 1.4-4), CAP can be directly applied to the tumor bulk or to a liquid, which is then injected into the tumor area as PAL (indirect treatment) [21]. The liquids often used for this application can include phosphate buffer saline (PBS), Ringer's saline solution, or cell culture media e.g., Dulbecco's modified Eagle's medium (DMEM) or Roswell Park Memorial Institute 1640 (RPMI). Both types of treatment are effective at reducing tumor size [20]. However, more research is

needed to fully understand the mechanisms of action and to determine the most effective protocols for plasma cancer therapy. In addition, the use of plasma-generated RONS as injections through the treatment of liquids or solutions with plasma devices is an area of active research and may be a promising future clinical application.

Two potential methods for using these liquids as a clinical treatment in the future have been proposed. The first involves injecting the liquid into the tumor bulk, while the second involves using it to wash the peritoneal cavity in cases of disseminated peritoneal carcinomatosis, a disease that is currently treated with Hyperthermic Intraperitoneal Chemotherapy (HIPEC) and Pressurized Intraperitoneal Aerosol Chemotherapy (PIPAC) therapy [21].

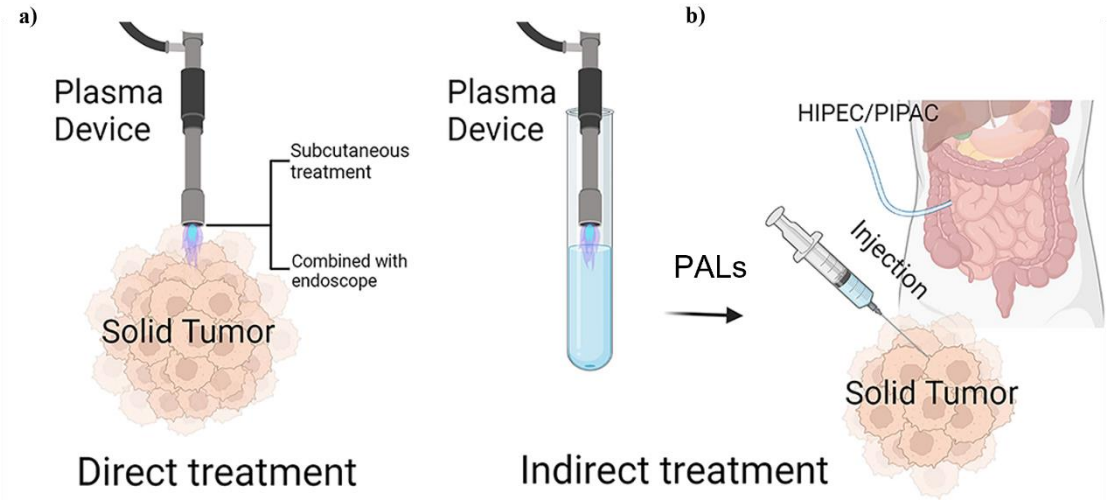

Figure 1.4-4 Plasma treatment in cancer therapy; (a) direct plasma treatment (b) indirect plasma treatment [22].

Early *in vitro* tests showed that plasma had several effects including apoptosis, necrosis and cell migration alteration [56]. Studies on cancer cell lines also showed similar effects and further analyses have suggested that plasma may selectively kill many types of cancer cells while causing minimal harm to healthy cells [55,57–61]. This selectivity has been observed in the treatment of various cancers, including head and neck cancer [62,63], brain cancer [64,65], leukemia [66,67], lung cancer [57], breast cancer [68], skin cancer [69], colorectal cancer [70], gastric cancer [71], pancreatic cancer [72], and ovarian cancer [21,61]. The reported selective nature of plasma as a cancer treatment has

resulted in an increase in the number of published studies on the topic (Figure 1.4-5) [73].

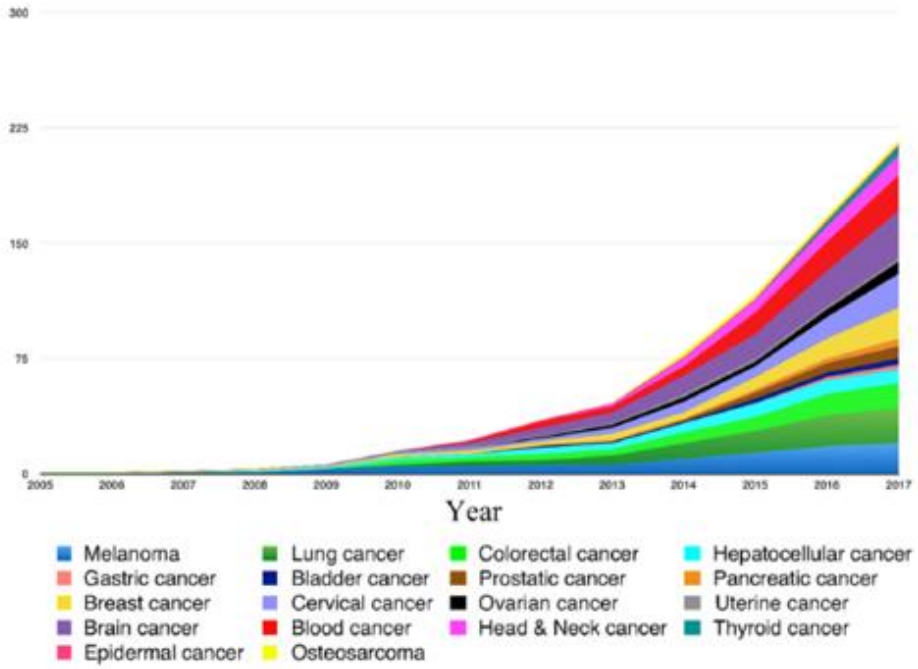

Figure 1.4-5 Chart showing the total number of articles published over time that focus on the use of plasma to treat specific types of cancer [73].

1.4.1 Plasma-activated liquid as an approach for the treatment of epithelial ovarian cancer

Epithelial Ovarian Cancer (EOC) is the most lethal gynecological cancer and it is characterized by intra-abdominal metastases which occur in the form of neoplastic nodules located on the peritoneal surface, a condition also referred to as peritoneal carcinomatosis [74]. About 75% of affected women are diagnosed in advanced stages, with a survival rate of 29% within 5 years from diagnosis, because of the asymptomatic nature of EOC [75,76]. Standard of care in advanced EOC, since the 1980s, is the combination of primary debulking surgery followed by platinum-taxane chemotherapy in an intravenous regimen [76,77]. Despite the improvements seen in survival rates in patients [78], these conventional therapies cannot eradicate the disease and the long-term survival rates remain low in patients with advanced EOC [75,77]. Indeed, about 80% of patients relapse because chemotherapeutic agents show low efficacy against resistant tumor subclones [79]. Furthermore, the disease presents a diffusion of nodules or plaques from the ovary to the peritoneal surfaces [79] and often

progress with an accumulation of ascitic fluid [77] that may contribute to the spread of cancer to secondary sites [80]. The complexity of the interaction between peritoneal cells and EOC cells is needed to be completely understood in order to develop new treatment strategies for peritoneal carcinosis [74]. However, innovations in the surgical and pharmacological fields are creating the conditions to make possible treating this type of neoplastic invasion. This could be accomplished by assisting the surgery through chemotherapy directly in the peritoneal cavity [81,82]. In this context, it would be possible to reduce the exposure of normal tissue to antineoplastic drugs and enhance antitumor activity while limiting the risk of toxicity [78]. Despite the promising results by intraperitoneal chemotherapy administration, such as HIPEC [75,78,83,84], innovative solutions have to be found to limit the severe side effects due to the chemotherapy drugs and to overcome chemoresistance.

Concerning the different liquids that are typically treated via plasma, *Tanaka et al.* made a significant discovery when they found that plasma-activated media (PAM) can kill glioblastoma cells and cause morphological changes consistent with apoptosis [65]. This finding has led to numerous studies on the use of PAM for the treatment of various types of cancer, showing its effectiveness both *in vitro* and *in vivo* [21,73]. It has been observed to induce a selective anticancer effect, meaning that it targets cancer cells with reduced damage to surrounding healthy cells. PAM has been found to be particularly effective against chemo-resistant ovarian cancer cells and has been administered intraperitoneally to patients with ovarian and gastric cancer to inhibit tumor growth and prevent cell metastasis in the abdominal cavity [85–87]. PAM has also been shown to reduce the adhesion capacity of cancer cells, which may improve survival rates in mice treated with PAM [85,87,88]. It is suggested that PAM may be a promising treatment option as a combined anticancer therapy.

While cell culture media contains many components that could potentially contribute to cytotoxic effects i.e, amino acids, fetal bovine serum or pyruvate, it is difficult to identify which specific compounds are responsible for the observed toxicity due to the complexity of the media's composition [21,89]. Additionally, the use of different types of cell culture mediums, such as RPMI and DMEM, and variations in their formulations make it challenging to compare results from plasma-activated media

studies [89]. In terms of clinical translation, solutions that have already been approved for medical use may be more suitable due to their defined composition and standardized, quality-controlled production methods [21]. Among this, *Tanaka et al*. were the first to suggest using Ringer's Lactate (RL) solution for the generation of PALs [90]. RL has a simple composition of NaCl, KCl, $CaCl_2$, and lactate, which makes it suitable for this purpose and minimizes the potential influence of other components of the medium on the final biological effect [21,91]. Their research demonstrated the effectiveness of plasma-activated Ringer's Lactate (PA-RL) against EOC cancer [90]. *Freund et al.* also found RL to be a clinically relevant plasma treatment solution with the potential to be stored long-term, making it a promising agent for further research in a clinical setting [92].

RONS and lactate treatment through CAP may be responsible for the effects of PA-RL [21,90,93]. It is important for an antineoplastic agent to selectively target cancer cells while protecting healthy tissue. While there is no evidence on the safety of any type of intraperitoneal administration of PAL in humans, PA-RL has been shown to have no side effects in mice, suggesting its safety and effectiveness. However, the exact mechanism by which CAP and PALs affect cells is not well understood. Further research is needed to determine the optimal dose of plasma-generated species from various sources and to establish the use of CAP in the clinic.

1.5 References

1. Fridman, A. & Friedman, G. *Plasma Medicine*. *Plasma Medicine* (John Wiley & Sons, Inc., 2012). doi:10.1002/9781118437704.
2. Langmuir, I. Oscillations in Ionized Gases. *Proc. Natl. Acad. Sci.* **14**, 627–637 (1928).
3. Braný, D., Dvorská, D., Halašová, E. & Škovierová, H. Cold Atmospheric Plasma: A Powerful Tool for Modern Medicine. *Int. J. Mol. Sci.* **21**, 2932 (2020).
4. Adachi, T., Matsuda, Y., Ishii, R., Kamiya, T. & Hara, H. Ability of plasma-activated acetated Ringer's solution to induce A549 cell injury is enhanced by a pre-treatment with histone deacetylase inhibitors. *J. Clin. Biochem. Nutr.* 1–8 (2020) doi:10.3164/jcbn.19-104.
5. Von Woedtke, T., Schmidt, A., Bekeschus, S., Wende, K. & Weltmann, K. D. Plasma medicine: A field of applied redox biology. *In Vivo (Brooklyn).* **33**, 1011–1026 (2019).
6. Xu, D. *et al.* The effects of cold atmospheric plasma on cell adhesion, differentiation, migration, apoptosis and drug sensitivity of multiple myeloma. *Biochem. Biophys. Res. Commun.* **473**, 1125–1132 (2016).
7. Bárdos, L. & Baránková, H. Plasma processes at atmospheric and low pressures. *Vacuum* **83**, 522–527 (2008).
8. Privat-Maldonado, A. *et al.* ROS from Physical Plasmas: Redox Chemistry for Biomedical Therapy. *Oxid. Med. Cell. Longev.* **2019**, (2019).
9. Haertel, B., Woedtke, T. von, Weltmann, K.-D. & Lindequist, U. Non-Thermal Atmospheric-Pressure Plasma Possible Application in Wound Healing. *Biomol. Ther. (Seoul).* **22**, 477–490 (2014).
10. Bruggeman, P. & Leys, C. Non-thermal plasmas in and in contact with liquids. *J. Phys. D. Appl. Phys.* **42**, (2009).
11. Bruggeman, P. J. *et al.* Plasma-liquid interactions: A review and roadmap. *Plasma Sources Sci. Technol.* **25**, (2016).
12. Magureanu, M., Lukes, P. & Parvulescu, I. V. *Plasma Chemistry and Catalysis in Gases and Liquids*. (2012).
13. Myers, B. *et al.* Measuring plasma-generated ˙OH and O atoms in liquid using

EPR spectroscopy and the non-selectivity of the HTA assay. *J. Phys. D. Appl. Phys.* **54**, 145202 (2021).

14. Bogaerts, A. *et al.* The 2020 plasma catalysis roadmap. *J. Phys. D. Appl. Phys.* **53**, 443001 (2020).
15. Khlyustova, A., Labay, C., Machala, Z., Ginebra, M.-P. & Canal, C. Important parameters in plasma jets for the production of RONS in liquids for plasma medicine: A brief review. *Front. Chem. Sci. Eng.* **13**, 238–252 (2019).
16. Ratovitski, E. A. *et al.* Anti-cancer therapies of 21st century: Novel approach to treat human cancers using cold atmospheric plasma. *Plasma Process. Polym.* **11**, 1128–1137 (2014).
17. Graves, D. B. Reactive species from cold atmospheric plasma: Implications for cancer therapy. *Plasma Process. Polym.* **11**, 1120–1127 (2014).
18. Kurake, N. *et al.* Cell survival of glioblastoma grown in medium containing hydrogen peroxide and/or nitrite, or in plasma-activated medium. *Arch. Biochem. Biophys.* **605**, 102–108 (2016).
19. Yan, D., Sherman, J. H. & Keidar, M. Cold atmospheric plasma , a novel promising anti-cancer treatment modality. **8**, 15977–15995 (2017).
20. Malyavko, A. *et al.* Cold atmospheric plasma cancer treatment, direct versus indirect approaches. *Mater. Adv.* **1**, 1494–1505 (2020).
21. Tanaka, H. *et al.* Plasma-Treated Solutions (PTS) in Cancer Therapy. *Cancers (Basel).* **13**, 1737 (2021).
22. Min, T. *et al.* Therapeutic Effects of Cold Atmospheric Plasma on Solid Tumor. *Front. Med.* **9**, (2022).
23. Gorbanev, Y., O'Connell, D. & Chechik, V. Non-Thermal Plasma in Contact with Water: The Origin of Species. *Chem. - A Eur. J.* **22**, 3496–3505 (2016).
24. Locke, B. R. & Shih, K. Y. Review of the methods to form hydrogen peroxide in electrical discharge plasma with liquid water. *Plasma Sources Sci. Technol.* **20**, 15 (2011).
25. Fridman, A. *Plasma chemistry*. *Plasma Chemistry* vol. 9780521847 (Cambridge University Press, 2008).
26. Norberg, S. A., Tian, W., Johnsen, E. & Kushner, M. J. Atmospheric pressure plasma jets interacting with liquid covered tissue: Touching and not-touching

the liquid. *J. Phys. D. Appl. Phys.* **47**, (2014).

27. Zel'dovich, Y. B. *The Oxidation of Nitrogen in Combustion Explosions*. *Acta Physicochimica U.S.S.R.* vol. 21 (1946).
28. Machala, Z., Tarabová, B., Sersenová, D., Janda, M. & Hensel, K. Chemical and antibacterial effects of plasma activated water: correlation with gaseous and aqueous reactive oxygen and nitrogen species, plasma sources and air flow conditions. *J. Phys. D. Appl. Phys.* **52**, 034002 (2019).
29. Lukes, P., Dolezalova, E., Sisrova, I. & Clupek, M. Aqueous-phase chemistry and bactericidal effects from an air discharge plasma in contact with water: Evidence for the formation of peroxynitrite through a pseudo-second-order post-discharge reaction of H2O 2 and HNO2. *Plasma Sources Sci. Technol.* **23**, (2014).
30. Yan, X. *et al.* Plasma medicine for neuroscience—an introduction. *Chinese Neurosurg. J.* **5**, 25 (2019).
31. Laroussi, M., Kong, M., Morfill, G and Stolz, W. *Plasma Medicine Applications of Low-Temperature Gas Plasmas in Medicine and Biology*. (Cambridge University Press, 2012).
32. von Woedtke, T., Laroussi, M. & Gherardi, M. Foundations of plasmas for medical applications. *Plasma Sources Sci. Technol.* **31**, 054002 (2022).
33. Mattson, M. P. Hormesis defined. *Ageing Res. Rev.* **7**, 1–7 (2008).
34. Farhood, B. *et al.* Disruption of the redox balance with either oxidative or anti-oxidative overloading as a promising target for cancer therapy. *J. Cell. Biochem.* **120**, 71–76 (2019).
35. Trachootham, D., Alexandre, J. & Huang, P. Targeting cancer cells by ROS-mediated mechanisms: a radical therapeutic approach? *Nat. Rev. Drug Discov.* **8**, 579–591 (2009).
36. Graves, D. B. The emerging role of reactive oxygen and nitrogen species in redox biology and some implications for plasma applications to medicine and biology. *J. Phys. D. Appl. Phys.* **45**, (2012).
37. Yan, D. *et al.* The Strong Cell-based Hydrogen Peroxide Generation Triggered by Cold Atmospheric Plasma. *Sci. Rep.* 1–9 (2017) doi:10.1038/s41598-017-11480-x.

38. Sauer, H., Wartenberg, M. & Hescheler, J. Reactive Oxygen Species as Intracellular Messengers During Cell Growth and Differentiation. *Cell Physiol Biochem* **11**, 173–186 (2001).
39. Veal, E. & Day, A. Hydrogen Peroxide as a Signaling Molecule. *Antioxid. Redox Signal.* **15**, 147–151 (2011).
40. Liou, G.-Y. & Storz, P. Reactive oxygen species in cancer. *Free Radic. Res.* **44**, 479–496 (2010).
41. DeBerardinis, R. J. & Chandel, N. S. Fundamentals of cancer metabolism. *Sci. Adv.* **2**, e1600200 (2016).
42. Kirtonia, A., Sethi, G. & Garg, M. The multifaceted role of reactive oxygen species in tumorigenesis. *Cell. Mol. Life Sci.* **77**, 4459–4483 (2020).
43. Patel, R. P. *et al.* Biological aspects of reactive nitrogen species. *Biochim. Biophys. Acta - Bioenerg.* **1411**, 385–400 (1999).
44. Gladwin, M. T. *et al.* The Emerging Biology of the Nitrite Anion. *Nat. Chem. Biol.* **1**, 308–314 (2005).
45. Sonveaux, P., Jordan, B. F., Gallez, B. & Feron, O. Nitric oxide delivery to cancer: Why and how? *Eur. J. Cancer* **45**, 1352–1369 (2009).
46. Keshet, R. & Erez, A. Arginine and the metabolic regulation of nitric oxide synthesis in cancer. *Dis. Model. Mech.* **11**, (2018).
47. Fukumura, D., Kashiwagi, S. & Jain, R. K. The role of nitric oxide in tumour progression. *Nat. Rev. Cancer* **6**, 521–534 (2006).
48. Burke, A. J., Sullivan, F. J., Giles, F. J. & Glynn, S. A. The yin and yang of nitric oxide in cancer progression. *Carcinogenesis* **34**, 503–512 (2013).
49. Patel, R. P. *et al.* Biological aspects of reactive nitrogen species. *Biochim. Biophys. Acta - Bioenerg.* **1411**, 385–400 (1999).
50. Weidinger, A. & Kozlov, A. Biological Activities of Reactive Oxygen and Nitrogen Species: Oxidative Stress versus Signal Transduction. *Biomolecules* **5**, 472–484 (2015).
51. Lu, X. *et al.* Reactive species in non-equilibrium atmospheric-pressure plasmas: Generation, transport, and biological effects. *Phys. Rep.* **630**, 1–84 (2016).
52. Laroussi, M. Cold Plasma in Medicine and Healthcare: The New Frontier in

Low Temperature Plasma Applications. *Front. Phys.* **8**, 1–7 (2020).

53. Bauer, G., Sersenová, D., Graves, D. B. & Machala, Z. Cold Atmospheric Plasma and Plasma-Activated Medium Trigger RONS-Based Tumor Cell Apoptosis. *Sci. Rep.* **9**, 14210 (2019).
54. Lee, B. W. L., Ghode, P. & Ong, D. S. T. Redox regulation of cell state and fate. *Redox Biol.* **25**, 101056 (2019).
55. Kim, S. J. & Chung, T. H. Cold atmospheric plasma jet-generated RONS and their selective effects on normal and carcinoma cells. *Sci. Rep.* **6**, 20332 (2016).
56. Hoffmann, C., Berganza, C. & Zhang, J. Cold Atmospheric Plasma: methods of production and application in dentistry and oncology. *Med. Gas Res.* **3**, 21 (2013).
57. Kim, J. Y. *et al.* Apoptosis of lung carcinoma cells induced by a flexible optical fiber-based cold microplasma. *Biosens. Bioelectron.* **28**, 333–338 (2011).
58. Recek, N. *et al.* Effect of Cold Plasma on Glial Cell Morphology Studied by Atomic Force Microscopy. *PLoS One* **10**, e0119111 (2015).
59. Keidar, M. *et al.* Cold plasma selectivity and the possibility of a paradigm shift in cancer therapy. *Br. J. Cancer* **105**, 1295–1301 (2011).
60. Utsumi, F. *et al.* Selective cytotoxicity of indirect nonequilibrium atmospheric pressure plasma against ovarian clear-cell carcinoma. *Springerplus* **3**, 1–9 (2014).
61. Bisag, A. *et al.* Plasma-activated Ringer's Lactate Solution Displays a Selective Cytotoxic Effect on Ovarian Cancer Cells. *Cancers (Basel).* **12**, 476 (2020).
62. Metelmann, H.-R. *et al.* Head and neck cancer treatment and physical plasma. *Clin. Plasma Med.* **3**, 17–23 (2015).
63. Kang, S. U. *et al.* Nonthermal plasma induces head and neck cancer cell death: the potential involvement of mitogen-activated protein kinase-dependent mitochondrial reactive oxygen species. *Cell Death Dis.* **5**, e1056–e1056 (2014).
64. Vandamme, M. *et al.* ROS implication in a new antitumor strategy based on

non-thermal plasma. *Int. J. Cancer* **130**, 2185–2194 (2012).

65. Tanaka, H. *et al.* Plasma-Activated Medium Selectively Kills Glioblastoma Brain Tumor Cells by Down-Regulating a Survival Signaling Molecule, AKT Kinase. *Plasma Med.* **1**, 265–277 (2011).
66. Thiyagarajan, M., Anderson, H. & Gonzales, X. F. Induction of apoptosis in human myeloid leukemia cells by remote exposure of resistive barrier cold plasma. *Biotechnol. Bioeng.* **111**, 565–574 (2014).
67. Barekzi, N. & Laroussi, M. Dose-dependent killing of leukemia cells by low-temperature plasma. *J. Phys. D. Appl. Phys.* **45**, 422002 (2012).
68. Kim, S. J., Chung, T. H., Bae, S. H. & Leem, S. H. Induction of apoptosis in human breast cancer cells by a pulsed atmospheric pressure plasma jet. *Appl. Phys. Lett.* **97**, 023702 (2010).
69. Gay-Mimbrera, J. *et al.* Clinical and Biological Principles of Cold Atmospheric Plasma Application in Skin Cancer. *Adv. Ther.* **33**, 894–909 (2016).
70. Ishaq, M., Evans, M. D. M. & Ostrikov, K. (Ken). Atmospheric pressure gas plasma-induced colorectal cancer cell death is mediated by Nox2–ASK1 apoptosis pathways and oxidative stress is mitigated by Srx–Nrf2 anti-oxidant system. *Biochim. Biophys. Acta - Mol. Cell Res.* **1843**, 2827–2837 (2014).
71. Hattori, N. *et al.* Effectiveness of plasma treatment on pancreatic cancer cells. *Int. J. Oncol.* **47**, 1655–1662 (2015).
72. Partecke, L. I. *et al.* Tissue Tolerable Plasma (TTP) induces apoptosis in pancreatic cancer cells in vitro and in vivo. *BMC Cancer* **12**, 473 (2012).
73. Dubuc, A. *et al.* Use of cold-atmospheric plasma in oncology: a concise systematic review. *Ther. Adv. Med. Oncol.* **10**, 175883591878647 (2018).
74. Baal, J. O. A. M. Van *et al.* Development of Peritoneal Carcinomatosis in Epithelial Ovarian Cancer : A Review. **66**, 67–83 (2018).
75. Jewell, A., Mcmahon, M. & Khabele, D. Heated Intraperitoneal Chemotherapy in the. (2018) doi:10.3390/cancers10090296.
76. Lheureux, S., Gourley, C., Vergote, I. & Oza, A. M. Epithelial ovarian cancer. *Lancet* **393**, 1240–1253 (2019).
77. Rynne-vidal, A., Au-yeung, C. L., Jiménez-heffernan, J. A. & Pérez-lozano,

M. L. Mesothelial-to-mesenchymal transition as a possible therapeutic target in peritoneal metastasis of ovarian cancer. 140–151 (2017) doi:10.1002/path.4889.

78. Pepa, C. Della *et al.* Ovarian cancer standard of care: are there real alternatives? *Chin. J. Cancer* **34**, 17–27 (2015).

79. Sant, M. *et al.* Survival for haematological malignancies in Europe between 1997 and 2008 by region and age: results of EUROCARE-5, a population-based study. *Lancet Oncol.* **15**, 931–942 (2014).

80. Puiffe, M. L. *et al.* Characterization of ovarian cancer ascites on cell invasion, proliferation, spheroid formation, and gene expression in an in vitro model of epithelial ovarian cancer. *Neoplasia* **9**, 820–829 (2007).

81. Chang, Y.-H. *et al.* Front-line intraperitoneal versus intravenous chemotherapy in stage III-IV epithelial ovarian, tubal, and peritoneal cancer with minimal residual disease: a competing risk analysis. *BMC Cancer* **16**, 235 (2016).

82. Tewari, D. *et al.* Long-Term Survival Advantage and Prognostic Factors Associated With Intraperitoneal Chemotherapy Treatment in Advanced Ovarian Cancer: A Gynecologic Oncology Group Study. *J. Clin. Oncol.* **33**, 1460–1466 (2015).

83. van Driel, W. J. *et al.* Hyperthermic Intraperitoneal Chemotherapy in Ovarian Cancer. *N. Engl. J. Med.* **378**, 230–240 (2018).

84. Wu, Q. *et al.* Efficacy of hyperthermic intraperitoneal chemotherapy in patients with epithelial ovarian cancer: a meta-analysis. *Int. J. Hyperth.* **36**, 562–572 (2019).

85. Utsumi, F. *et al.* Effect of indirect nonequilibrium atmospheric pressure plasma on anti-proliferative activity against chronic chemo-resistant ovarian cancer cells in vitro and in vivo. *PLoS One* **8**, 1–10 (2013).

86. Torii, K. *et al.* Effectiveness of plasma treatment on gastric cancer cells. *Gastric Cancer* **18**, 635–643 (2015).

87. Nakamura, K., Peng, Y., Utsumi, F., Tanaka, H. & Mizuno, M. Novel Intraperitoneal Treatment With Non-Thermal Plasma- Activated Medium Inhibits Metastatic Potential of Ovarian Cancer Cells. *Sci. Rep.* 1–14 (2017)

doi:10.1038/s41598-017-05620-6.

88. Takeda, S. *et al.* Intraperitoneal Administration of Plasma-Activated Medium: Proposal of a Novel Treatment Option for Peritoneal Metastasis From Gastric Cancer. *Ann. Surg. Oncol.* **24**, 1188–1194 (2017).
89. Bergemann, C., Rebl, H., Otto, A., Matschke, S. & Nebe, B. Pyruvate as a cell-protective agent during cold atmospheric plasma treatment in vitro: Impact on basic research for selective killing of tumor cells. *Plasma Process. Polym.* **16**, (2019).
90. Tanaka, H. *et al.* Non-thermal atmospheric pressure plasma activates lactate in Ringer's solution for anti-tumor effects. *Sci. Rep.* **6**, 36282 (2016).
91. Nakamura, K. *et al.* Preclinical Verification of the Efficacy and Safety of Aqueous Plasma for Ovarian Cancer Therapy. *Cancers (Basel).* **13**, 1141 (2021).
92. Freund, E. *et al.* In Vitro Anticancer Efficacy of Six Different Clinically Approved Types of Liquids Exposed to Physical Plasma. *IEEE Trans. Radiat. Plasma Med. Sci.* **3**, 588–596 (2019).
93. Tanaka, H. *et al.* Oxidative stress-dependent and -independent death of glioblastoma cells induced by non-thermal plasma-exposed solutions. *Sci. Rep.* **9**, 13657 (2019).

CHAPTER 2

Examining the cytotoxic effect of different plasma-activated liquids on Epithelial Ovarian Cancer cells

2.1 Introduction

The following discussion concerns the experimental approach over these years. The long work carried out has involved more people and led to the publishing of a scientific publication in an international journal, which will be mentioned [1].

In particular, the first part of this section derives from a joint research work conducted with Dr Alina Bisag. Her essential contribution dealt with the development and characterization of a novel multiwire plasma source employed in this study, and the production of Plasma-Activated Liquids (PALs). With regard to the cell culturing and biological analyses, the experiments on cancer cells were performed in the Golgi BioPlasma Cell laboratory (DIN), while experiments on primary fibroblasts were carried out at U.O. di Genetica Medica, Genetica Medica laboratory, Pol. S.Orsola (DIMEC). The analyses conducted on primary models derive from a joint work with Dr Giulia Girolimetti and Dr Sara Coluccelli.

A part of these activities was supported by the UNIBO AlmaIDEA Grant Senior project entitled “Chemo-physical and biological mechanisms behind the anticancer activity of plasma activated liquids for the treatment of peritoneal carcinosis from primitive epithelial ovarian/tubular tumor” and supervised by Prof. Pierandrea De Iaco from the Department of Gynecology and Obstetrics, S. Orsola-Malpighi Hospital, Alma Mater Studiorum-Università di Bologna. The aim of this project was the development of a novel intraperitoneal therapy for Epithelial Ovarian Cancer (EOC) treatment using Plasma-Activated Liquids.

In this research, Cold Atmospheric Plasma (CAP) generated through an innovative plasma source (Figure 2.2-1), developed by the Research Group for Industrial Application of Plasmas (IAP group) at the Alma Mater Studiorum – University of Bologna was employed for the first time to produce Plasma-Activated Liquids (PALs) for the treatment of Epithelial Ovarian Cancer (EOC) [1]. EOC is the fifth leading cause of cancer-related death among women and it is characterized by intraperitoneal dissemination [2]. Hence, it is the most lethal and silent gynecological tumor and in advanced stages (III-IV) it presents a poor prognosis at diagnosis (29% of survival rate within 5 years) [3,4]. Currently available therapeutic options include

tumor debulking surgery and intraperitoneal platinum-taxane chemotherapy, which cannot eradicate the disease and about 80% of patients relapse [4–7]. The treatment of liquids through CAP technology enables the production of PALs containing reactive oxygen and nitrogen species having anticancer activity. In this perspective, delivering RONS to cancer tissues by washing the peritoneal cavities with PALs, might be an adjuvant strategy to aid conventional EOC therapies [1,8]. In this work, *in vitro* experiments on EOC, non-cancer and fibroblast cell lines are conducted with the aim to evaluate the cytotoxic effect and the selectivity of PALs. PALs are produced by exposing cell culture medium or Ringer's Lactate solution (RL) to a micropulsed corona discharge to produce plasma-activated medium (PAM) and plasma-activated Ringer's Lactate solution (PA-RL), respectively. PAM and PA-RL dilutions are used for the treatment of EOC in order to define the dose-response profile of PALs. Therefore, two PAL-synthetic solutions are produced to evaluate whether PALs-induced cell injury may depend on the presence of H_2O_2. Both PAM and PA-RL dilutions reveal a cytotoxic effect. However, only PA-RL 1:16 dilution exerts a significantly higher cytotoxic effect on EOC, not only related to reactive species presence, with respect to PAM. PA-RL is also diluted in cell culture media to investigate whether its cytotoxicity may depend on a strict interaction between the CAP bio-active species and the liquid used. The analyses reveal that the CAP-generated RONS only partly contribute to the cytotoxic activity of PALs, to which additional species such as the organic elements therein involved also contribute. Therefore, when PALs cytotoxicity is correlated with EOC metabolic profile, a correlation between PALs and cell type strictly associated with cancer metabolic plasticity is also observed. In order to find the applicability of PALs in the clinics, it is investigated whether the PA-RL powerful cytotoxicity may display such a selective effect on cancer cells. PA-RL dilutions are used to treat ovarian cancer cell lines as well as non-cancer epithelial and fibroblast cell models. The analyses show that PA-RL 1:16 could compromise EOC cell growth displaying a selective cytotoxic effect concerning non-cancer cells. Altogether, these results suggest that PALs activity is characterized by different intracellular molecular mechanisms since other CAP-generated RONS are involved. Albeit there is a need for further studies to confirm the mechanism by which PALs exert cytotoxicity in the context of ovarian

cancer, PALs could be a promising option to contribute to the development of new adjuvant and personalized anticancer therapies.

2.2 Materials and Methods

2.2.1 Plasma device and electrical characterization

A multiwire plasma source (developed at the Alma Mater Studiorum – University of Bologna) was used to produce PALs by exposing liquids to a micropulsed corona discharge (Figure 2.2-1). The plasma source consists of a multiwire corona driven by a high voltage generator (AlmaPULSE, AlmaPlasma s.r.l.) delivering a peak voltage of 18 kV, pulse duration full width at half maximum of 8 μs and pulse repetition rate set at 1 kHz. The high voltage (HV) electrode consists of four steel wires individually fixed on aluminium supports through threaded screws and connected to high voltage generator through a ballast resistor of 70 kΩ. The ground electrode consists of an aluminium sheet fixed on the bottom of the polymethylmethacrylate (PMMA) vessel containing the liquid substrate; it is connected to the ground through a 30 kΩ resistor. To guarantee a controlled atmosphere during the CAP treatment, the plasma source structure is encased in a PMMA box and equipped with a fan able to direct the plasma effluent towards the liquid surface.

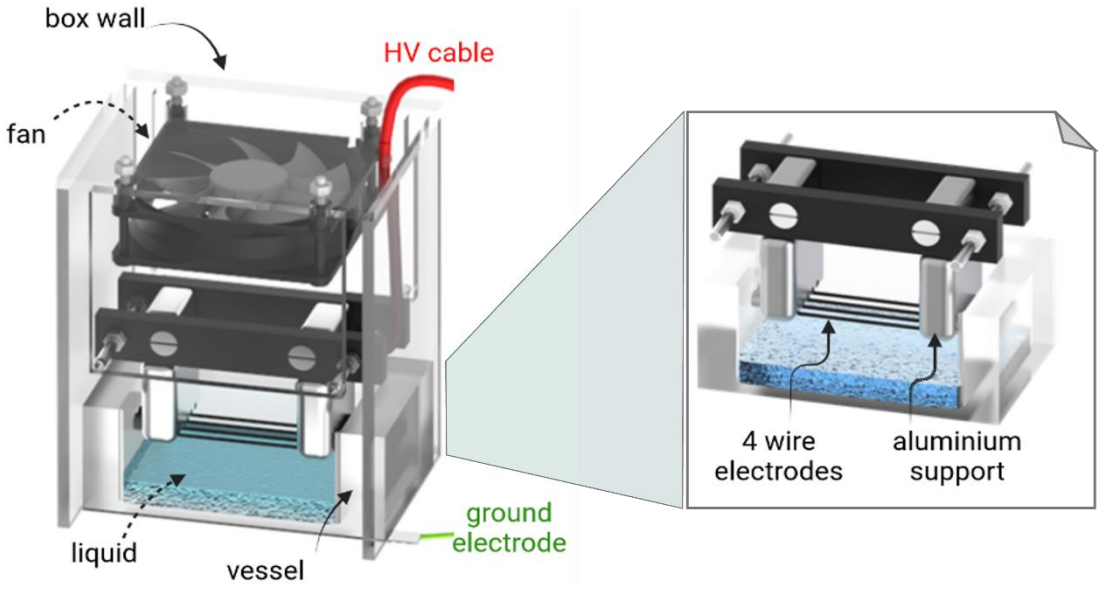

Figure 2.2-1 Render of the corona multiwire plasma source

To measure the time evolution of the plasma discharge electrical parameters 5 mm gap value was fixed between the HV electrodes and liquid surface; the setup used for the analysis is reported in Figure 2.2-2. In addition, two HV probes (Textronix P6015A) were used to measure the voltage before and after the high voltage resistor (70 kΩ), while the discharge current was measured employing a current probe (Pearson 6585). All the probes were connected to an oscilloscope (Tektornix DPO4034, 350 MHz, 2.5 GSa s-1) and the average power (P) over a period (T) was calculated starting from current (I) and voltage (V) measurements:

$$P = \frac{1}{T}\int_T VI\,dt \qquad (1)$$

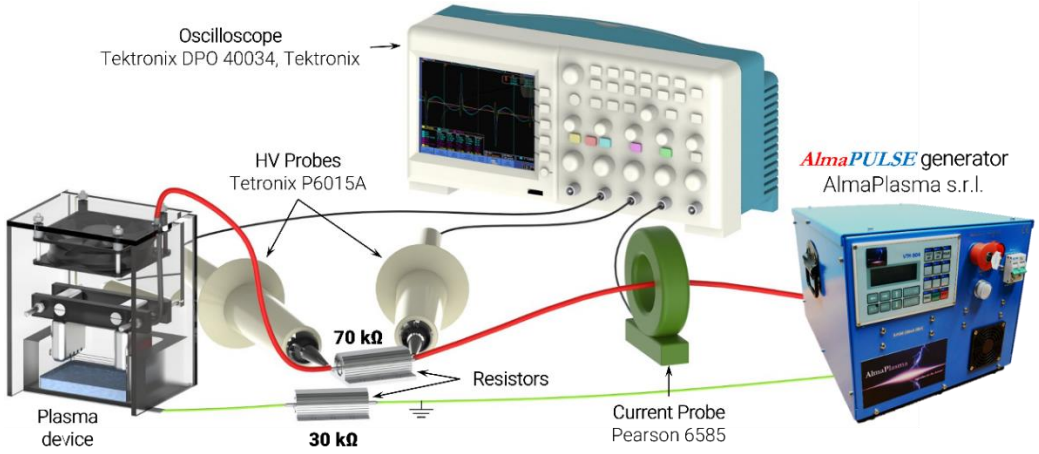

Figure 2.2-2 Setup used for electrical characterization

2.2.2 PALs and synthetic solutions production

PAM and PA-RL solutions were produced by exposing 20 ml of RPMI medium without FBS or 20 ml of RL to plasma for 10 minutes, respectively. The gap between high voltage electrodes and the liquid surface was fixed to 5 mm, while peak voltage (PV) and pulse repetition frequency (PRF) was set to 18 kV and 1 kHz, respectively. After plasma treatment, quantitative determination of H_2O_2 and NO_2^- related PAM and PA-RL were performed using Amplex® Red Hydrogen Peroxide Assay Kit (Thermo Fisher Scientific #A22188, Waltham, MA, USA) and Nitrite/Nitrate colorimetric assay (ROCHE #11746081001, Basel, Switzerland). In addition, before and after exposure to plasma, the pH and the conductivity of the liquid substrates

were evaluated by means of inoLab® pH 7110 and Oakton Instrument: Con 6+ Meter, respectively.

PAM and PA-RL were diluted by two-fold serial dilutions (from 1:2 to 1:16) in RPMI or RL, respectively. Moreover, undiluted PA-RL was also used to produce a new plasma-activated liquid namely RPMI+PA-RL i.e., PA-RL was serially diluted in RPMI, as mentioned before.

Synthetic solutions were also prepared to serve as positive controls. PAM/PA-RL-synthetic solutions were also produced adding a proper amount of H_2O_2 (Sigma-Aldrich, 216763) and of NO_2^- (Alfa Aesar by Thermo Fisher (Kandel) GmbH, #43015, Karlsruhe, Germany), in order to reach the same concentration of RONS generated in PAM and PA-RL. An additional PA-RL-synthetic solution was prepared by adjusting the pH of RL to 5.36 with a solution of 0.01M HCl, according to the pH value gauged in PA-RL. The above mixtures were also diluted in RPMI or RL, as reported before.

PAM and PA-RL dilutions and synthetic solutions were immediately used to treat cells after preparation.

2.2.3 Cell lines and culture conditions

Human EOC cell lines SKOV-3, OV-90, OVSAHO and OC314 were purchased from ATCC®, while HOSE cell line was purchased from ScienCell Research Laboratories, Inc. As non-cancer controls, two lines of immortalized fibroblasts (F1 and F2) derived from two patients' skin biopsies, obtained in the context of a protocol approved by the Independent Ethics Committee of S. Orsola-Malpighi Hospital (107/2011/U/Tess of MiPEO studies) were used. EOC, HOSE and fibroblast cell lines were grown in RPMI medium (EuroClone, Milan, Italy), Ovarian Epithelial Cell Medium (OEpiCM, ScienCell Research Laboratories, Inc., Carlsbad, CA, USA) and DMEM High glucose (EuroClone), respectively. The cell culture media were supplemented with 10% heat-inactivated fetal bovine serum (FBS), 2 mM L-glutamine, 100 U/mL penicillin and 100 μg/mL streptomycin (EuroClone). Cells were cultured at 37°C in a 5% CO_2 humidified atmosphere and observed using Eclipse TS100 microscope (Nikon, Tokyo, Japan).

2.2.4 Cell treatment and viability assay

EOC, HOSE and fibroblast cell lines were seeded in 96-well plates in complete medium, at the conditions reported in Table 2.2-1.

	EOC				Non-cancer		
Cell line	SKOV-3	OV-90	OVSAHO	OC314	HOSE	F1	F2
No. of cells/well	2×10^3	4×10^3	5.5×10^2	3.5×10^2	7×10^3	9×10^3	1×10^4

Table 2.2-1 Cell lines seeding conditions for cell viability assay

After 24 hours of incubation, cells were treated with 100 µl of appropriately diluted PALs or its corresponding untreated control liquids for 2 hours. Afterwards, cells were washed in phosphate buffered solution (PBS) and cultured in complete medium at 37°C and 5% CO_2 (Figure 2.2-3). Cell viability was assayed using Sulforhodamine B (SRB; Sigma-Aldrich, #S1402, St. Louis, MO, USA) at the following time points: 2, 24, 48 and 72 h after treatment. Treated cells were fixed with 50% cold trichloroacetic acid (TCA) for 1 h, washed 5 times with distilled water to eliminate TCA, and stained with 0.4 % SRB for 30 minutes. Unbound dye was removed after 4 washes with 1 % acetic acid. Protein-bound dye was dissolved in 10 mM pH 10.5 Tris base solution. Then, absorbance values were determined at 570 nm using a 96-well Multilabel Plate Reader VICTOR^3 (1420 Multilabel Counter-PerkinElmer, Turku, Finland). Percentage of growth was calculated considering PAL-untreated cells as control.

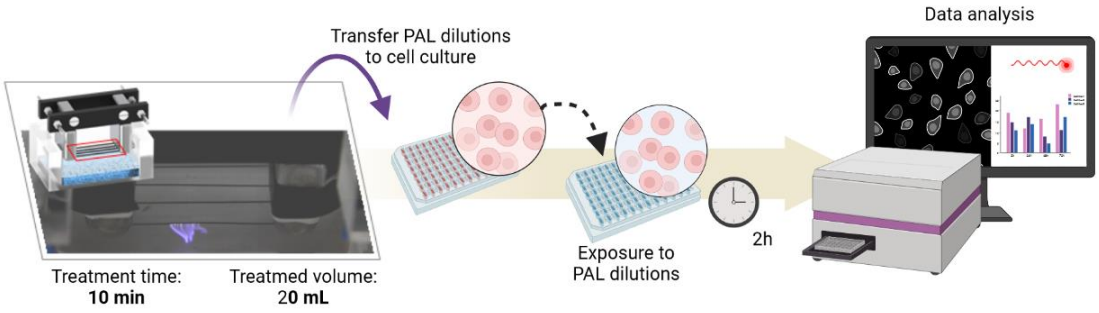

Figure 2.2-3 Workflow of PAL treatments on cell models

2.2.5 ROS detection and cytotoxicity assays

The total ROS detection and cytotoxicity assay were performed by using the IncuCyte S3 Live-Cell Analysis System (at the Centre for Applied Biomedical Research – CRBA - University of Bologna). The total ROS detection was performed by seeding EOC in a 96-wells plate, at the conditions mentioned in Table 2.2-1. After 24 hours, cells were treated for 2 hours with PALs dilutions and then incubated with the CellROX Deep Red Reagent 5 µM (Invitrogen®, Carlsbad, USA) diluted in complete fresh medium, useful to detect total ROS levels. The set acquisition protocol was set for acquiring 1 image/well every 2 hours from the end of the treatment to 24 hours post-treatment.

Regarding the cytotoxic assay, EOC cells were seeded in a 96-wells plate, at the conditions mentioned in Table 2.2-2Table 2.2-1 Cell lines seeding conditions. After PALs dilutions treatment, EOC lines were incubated with the Incucyte® Cytotox Green Dye (to detect dead cells) and the Incucyte® NucLight Rapid Red Reagent (to stain nuclei of live cells). The set acquisition protocol was set for acquiring 1 image/well at the end of the treatment, 2-, 12- and 24-hours post-treatment. Data analyses were performed using IncuCyte™ S3 software. Raw data were exported from the instrument and represented in GraphPad.

The intracellular levels of ROS were measured using cell-permeant 2',7'-dichlorodihydrofluorescein diacetate (H_2DCFDA) 2µM after treatment and fluorescence ($\lambda_{ex/em}$ = 490/530 nm) was measured at the end of treatment, 2 h and 4 h post-treatment.

	EOC			
Cell line	SKOV-3	OV-90	OVSAHO	OC314
No. of cells/well	6 x 10^3	8 x 10^3	12 x 10^3	4 x 10^3

Table 2.2-2 Cell lines seeding conditions for the cytotoxic assay.

2.2.6 Colony formation assay

The ability of a single cancer cell to grow forming a colony was evaluated by seeding 2 x 10^3 cells/well in a 6-well plate. After seeding, cells were incubated at 37° C in a humidified 5% CO_2 atmosphere for 24 hours. The anti-tumorigenic potential of

PALs was assessed by treating EOC for 2 h with PALs. Then, cells were grown for 10 days, changing the media every 3 days. Colonies were fixed using 50% TCA for 1 h and stained with 0.4% SRB and then counted. Images were acquired using Gel Logic 1500 Imaging System (Kodak, Ronchester, NY, USA).

2.2.7 SDS-PAGE and Western Blot Analysis

EOC cell lines and fibroblasts were seeded and after 24 h were treated for 2 h with RL and PA-RL 1:16 dilution. After treatments, cells were washed in PBS and cultured in complete media at 37°C and 5% CO_2. An untreated (UT) sample was also collected for each cell line. Then, cells were harvested at 72 h post-treatment and resuspended in RIPA buffer (50 mM Tris–HCl pH 7.4, 150 mM NaCl, 1 % SDS, 1 % Triton X-100 and 1 mM EDTA pH 7.6) supplemented with protease and phosphatase inhibitors (ThermoFisher #A32955, Waltham, MA, USA). The protein content was quantified using Lowry protein assay (Bio-Rad #5000116, Hercules, CA, USA). 30 µg of total protein were separated by using SDS-PAGE on a 12 % polyacrylamide gel and then transferred onto a Trans-Blot Turbo Midi Nitrocellulose membrane (Bio-Rad #1704159). Membranes were incubated with 5 % TBS-Tween/milk (0.1 % Tween 20 (Sigma-Aldrich #P9416, St. Louis, MO, USA) and incubated with primary antibodies using the following dilutions/conditions: anti-SOD-1 (Santa Cruz Biotechnology #sc-11407, Dallas, TX, USA) 1:1000, overnight at 4°C; anti-β-actin (Sigma-Aldrich #A5316) 1:10000, 1 h at room temperature. Membranes were washed 4 times with TBS-Tween and incubated with proper secondary antibodies (Jackson ImmunoResearch Laboratories #111035144 and #111035146, West Grove, PA, USA), diluted 1:20000 (anti-rabbit) and 1:10000 (anti-mouse) for 30 min at room temperature. Chemiluminescence signal was obtained by Clarity Western ECL Substrate (Bio-Rad #1705061). Images were acquired using ChemiDoc XRS+ (Bio-Rad). Protein levels were determined by densitometry of each specific band normalizing on β-actin as housekeeping.

Regarding the amount of antioxidant enzymes in basal condition, 40 µg of total protein were separated by using SDS-PAGE on a 12 % polyacrylamide gel and then transferred onto a Nitrocellulose membrane 0.45 mm in a full-wet system in Western Transfer Buffer (25 mM Tris pH 8.3, 93 mM glycine, 20 % methanol) using Bio-Rad

Mini Trans-Blot Cell system. Then, membrane was incubated with primary antibodies using the following dilutions/conditions: anti-SOD-2 (or anti-MnSOD; Abcam #06984) 1:1000, overnight at 4°C; anti-CAT (Sigma-Aldrich #C0979) 1:4000; anti-HSP70 (Abcam #ab2787) 1:1000, 1 h at room temperature. Membranes were washed 4 times with TBS-Tween and incubated with proper secondary antibodies (Jackson ImmunoResearch Laboratories #111035144 and #111035146, West Grove, PA, USA), diluted 1:20000 (anti-rabbit) and 1:10000 (anti-mouse) for 30 min at room temperature. Protein levels were determined by densitometry of each specific band normalizing on HSP70 as housekeeping.

The densitometric analysis of protein levels was performed using ImageJ software (Version 1.53m, Bethesda, MD, USA).

2.2.8 Statistical Analyses

Statistical analyses were performed using GraphPad Prism version 8. Continuous variables were expressed as mean ± standard error of the mean (SEM; $n \geq 3$). To compare groups, Student's *t-test* was used, and statistical significance is specified with asterisks (* $p \leq 0.05$, ** $p \leq 0.001$).

2.3 Results and discussion

2.3.1 Electrical characterization of multiwire plasma source and chemical features of liquid substrates

2.3.1.1 Electrical characterization

The temporal evolution of voltage and current waveforms during the treatment of RPMI and RL solution was evaluated (Figure 2.3-1). The dynamic behaviour of voltage and current waveforms related to RPMI treatment corresponded to a maximum peak value of 18.4 kW and 184 mA, and a minimum peak reached -18 kV and -188 mA, respectively. While voltage waveforms during RL treatment raged maximum and minimum values from 20 kV to -19.6 kV. The respective current waveforms reached a peak of 288 mA to -268 mA. Thus, according to equation (1), the average power (P) applied on both liquid substrates was calculated showing that the P during RPMI treatment was 12.11 W while during RL treatment was 12.42 W.

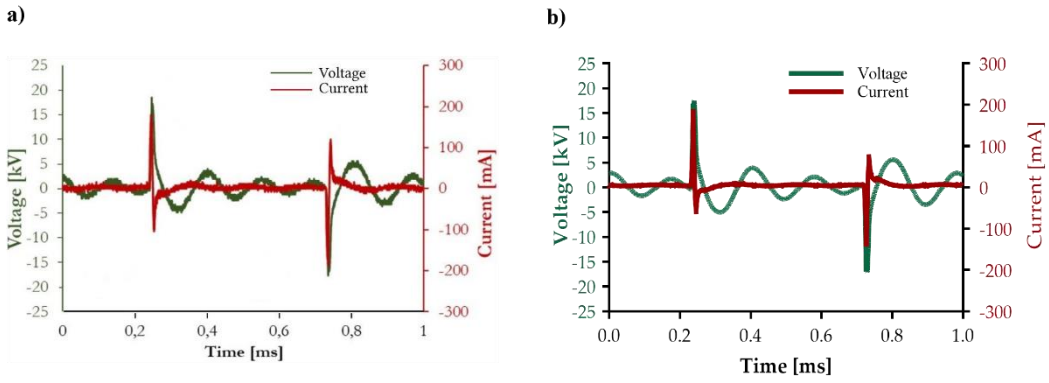

Figure 2.3-1 Electrical characterization of plasma source during treatment of (a) RPMI and (b) Ringer's Lactate solution at 18kV and 1kHz. Data are presented as mean ± SEM (n = 3).

2.3.1.2 Chemical features of the treated liquid

The exposure of a liquid to plasma discharges induces the production of reactive oxygen and nitrogen species, giving anti-cancer properties to the treated solution [9–11]. Hence, RONS concentrations measured after the plasma treatment in PAM and PA-RL are shown in Figure 2.3-2 and Figure 2.3-3. More specifically, the H_2O_2 and NO_2^- concentrations increased linearly with the treatment time in both treated solutions (Figure 2.3-2). The amount of H_2O_2 and NO_2^- reached 265.0 ± 4.5 µM and 672.9 ± 11.0 µM for PAM, while in PA-RL ranged 226.0 ± 12.5 µM and 658.6 ± 15.2 µM, respectively. Thus, the ratio NO_2^- /H_2O_2 in PAM resulted to be 2.54, while in PA-RL resulted to be 2.91.

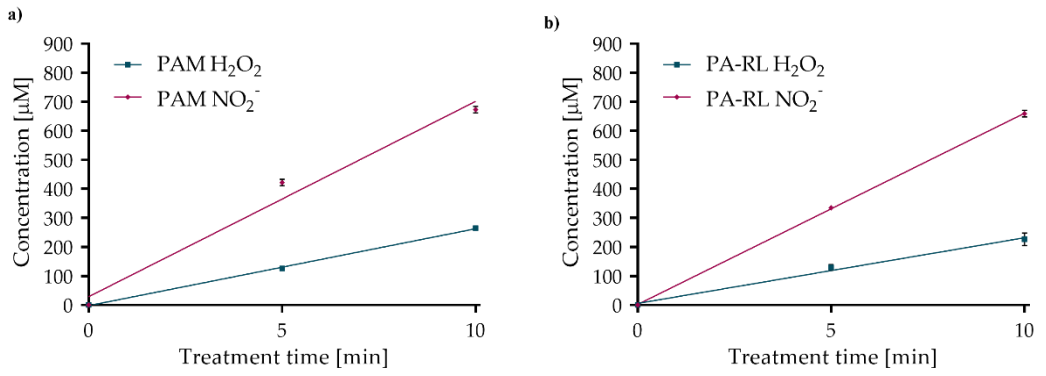

Figure 2.3-2 Plasma treatment leads to the formation of H_2O_2 and NO_2^-. RONS concentrations in (a) PAM and (b) PA-RL as a function of treatment time. Data are presented as mean ± SEM (n=3).

Moreover, were also reported RONS concentration of diluted PALs solution (Figure 2.3-3). One of the main focuses is to assess the dose-response profile of PALs solution as a function of different RONS concentrations. Thus, PALs dilutions were obtained by performing 2-fold serial dilution in the proper liquid and as expected, an H_2O_2- and NO_2^--dependent decrease was observed.

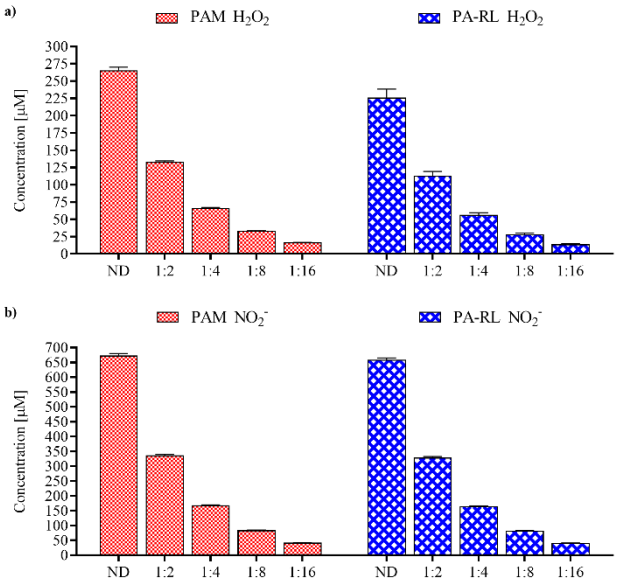

Figure 2.3-3 H_2O_2 (a) and NO_2^- (b) concentration in PAM and PA-RL not diluted (ND) and diluted solutions. Data are presented as mean ± SEM (n=3).

Figure 2.3-4 reported the evolution of pH and conductivity of PALs and their dilutions. After 10 minutes of CAP treatment, the pH decreases to 5.36 in PA-RL solution as opposed to PAM, while the conductivity increased in both treated solutions. Thus, these results led to excluding the undiluted PA-RL solution, and consequently its PAM counterpart, for subsequent cell treatments.

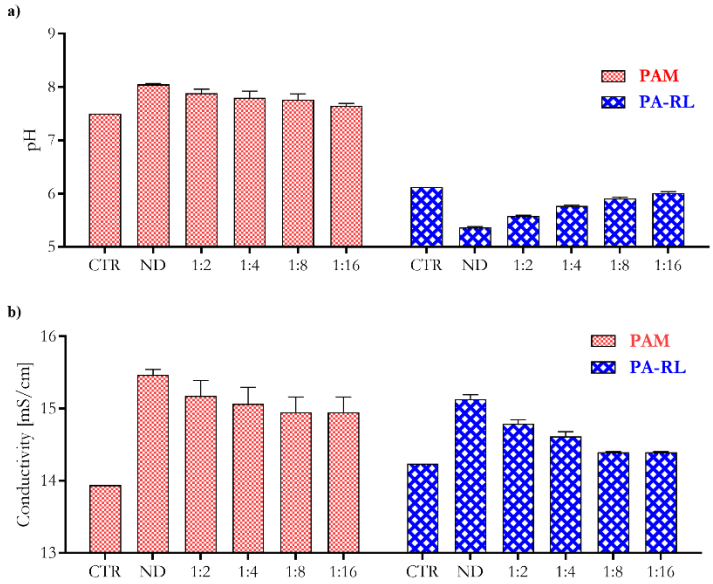

Figure 2.3-4 pH (a) and conductivity (b)in PAM and PA-RL as a function of serial dilutions. Data are presented as mean ± SEM (n = 3)

2.3.2 Epithelial Ovarian Cancer cells exhibit different sensitivities to Plasma-Activated Medium and Plasma-Activated Ringer's Lactate

2.3.2.1 PA-RL inhibits cell proliferation more efficiently than PAM in EOC cell lines

To assess the impact of PAM and PA-RL on the proliferative profile, the viability assay on two EOC cell lines, namely OV-90 and SKOV-3, was performed. EOC cells were exposed to a gradient ratio of PAM and PA-RL (dilutions 1:2 to 1:16) for two hours. As shown in Figure 2.3-5, OV-90 appeared to be more sensitive to PA-RL with respect to PAM even after two hours of exposure. Moreover, PA-RL showed a significant dose-dependent trend on OV-90, with a viability decrease from 35 % to 65 %, through a partial cytostatic effect up to PA-RL 1:8. In SKOV-3 cancer cells, PAM and PA-RL showed the same antiproliferative trend; and these effects were not dose-dependent. In particular, PAM and PA-RL showed a significant efficiency difference only when SKOV-3 were treated with 1:16 dilution. The 50 % of SKOV-3 viability was affected by PA-RL 1:16 treatment showing a cytostatic effect over time, whereas PAM 1:16 seems not to exert influence on the proliferative capability. Overall, PAM and PA-RL dilutions induced different effects on different types of EOC cells. The effect recorded on OV-90 was dose-dependent in contrast with the

one induced on SKOV-3. Furthermore, SKOV-3 were more sensitive to PAM and PA-RL treatments with respect to OV-90. Together, these results showed that PA-RL exerted better effectiveness and steadiness to inhibit EOC proliferation than PAM; indeed, PA-RL exerted a substantial cytostatic trend in all the cases investigated up to 72h post-treatment.

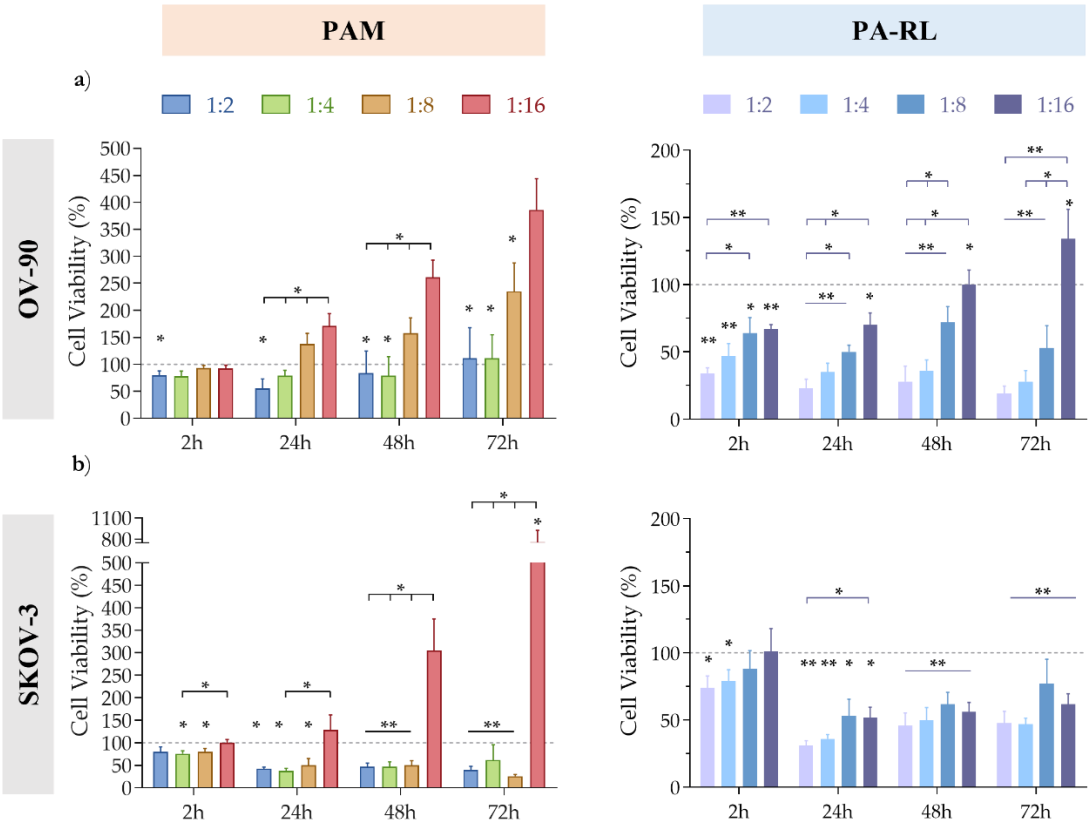

Figure 2.3-5 PA-RL inhibits cell proliferation more efficiently than PAM in Epithelial Ovarian Cancer (EOC) cell lines. Viability of OV-90 (a) and SKOV-3 (b) cell line after PAM and PA-RL dilutions treatments. Data are mean ± SEM ($n \geq 3$) normalized considering untreated cells at t = 2 h as 100%. The statistical significance is specified with asterisks ($p \leq 0.05$, ** $p \leq 0.001$ as determined by a paired Student's t-test).*

2.3.2.2 Hydrogen peroxide contributes to the activity of PALs depending on the cell type

Several studies indicated that hydrogen peroxide (H_2O_2) plays a key role in the anticancer activity of plasma-activated solutions [12–15]. Hence, the H_2O_2 contribution to the activity of PAM and PA-RL solutions was assessed. The scope was to evaluate which liquid, once exposed to CAP, could be the best option for cancer therapy and

if its activity could be more effective than hydrogen peroxide solution. Concerning the H_2O_2 concentration in undiluted PAM and PA-RL reported in Figure 2.3-3, two PALs-synthetic solutions namely RPMI+H_2O_2 and RL+H_2O_2 were prepared and diluted 2-, 4-, 8- and 16-fold. EOC cells were exposed to them, and the viability was monitored as stated for PAM and PA-RL treatment (Figure 2.3-6).

The analysis showed that H_2O_2 content can reduce SKOV-3 viability in all cases investigated, except at 1:16 dilution, while OV-90 cells seem not to be significantly affected by the presence of H_2O_2. More specifically, OV-90 suffered a higher and more significant susceptibility to PA-RL compared to PAM and RPMI+H_2O_2 solutions. On contrary, SKOV-3 cells demonstrated high sensitivity for each analysed condition, with no dose-dependent fashion and viability rate of decrease over 90%. Only PAM 1:16 and RPMI+H_2O_2 1:16 showed a high survival rate on SKOV-3. Overall, comparing the antiproliferative activity of PAM and PA-RL with their corresponding H_2O_2-containing solution, H_2O_2 content plays an important role in reducing SKOV-3 viability in all cases investigated, except at 1:16 dilution. On the other hand, OV-90 cells seem not to be significantly affected by the presence of H_2O_2.

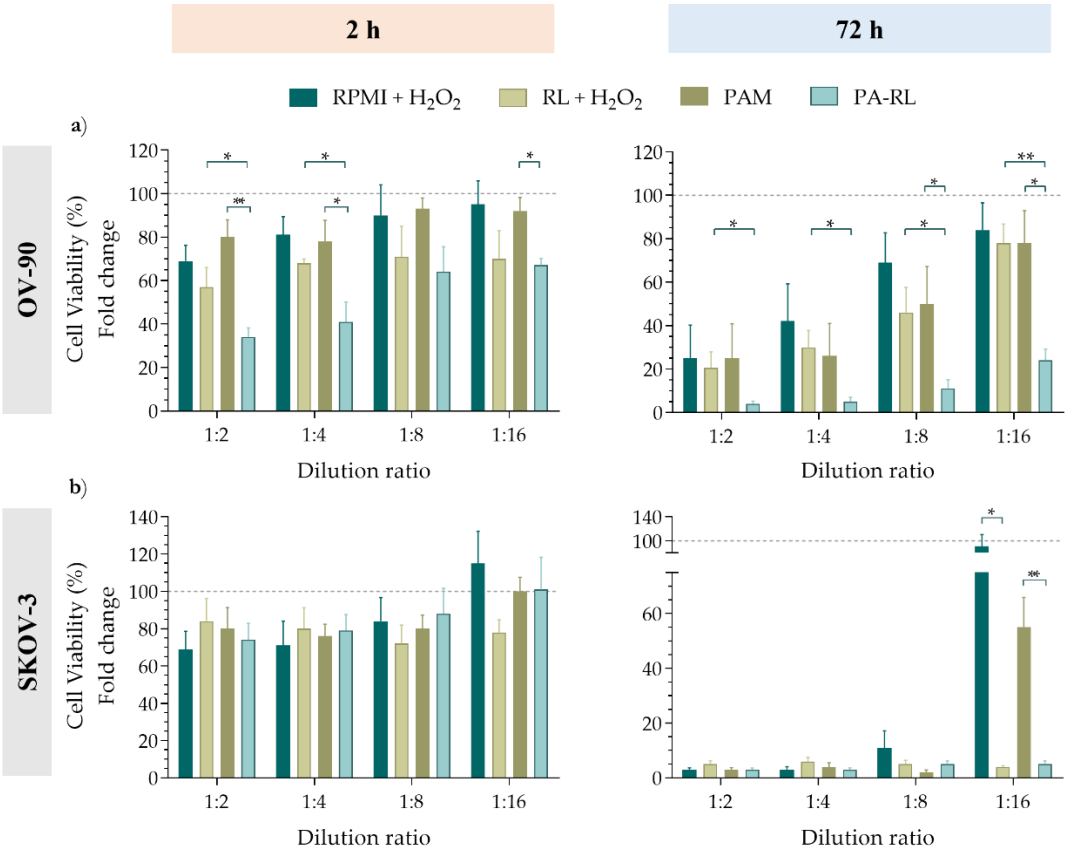

Figure 2.3-6 Hydrogen Peroxide contributes to the activity of plasma-activated solutions depending on the cell type. Viability of OV-90 (a) and SKOV-3 (b) treated with PAM, PA-RL and H_2O_2-synthetic solutions at 2 and 72 hours post-treatment. Data are mean ± SEM ($n \geq 3$) normalized considering untreated cells at t = 2 h as 100% and plotted as percentage relative to the corresponding untreated, for both time points. The statistical significance is specified with asterisks ($p \leq 0.05$, ** $p \leq 0.001$ as determined by a paired Student's t-test).*

These results were accomplished by microscopy images reported in Figure 2.3-7, which revealed morphological changes in EOC cells, in particular after PA-RL 1:16 treatments. During the entire experiment, the untreated cells were healthy, adherent to the substrate and showed the typical epithelial shape with clear contours. After 72 h H_2O_2-synthetic solutions treatment, only SKOV-3 appeared to be affected by the presence of that reactive species in particular when supplemented in RL. Indeed, the cells presented a scatter distribution and debris, whereas OV-90 morphology was the same as the corresponding untreated. Furthermore, PAM did not affect the SKOV-3 morphology, while PA-RL induced evident morphological changes as the cells appeared bigger than the control. After PAM and PA-RL treatment at 1:16 dilution,

OV-90 showed a considerable decrease in the amount of adherent cells. Also, OV-90 appeared smaller than untreated ones when exposed to PA-RL 1:16.

Altogether, these outcomes highlighted that PAM was able to inhibit EOC cell proliferation thanks to its content of H_2O_2, whereas PA-RL exerted its antiproliferative activity with more complex mechanisms not only related to H_2O_2 presence. Indeed, the contribution of this ROS in the induction of cytotoxicity seems to be related to the cell line sensitivity and capability to adapt to the oxidative burst [16,17]. Hence, these results showed a correlation between H_2O_2, PALs and cell type, and that PA-RL 1:16 could be a good option to compromise both EOC cells' growth.

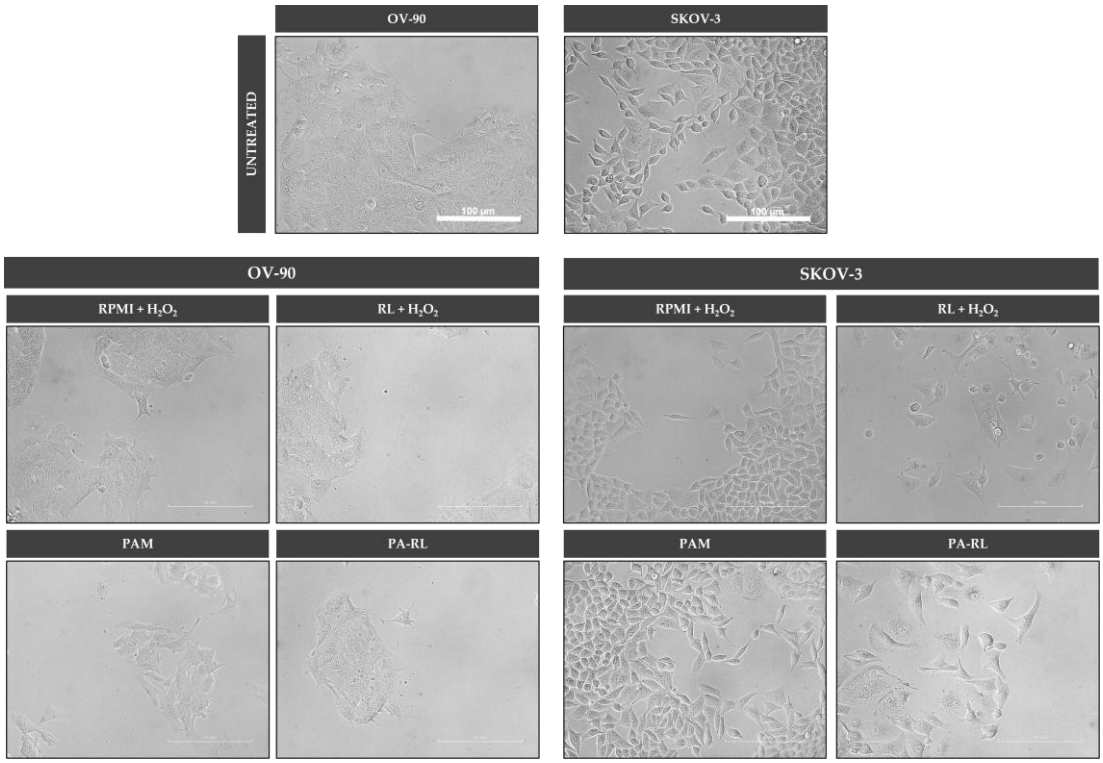

Figure 2.3-7 Representative images of morphological changes evoked in OV-90 and SKOV-3 cells after 72 h of treatment with PAM, PA-RL and H_2O_2-synthetic solutions at dilution 1:16. Scale bar =100 µm.

2.3.2.3 PA-RL inhibits EOC tumorigenic potential more than PAM

Cancer cells retain stemness, self-renewal and the potency to undergo epigenetic alterations leading to asymmetric cell division, generation of colonies of single-cell-derived clonal population and initiate tumorigenesis [18]. Given the interesting results related to the cytotoxic effects due to PAM and PA-RL dilutions observed in Figure

2.3-5, their anti-tumorigenic potential was also evaluated by performing a colony formation assay (Figure 2.3-8). In particular, this *in vitro* analysis was focused on the 1:8 and 1:16 dilutions, conditions to which SKOV-3 and OV-90 seem to respond in mildly different behaviour. When SKOV-3 and OV-90 have been exposed to PAM and PA-RL dilutions a significant reduction in the number of EOC colonies formed was observed with respect to the control. More specifically, PAM and PA-RL were the more effective on SKOV-3, while OV-90 showed percentages of residual colonies of 0.3% and 3.4% after PAM 1:8 and PAM 1:16 treatments, respectively. Thereby, PA-RL showed the ability to better blunt colony formation than PAM in both EOC cell lines.

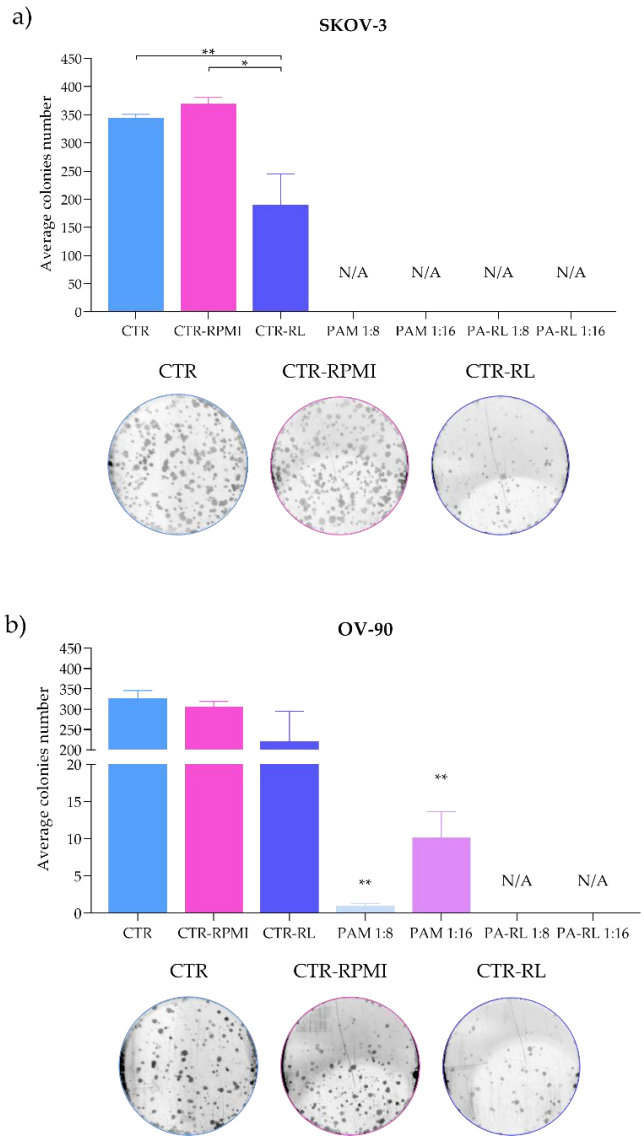

Figure 2.3-8 PA-RL inhibits EOC cell tumorigenic potential more than PAM. Capacity of SKOV-3 (a) and OV-90 (b) cells to form colonies analyzed in basal conditions (CTR), and after exposure to not

supplemented RPMI (CTR-RPMI), RL (CTR-RL) solutions and PAM and PA-RL dilutions. Data are presented as mean absolute value ± SEM (n ≥ 3). The statistical significance is specified with asterisks (p ≤ 0.05, ** p ≤ 0.001 as determined by unpaired Student's t-test).*

2.3.2.4 Effect of the liquid composition on PA-RL activity

The microenvironment of solid tumors is a complex and heterogeneous system which has a pivotal role in the growth and survival of tumor as well as the maintenance of drug resistance [19]. Cancer cells are characterized by the ability to control the cellular and non-cellular components' function, through complex signalling, for their benefit gain [20]. Therefore, cancer cells are characterized by metabolic plasticity which led them to adapt better to drastic changes in nutrient availability [21,22]. Most cancer research has been done in 2D cultures, which leads to understanding preliminary cues regarding cell biology, mechanisms of diseases or drug action [23]. In this context, it is important to consider that even the medium components could influence the biological efficiency of treatments [24,25]. In this regard, PA-RL was diluted in cell culture media producing a new PAL solution, namely RPMI+PA-RL. The focus of this analysis was to investigate whether PA-RL-induced cell injury may depend closely on its composition due to a strict interaction among the CAP bio-active species and the RL solution. For this purpose, EOC cells were stimulated with this latter PAL solution to evaluate if the components of cell culture media could affect the efficiency of PA-RL (Figure 2.3-9). EOC cells were exposed to different dilutions (1:2 to 1:16) of RPMI+PA-RL for two hours. After treatments, the antiproliferative activity of RPMI+PA-RL on EOC could be correlated to the inhibition capability of PAM. In particular, RPMI+PA-RL 1:16 showed the same biological efficiency induced by PAM 1:16 on EOC, while PA-RL was able to significantly reduce cancer cell proliferation capability in all cases investigated.

These data showed that there is a strict correlation between CAP activity and treated liquid composition. Indeed, in RPMI+PA-RL a strong influence of cell culture media on its cytotoxic response was observed and a significant decrease in cytotoxicity was recorded compared to PA-RL. This evidence correlates with data reported in the literature whereby the components of the culture medium influence the half-life of the reactive species produced by CAP and thus affect the activity of PALs [25,26].

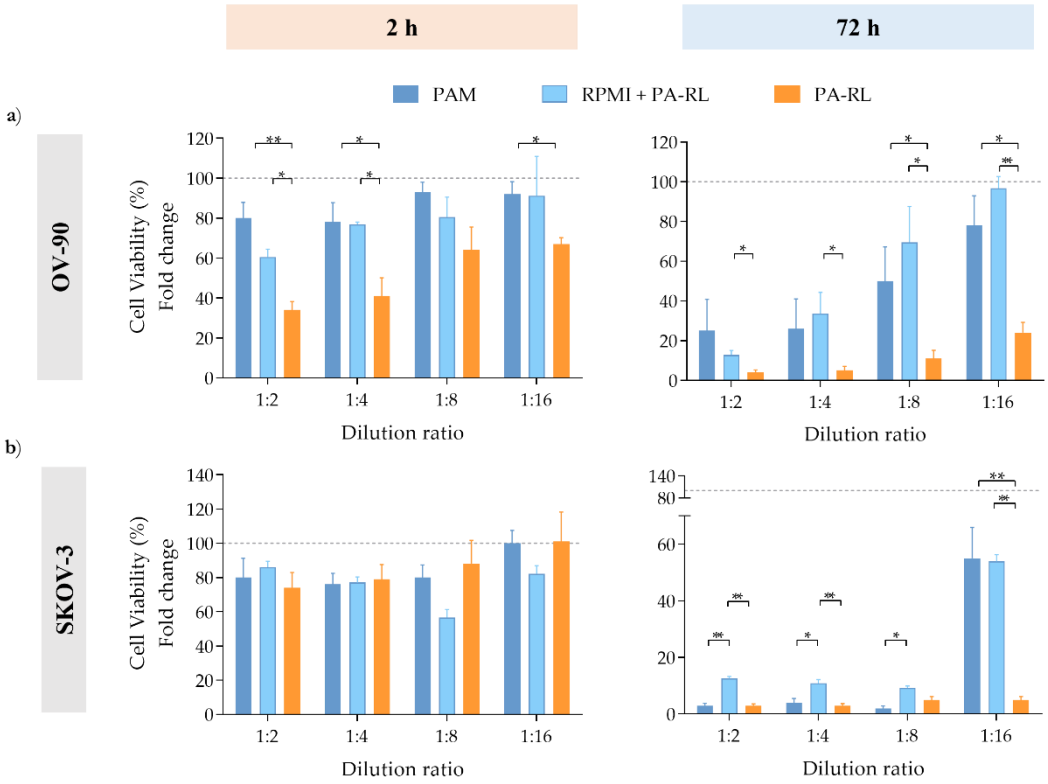

Figure 2.3-9 PA-RL inhibits EOC cell proliferation more than PAM and RPMI+PA- RL. Viability of OV-90 (a) and SKOV-3 (b) treated with PAM, PA-RL, and RPMI+PA-RL solutions at 2 and 72 hours post-treatment. Data are mean ± SEM ($n \geq 3$) normalized considering untreated cells at $t = 2$ h as 100% and plotted as percentage relative to the corresponding untreated, for both time points. The statistical significance is specified with asterisks ($p \leq 0.05$, ** $p \leq 0.001$ as determined by unpaired Student's t-test).*

In this context, the ability of PALs to trigger ROS production in EOC was observed (Figure 2.3-10). Total ROS levels measured in OV-90 and SKOV-3 treated with PALs 1:16 dilution, confirmed that the induction of ROS-mediated oxidative stress in cells due to RPMI+PA-RL was comparable to that of PAM. While PA-RL treatment induced a mild progressive increase in ROS levels with respect to that of PAM and RPMI+PA-RL. Overall, the antiproliferative effect induced by RPMI+PA-RL was in line with the one induced by PAM; while PA-RL, with its complexity and blend of bio-active species, showed better effectiveness and steadiness to inhibit both EOC cell growth. Furthermore, PA-RL 1:16 dilution has once again shown a high degree of mortality in both EOC models despite PAM and RPMI+PA-RL. Thus, it may be still considered a good candidate for more detailed studies of anti-tumorigenic activity.

These outcomes also suggested that the survival rate of reactive species produced by CAP is influenced by the liquid substrate exposed to plasma treatment; thus, influencing the PALs efficiency and the cell response.

Because the RPMI+PA-RL activity showed an equivalent effect on EOC cells to the PAM one, the subsequent analysis will be focused only on PAM and PA-RL.

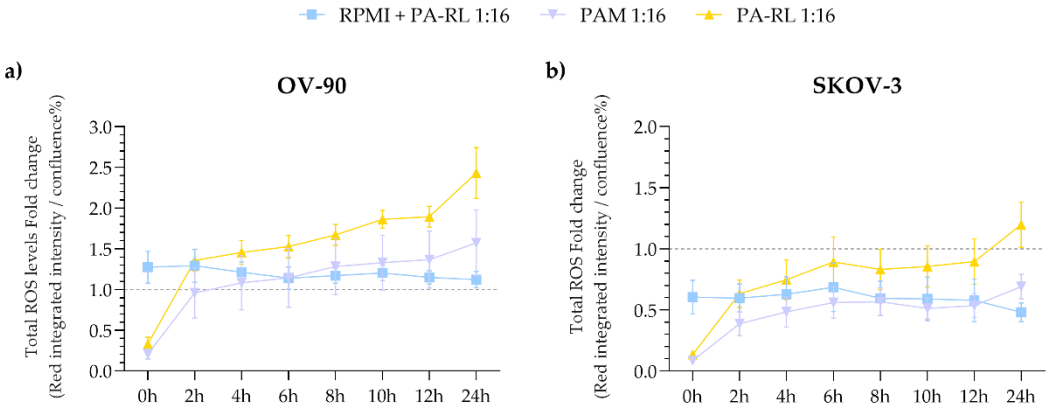

Figure 2.3-10 Total ROS levels in OV-90 (a) and SKOV-3 (b) generated in response to RPMI+PA-RL, PAM and PA-RL 1:16 dilutions at the end of the treatments (t = 0 h) to 24 h post-treatment. Total ROS levels were plotted as fold change relative to the respective untreated sample and data are presented as mean ± SEM (n ≥ 3).

2.3.2.5 PA-RL activity could be dependent on cancer cell metabolism

EOC is one of the most heterogeneous human tumors, which is mainly classified by different histological subtypes [16,17,27]. Recent studies revealed the existence of EOC subgroups depending on preferential metabolic modulation [28]. Especially, EOC cells can be classified into high-OXPHOS subgroups and low-OXPHOS subgroups according to their major or minor ability to adapt to the oxidative burst, respectively [16,28]. In the era of personalized medicine, the development of new therapeutic approaches is nowadays focused on specific targets based on the mechanistic underlying causes of diseases. Therefore, the metabolic classification of EOC, which has now taken hold, would allow exploring the tumor response to therapy and thus contribute to the development of personalized medicine in EOC. Literature reported that OV-90 and SKOV-3 cancer cells exploited different metabolic profiles [16,28]. In particular, evidence showed that SKOV-3 is characterized by a low-OXPHOS metabolism, while OV-90 such as a middle-OXPHOS [16]. In order to assess whether

the antiproliferative efficiency of PAM and PA-RL could be strictly correlated to cancer cells metabolism, two EOC cell models, namely OVSAHO and OC314 as models belong to middle-OXPHOS and high-OXPHOS subgroups respectively were implemented in this study [16,17]. The viability assay on OVSAHO and OC314 was performed at the same condition fixed for OV-90 and SKOV-3. As shown in Figure 2.3-11, both PAM and PA-RL dilutions displayed high cytotoxic effects on OVSAHO and OC314. In particular, PALs' biological efficiency was evident in those models characterized by lower (SKOV-3, Figure 2.3-9) or higher (OC314) metabolic activity. Thus, the different metabolic profiles of cancer cells could be a cogent issue to understand the mechanisms responsible for the anti-tumorigenic activity of PALs, for which further functional experiments will be unequivocally required to understand the underlying mechanism.

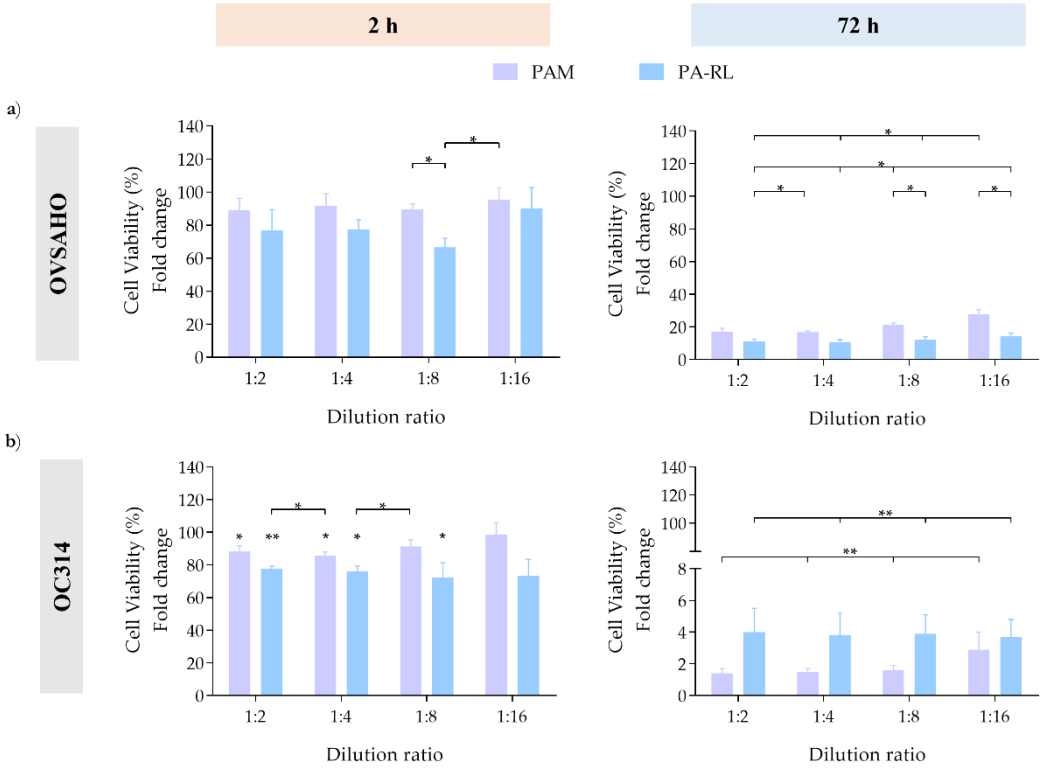

Figure 2.3-11 PAM and PA-RL efficiency are influenced by EOC metabolism classification. Viability of OVSAHO (a) and OC314 (b) cells treated with PAM and PA-RL dilutions at 2 and 72 hours post-treatment. Data are mean ± SEM (n ≥ 3) normalized considering untreated cells at t = 2 h as 100% and plotted as percentage relative to the corresponding untreated, for both time points. The statistical significance is specified with asterisks (p ≤ 0.05, ** p ≤ 0.001 as determined by unpaired Student's t-test)*

Then, because PA-RL 1:16 has proven to be a very effective candidate to inhibit EOC cell proliferation in all four models, its cytotoxic kinetic and simultaneously associated morphological changes were monitored over time on EOC. The analyses showed a rapid induction of the cytotoxic response in each EOC line after 2 hours of treatment (t = 0 h in Figure 2.3-12), thus reaching its peak at 12 hours post-treatment correlated with a drastic morphological change that occurred because of membrane loss integrity. Indeed, the cellular response to cytotoxic exposure is controlled by complex biochemical pathways, which induce morphological changes and eventually loss of plasma membrane integrity and resulting in cell death [29,30]. Together, these results suggest that PA-RL treatment is able to exert its cytotoxic activity up to 12 hours post-treatment, confirming the hypothesis that it can be used as a promising approach for the treatment of ovarian cancer.

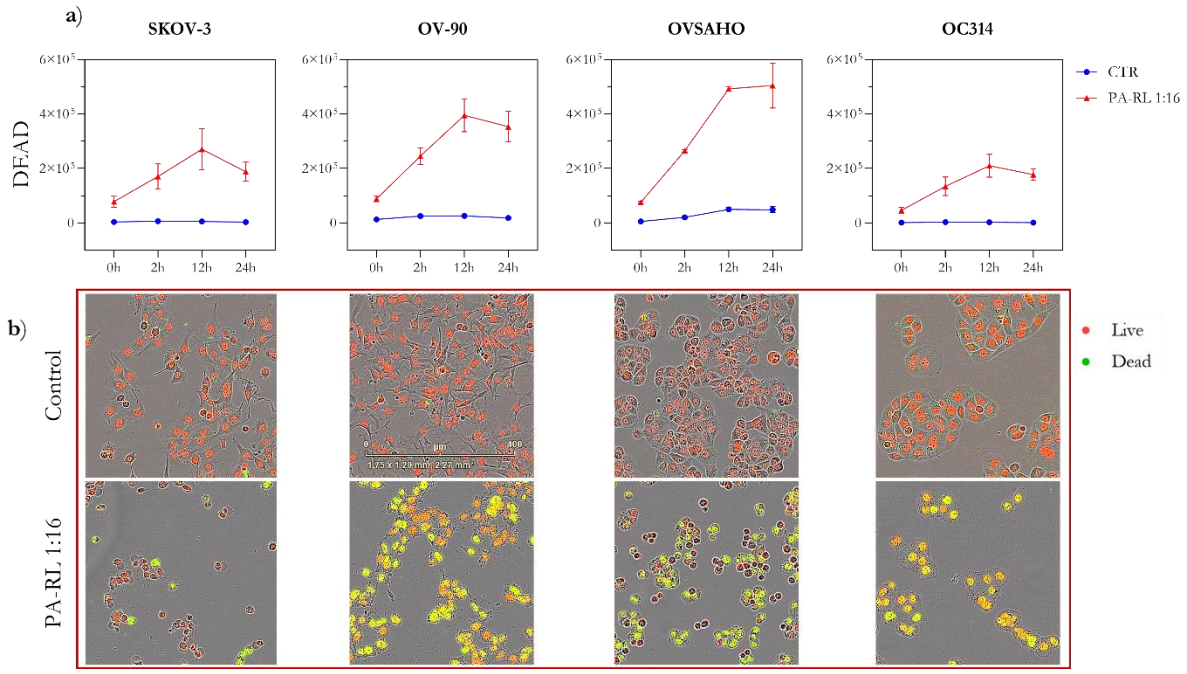

Figure 2.3-12 PA-RL cytotoxic response in EOC. Time-course for the effects of PA-RL 1:16 on EOC cell death up to 24 h post-treatment (a) Dead fluorescence signal was determined by analyzing green integrated intensity / Confluence%. Data are mean ± SEM (n ≥ 3). Phase-contrast and fluorescent images of EOC at 12 h post-treatment showing morphological changes in response to PA-RL 1:16 (b). Scale bar =400 µm.

2.3.2.6 Sodium pyruvate attenuates PALs cytotoxicity

As previously discussed, the different PA-RL activity, compared with PAM, is not due exclusively to the amount of H_2O_2. The cytotoxicity of these liquids depends closely on their overall composition, i.e., the organic elements therein contained, and their specific cancer metabolic profiles. Pyruvate is a metabolite of glucose and a key molecule in cellular metabolism representing a pivotal point between relevant metabolic pathways, which concerns carbohydrates, fatty acids and amino acids [31]. Pyruvate is also added as a supplementary source of energy to most cell culture media. Furthermore, it is known for its role as an efficient scavenger of hydrogen peroxide, and several studies reported its protective effect on CAP-induced oxidative burst [25,26,32]. In this context, EOC lines were cultured in RPMI medium supplemented with 1 mM of sodium pyruvate (Pyr) and then exposed to PAM diluted 1:16 with and without 1 mM Pyr (Figure 2.3-13a). PAM caused an overall reduction in EOC growth, up to 72 h post-treatment. However, the presence of pyruvate in RPMI during CAP treatment resulted in a strikingly different effect of PAM on EOC viability, significantly reducing the PAM cytotoxic activity. These data suggested that pyruvate influenced PAM activity by acting as a possible protective agent against the exogenous oxidative stress it caused. Indeed, when pyruvate is also present in the substrate exposed to CAP treatment, it has been observed that plasma-generated H_2O_2 reacts immediately with this component leading to its degradation and reducing the PAM cytotoxicity [25,26]. In the case of PA-RL treatment, EOC cells were cultured in presence or absence of 1 mM Pyr and then exposed to PA-RL diluted 1:16 in RL without 1 mM Pyr (Figure 2.3-13b). The analysis showed a coherent PA-RL antiproliferative effect of both treated EOC cultured conditions, thus because probably the exogenous amount of pyruvate in the solution can acts as a bioenergetic fuel readily oxidizable in case of energy crisis due, as in this case, to PA-RL treatment [33]. Together, these results supported the fact that medium components influence the biological efficiency of plasma-treated liquids, as also reported in section 2.3.2.4. This corroborates the fact that PAM is not a useful clinical approach, unlike PA-RL which instead has been shown to retain a high inhibition efficiency independent of the growth conditions of the cells themselves.

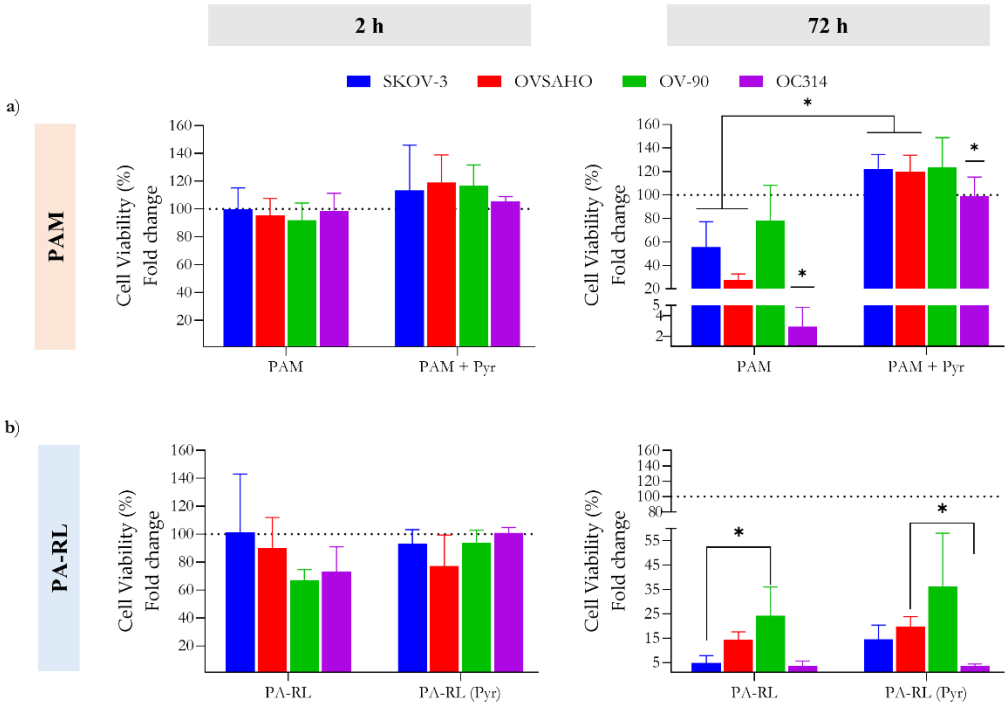

Figure 2.3-13 Sodium pyruvate attenuates PALs cytotoxicity on EOC cell proliferation. Effects of PAM (a) and PA-RL (b) at 1:16 dilution ± 1 mM Pyr on EOC cell models at 2- and 72 hours post-treatment. Data are mean ± SEM ($n \geq 3$) normalized considering untreated cells at $t = 2$ h as 100% and plotted as percentage relative to the corresponding untreated, for both time points. The statistical significance is specified with asterisks ($p \leq 0.05$, as determined by unpaired Student's t-test).*

Because PA-RL 1:16 seems to retain a similarly cytotoxic effect both in the presence and absence of Pyr, the intracellular ROS levels in all EOC models were measured at the end of treatment (Figure 2.3-14a). In particular, PA-RL triggered ROS production in SKOV-3 and OC314, whereas the ROS levels in OV-90 and OVSAHO seem not to be perturbated by treatment. Furthermore, the amount of intracellular ROS recorded did not change over time, suggesting that this reactive specie may have rapidly reached a plateau. Detoxification of reactive oxygen species is paramount to the survival of cancer cells, which can withstand a high degree of oxidative stress due to their higher levels of antioxidant proteins [1,34]. Hence, to ascertain if indeed EOC cells expressed higher levels of the main molecular players in ROS detoxification, the expression levels of Superoxide Dismutase (MnSOD) and Catalase (CAT) enzymes were measured in basal conditions (Figure 2.3-14b). SKOV-3 was characterized by a good expression of both antioxidant enzymes, while OC314 showed a higher expression profile only in MnSOD. Although SKOV-3 was

more enriched in this defence system, the expression levels of MnSOD and CAT were not enough to detoxify PARL-induced ROS, probably due to the SKOV-3 metabolism profile (low-OXPHOS) which did not make it particularly prone to this type of response. However, even a more energetic metabolism as well as in OC314 (high-OXPHOS) was not sufficient to counteract the further exogenous burst induced by PA-RL, leading to its increased sensitivity to treatment. OVSAHO and OV-90 did not appear to undergo fluctuations in ROS levels probably because of their mild metabolic profile which made them more responsive to oxidative changes. Overall, these data showed that PA-RL treatment has a greater cytotoxic effect on EOC models, in particular on those EOC characterized by a high or low metabolic rate e.g., OC314 (high-OXPHOS) and SKOV-3 (low-OXPHOS).

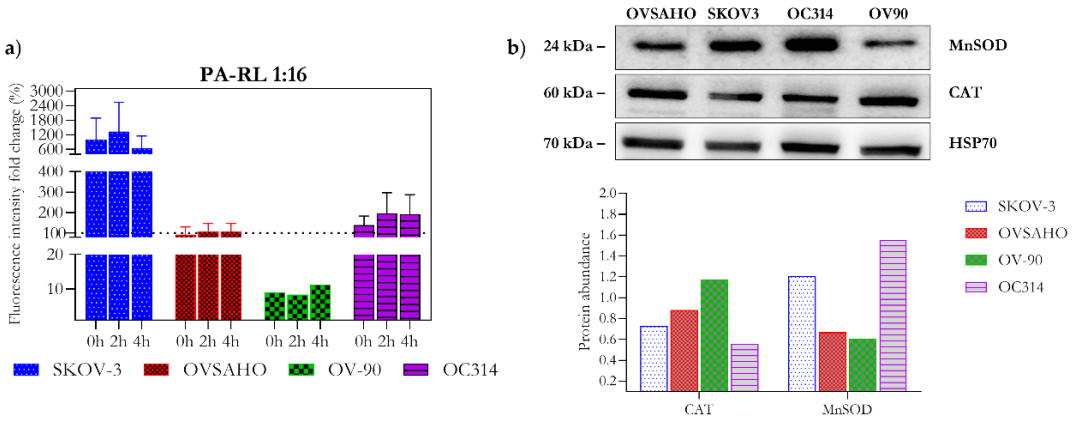

Figure 2.3-14 PA-RL-induced oxidative stress in EOC. Intracellular ROS measurement (a) after PA-RL 1:16 treatment by using dichlorofluorescein diacetate 2 µM. Data are mean ± SD relativized to negative control. Basal Antioxidant enzymes levels (b) in untreated EOC cells cultured in complete RPMI + 1mM Pyr.

2.3.3 PA-RL display a selective cytotoxic effect on EOC cells

2.3.3.1 PA-RL displays a cytotoxic effect on EOC cell lines, which does not depend exclusively on hydrogen peroxide or nitrites

In the perspective to propose PA-RL in clinical applications, it is important to properly assess the influence of the main elements therein contained. In section 2.3.2.2 it was discussed that PA-RL activity did not depend exclusively on the presence of H_2O_2 in the solution; however, PA-RL composition also provides to other two main components such as nitrites concentration or pH fluctuations. With the purpose of analysing their role in PA-RL mechanism, the cytotoxic effect of PA-RL 1:16 was compared to that one induced by solutions containing the same amount of NO_2^- and at the same pH as measured in the corresponding PA-RL dilution. In these conditions, OV-90 was confirmed to undergo a more immediate loss of viability of about 20 – 30 % after 2 hours of exposure in all cases investigated, while SKOV-3 appeared to only mild suffering loss of viability during the same time frame (Figure 2.3-15). After 72 hours, nitrites did not affect cell viability for both cell lines, while pH and H_2O_2 only mildly affected cell growth. Overall, only PA-RL was able to significantly reduce the viability of both EOC models, confirming that the only presence of H_2O_2, NO_2^- or pH shift is not sufficient to exert a significant cytotoxic effect on EOC, but that this may be due to different RONS therein contained which in synergy cause the induction of cytotoxicity. These results demonstrated that the complexity of the PA-RL may not be replaced by synthetic solutions.

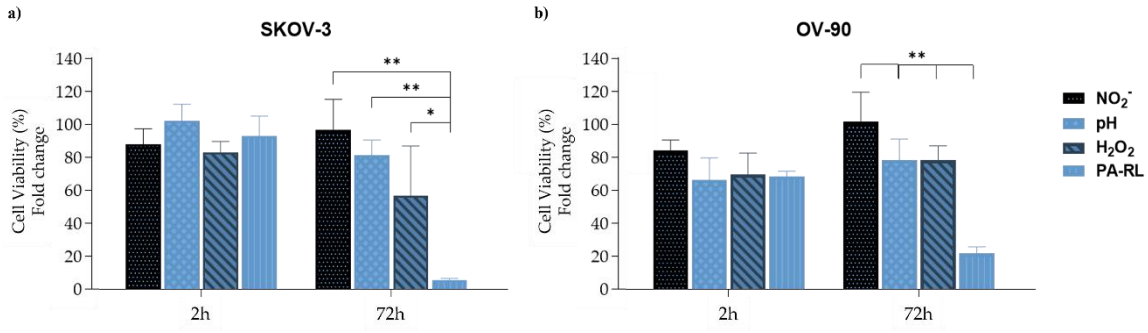

Figure 2.3-15 Viability of SKOV-3 (a) and OV-90 (b) cell lines treated with PA-RL 1:16 and corresponding H_2O_2-, NO_2^-- and pH-adjusted synthetic solutions diluted in RL. Data are presented as mean ± SEM ($n \geq 3$) normalized considering untreated cells at t = 2 h as 100% and plotted as

percentage relative to the corresponding untreated, for both time points. The statistical significance is specified with asterisks ($p \leq 0.05$, as determined by unpaired Student's t-test).*

2.3.3.2 PA-RL is selective for EOC cells with respect to non-cancer epithelial ovarian cell lines

As one of the main requisites for clinical application is that PA-RL cytotoxic action ought to be specific for cancer cells. Hence, the PA-RL efficiency was explored with the aim to observe such a specific effect. The PA-RL dilutions were tested on EOC cell lines and two different non-cancer cell models. The non-cancer epithelial cell model HOSE was used in this study as the healthy counterpart for both EOC, while two different humans immortalized fibroblast lines were used to evaluate the response of the mesenchymal tissue component to PA-RL (Figure 2.3-16). PA-RL dilutions induced a significantly different cytotoxic effect in non-cancer and cancer cells, in terms of viability rate. More specifically, both HOSE and fibroblast lines were similarly affected by the treatments in a dose-independent trend, with a decrease of viability in a range between 60 – 70 % at 72 hours post-treatment, and the highest survival at the 1:16 dilution. Thus, the PA-RL 1:16 dilution showed significant selectivity for cancer cells compared to the non-cancer population, which may represent the best compromise to treat cancer cells while sparing the surrounding healthy tissues. Indeed, a significant difference in cell survival rate in cancer versus non-cancer cells was evident as early as 24 hours post-treatment (Figure 2.3-16b).

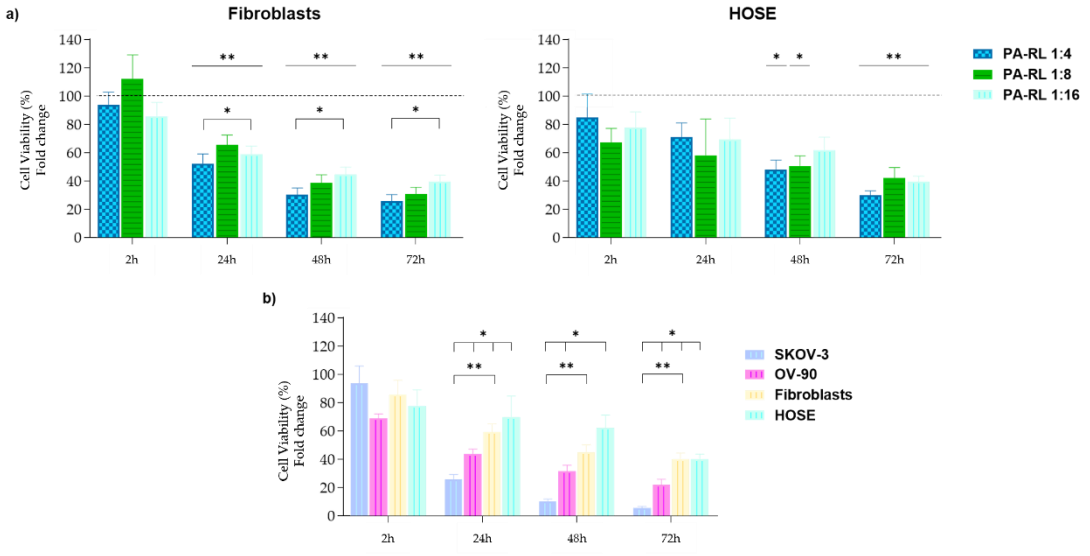

Figure 2.3-16 PA-RL displays a selective cytotoxic effect on EOC cell lines. Viability of non-cancer cells (a), namely human fibroblasts (n = 9) and HOSE (n = 4) treated with PA-RL dilutions (1:4, 1:8 and 1:16). PA-RL 1:16 efficacy on non-cancer and EOC cell viability (b). Data are presented as mean ± SEM normalized considering untreated cells at t = 2 h as 100% and plotted as percentage relative to the corresponding untreated, for both time points at 2-, 24-, 48- and 72-hours post-treatment. Statistical significance is specified with asterisks ($p \leq 0.05$, ** $p \leq 0.001$ as determined by a paired Student's t-test).*

2.3.3.3 Differentially activated antioxidant defenses mechanisms may underlie cancer cells-specific PA-RL toxicity

As claimed in section 2.3.2.6, paramount to the survival of cancer cells and to sustaining the fast proliferation is their higher expression levels of antioxidant proteins as a defense mechanism against the high degree of oxidative stress.

Thus, the basal levels of one of the most active cytosolic antioxidant enzymes involved in radical species detoxyfication, namely superoxide dismutase-1 (SOD-1) were measured both in EOC cell lines and in human fibroblasts (Figure 2.3-17). As expected, EOC cells showed higher levels of SOD-1 with respect to fibroblast lines. However, when all four cell lines were treated with PA-RL 1:16, the levels of this enzyme remained unchanged in cancer cells, whereas fibroblasts were able to enhance SOD-1 expression which could have determined the achievement of protective activity against PA-RL-induced oxidative stress. These data suggested that the antioxidant response in cancer cells may have likely reached a plateau over which

enzyme levels may not be increased, which could be one explanation for the higher efficiency of PA-RL on EOC with respect to their healthy counterpart.

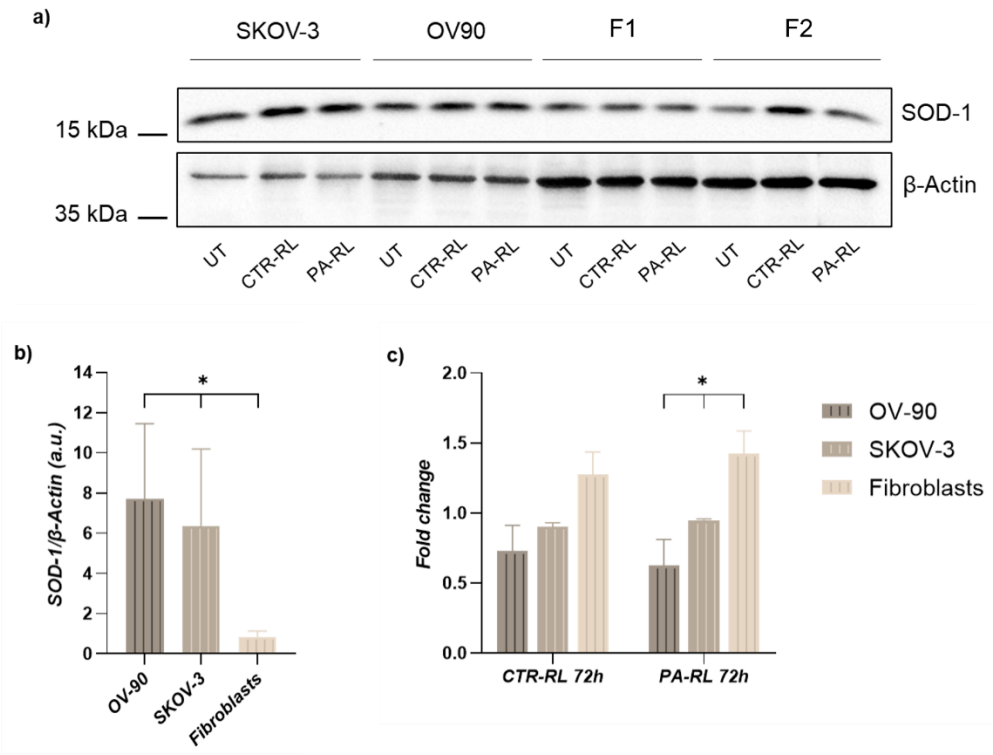

*Figure 2.3-17 PA-RL solution induces an increase in SOD-1 expression in fibroblasts but not in EOC cell lines. (a) Western blot analysis Superoxide dismutase-1 (SOD-1) levels in EOC cell lines and fibroblasts (F1 and F2) at 72 hours after treatment with PA-RL 1:16 (UT, untreated cells). (b) SOD-1 levels in untreated fibroblasts and cancer cell lines. Histograms show densitometric values of the SOD-1 protein normalized to the β-actin used as a loading control. (c) Relative densities of SOD-1 and β-actin were measured using densitometric analysis. SOD-1 levels of CTR-RT and PA-RL 1:16 after 72 h of treatment were normalized to β-actin and plotted as fold change relative to UT sample. All data are presented as mean ± SEM (n = 3). Statistical significance is specified with asterisks * $p \leq 0.05$*

2.4 Conclusions

The multiwire plasma source in Figure 2.2-1 has a robust design, an innovative feature able to work without the use of a technical gas and it can be easily scaled to produce higher plasma-activated liquid volumes than 20 mL. Furthermore, the source architecture leads to the formation of a high H_2O_2 concentration into liquids, which contributes to both PAM and PA-RL cytotoxic effects on cancer cells. However, *in vitro* results showed that PAM antiproliferative effect is mainly due to the presence

of H_2O_2, while PA-RL activity does not depend exclusively on this reactive species or nitrites. These outcomes are encouraging, in particular from the perspective to propose PALs in clinical applications. Indeed, PA-RL showed a selective cytotoxic effect on cancer cells, while non-cancer cells and fibroblasts cell viability 72 hours after the treatment retains a high survival at the 1:16 dilution. In summary, although additional investigations have to be performed to evaluate the exact mechanism by which PA-RL exerts its selective cytotoxicity in the frame to develop a new selective approach for ovarian cancer therapy, the clinical use of plasma-activated liquid could be promising as a new therapeutic strategy to be used in combination with other standard therapies, especially in the field of personalized medicine.

2.5 References

1. Bisag, A. *et al.* Plasma-activated Ringer's Lactate Solution Displays a Selective Cytotoxic Effect on Ovarian Cancer Cells. *Cancers (Basel).* **12**, 476 (2020).
2. Brett M., R., Jennifer B., P. & Thomas A., S. Epidemiology of ovarian cancer: a review. *Cancer Biol. Med.* **14**, 9–32 (2017).
3. Prat, J. FIGO's staging classification for cancer of the ovary, fallopian tube, and peritoneum: abridged republication. *J. Gynecol. Oncol.* **26**, 87 (2015).
4. Lheureux, S., Gourley, C., Vergote, I. & Oza, A. M. Epithelial ovarian cancer. *Lancet* **393**, 1240–1253 (2019).
5. Rynne-Vidal, A. *et al.* Mesothelial-to-mesenchymal transition as a possible therapeutic target in peritoneal metastasis of ovarian cancer. *J. Pathol.* **242**, 140–151 (2017).
6. Sant, M. *et al.* Survival for haematological malignancies in Europe between 1997 and 2008 by region and age: results of EUROCARE-5, a population-based study. *Lancet Oncol.* **15**, 931–942 (2014).
7. Jewell, A., Mcmahon, M. & Khabele, D. Heated Intraperitoneal Chemotherapy in the. (2018) doi:10.3390/cancers10090296.
8. Vander Heiden, M. G. & DeBerardinis, R. J. Understanding the Intersections between Metabolism and Cancer Biology. *Cell* **168**, 657–669 (2017).
9. Locke, B. R., Lukes, P. & Brisset, J. L. Elementary chemical and physical phenomena in electrical discharge plasma in gas-liquid environments and in liquids. in *Plasma Chemistry and Catalysis in Gases and Liquids* (eds. Parvulescu, V. I., Magureanu, M. & Lukes, P.) 185–242 (Wiley-VCH Verlag GmbH & Co. KGaA, 2012).
10. Graves, D. B. The emerging role of reactive oxygen and nitrogen species in redox biology and some implications for plasma applications to medicine and biology. *J. Phys. D. Appl. Phys.* **45**, (2012).
11. Graves, D. B. Reactive species from cold atmospheric plasma: Implications for cancer therapy. *Plasma Process. Polym.* **11**, 1120–1127 (2014).
12. Adachi, T., Matsuda, Y., Ishii, R., Kamiya, T. & Hara, H. Ability of plasma-activated acetated Ringer's solution to induce A549 cell injury is enhanced by

a pre-treatment with histone deacetylase inhibitors. *J. Clin. Biochem. Nutr.* 1–8 (2020) doi:10.3164/jcbn.19-104.

13. Matsuzaki, T., Kano, A., Kamiya, T., Hara, H. & Adachi, T. Enhanced ability of plasma-activated lactated Ringer's solution to induce A549 cell injury. *Arch. Biochem. Biophys.* **656**, 19–30 (2018).
14. Laroussi, M. Cold Plasma in Medicine and Healthcare: The New Frontier in Low Temperature Plasma Applications. *Front. Phys.* **8**, 1–7 (2020).
15. Vandamme, M. *et al.* ROS implication in a new antitumor strategy based on non-thermal plasma. *Int. J. Cancer* **130**, 2185–2194 (2012).
16. Gentric, G. *et al.* PML-Regulated Mitochondrial Metabolism Enhances Chemosensitivity in Human Ovarian Cancers. *Cell Metab.* **29**, 156-173.e10 (2019).
17. De Luise, M. *et al.* Inducing respiratory complex I impairment elicits an increase in PGC1α in ovarian cancer. *Sci. Rep.* **12**, 8020 (2022).
18. Rajendran, V. & Jain, M. V. In Vitro Tumorigenic Assay: Colony Forming Assay for Cancer Stem Cells. in 89–95 (2018). doi:10.1007/978-1-4939-7401-6_8.
19. Lunt, S. J., Chaudary, N. & Hill, R. P. The tumor microenvironment and metastatic disease. *Clin. Exp. Metastasis* **26**, 19–34 (2009).
20. Baghban, R. *et al.* Tumor microenvironment complexity and therapeutic implications at a glance. *Cell Commun. Signal.* **18**, 59 (2020).
21. Dang, C. V. Links between metabolism and cancer. *Genes Dev.* **26**, 877–890 (2012).
22. Palm, W. Metabolic plasticity allows cancer cells to thrive under nutrient starvation. *Proc. Natl. Acad. Sci.* **118**, (2021).
23. Kapałczyńska, M. *et al.* 2D and 3D cell cultures – a comparison of different types of cancer cell cultures. *Arch. Med. Sci.* (2016) doi:10.5114/aoms.2016.63743.
24. Halliwell, B. Cell culture, oxidative stress, and antioxidants: Avoiding pitfalls. *Biomed. J.* (2014) doi:10.4103/2319-4170.128725.
25. Bergemann, C., Rebl, H., Otto, A., Matschke, S. & Nebe, B. Pyruvate as a cell-protective agent during cold atmospheric plasma treatment in vitro:

Impact on basic research for selective killing of tumor cells. *Plasma Process. Polym.* **16**, (2019).

26. Tornin, J. *et al.* Pyruvate Plays a Main Role in the Antitumoral Selectivity of Cold Atmospheric Plasma in Osteosarcoma. *Sci. Rep.* **9**, 10681 (2019).
27. Nantasupha, C., Thonusin, C., Charoenkwan, K., Chattipakorn, S. & Chattipakorn, N. Metabolic reprogramming in epithelial ovarian cancer. *Am. J. Transl. Res.* **13**, 9950–9973 (2021).
28. Gentric, G., Mieulet, V. & Mechta-Grigoriou, F. Heterogeneity in Cancer Metabolism: New Concepts in an Old Field. *Antioxid. Redox Signal.* **26**, 462–485 (2017).
29. Kepp, O., Galluzzi, L., Lipinski, M., Yuan, J. & Kroemer, G. Cell death assays for drug discovery. *Nat. Rev. Drug Discov.* **10**, 221–237 (2011).
30. Zhang, Y., Chen, X., Gueydan, C. & Han, J. Plasma membrane changes during programmed cell deaths. *Cell Res.* **28**, 9–21 (2018).
31. Gray, L. R., Tompkins, S. C. & Taylor, E. B. Regulation of pyruvate metabolism and human disease. *Cell. Mol. Life Sci.* **71**, 2577–2604 (2014).
32. Guarino, V. A., Oldham, W. M., Loscalzo, J. & Zhang, Y. Y. Reaction rate of pyruvate and hydrogen peroxide: assessing antioxidant capacity of pyruvate under biological conditions. *Sci. Rep.* **9**, 1–9 (2019).
33. Ichai, C., Orban, J.-C. & Fontaine, E. Sodium lactate for fluid resuscitation: the preferred solution for the coming decades? *Crit. Care* **18**, 163 (2014).
34. DeBerardinis, R. J. & Chandel, N. S. Fundamentals of cancer metabolism. *Sci. Adv.* **2**, e1600200 (2016).

CHAPTER 3

The oxidation of lactate to pyruvate influences the cytotoxic activity of plasma-activated liquids on Epithelial Ovarian Cancer cells

3.1 Introduction

The following discussion derives from a research joint project held in the frame of the COST Action CA20114 - Therapeutical applications of Cold Plasmas (PlasTHER), a consortium of European experts in the field of plasma medicine. The aim of this Action is to improve the knowledge of the mechanisms involved in the therapeutic action of plasmas and plasma-conditioned liquids by establishing a synergistic network and interdisciplinary exchange of knowledge and know-how between the researchers, the medical community, industry or patient associations. In order to achieve this aim, the COST Action also provided grants for short-term scientific missions (STSMs) in institutions or laboratories in foreign COST Countries. In particular, the following research was carried out in Prof. Cristina Canal's research group, which is part of the Biomaterials, Biomechanics & Tissue Engineering – BBT at the Universitat Politècnica de Catalunya (Barcelona), and it was aimed at broadening my knowledge on plasma-biological interaction mechanisms, exploitable in the field of anticancer therapy and thus clinical application, spanning from engineering to medicine.

The work carried out has involved several people to whom all my gratitude and affection goes, Dr Francesco Tampieri, Dr Miguel Mateu-Sanz and especially Professor Cristina Canal. Also, I would like to thank the entire BBT research group, especially Dr Milica Živanić, Dr Albert Espona, Dr Daniel Moreno, Dr Marc Iglesias and Dr Vincenzo Migliaccio, for their support and friendship.

Cold atmospheric plasma, with its blend of bio-active agents, enables the production of reactive oxygen and nitrogen species into liquids, making it a promising tool for cancer therapy. Because of the focus on the medical field, exploring the chemical features of plasma-activated clinically suitable liquids is a cogent issue to propose their use in the clinical field.

Recently, the exposure of physiological Ringer's lactate solution (RL) to CAP resulted in the production of plasma-activated Ringer's lactate solution (PARL), which showed a selective cytotoxic effect on ovarian cancer cells [1]. Along that, the cytotoxic effect ascribed to another clinically suitable solution, i.e. Ringer's saline

(R), on osteosarcoma was established [2], which also showed a synergistic effect with doxorubicin and compromised metastatic potential [3]. RL and R solutions are isotonic fluids whose simple composition has been used in hospitals and healthcare settings. They share the same basic composition (NaCl, KCl, $CaCl_2$), although RL contains also lactate, in the form of sodium salt [4]. Lactate is a by-product of glucose metabolism during cell anaerobic phase, a cell state which requires an increase in energy demand [5]. During their life cycle, cells go through aerobic and anaerobic phases, which cause the continuous pyruvate oxidation-reduction in lactate to maintain a balanced energy ratio [6]. When lactate is oxidated to pyruvate, it contributes to the maintenance of glycolytic flux and acts, in turn, as a buffer system [5,7,8]. Indeed, it was reported that organic elements as the medium components could influence the CAP final biological effect, especially pyruvate which has been reported to mitigate PAL efficiency given to its H_2O_2 scavenging activity [9,10].

In this research, ready to be published, the lactate-mediated biological efficiency of plasma-activated saline solutions in ovarian cancer was investigated for the first time. Thus, RL and R were exposed to kINPen plasma jet for several treatment times to produce PARL and PAR, respectively. RONS generated by plasma in R and RL were quantified by colorimetric methods and the direct effect of plasma on lactate was studied by chromatography coupled with diode array detector. Hence, PARL and PAR cytotoxicity was examined for the first time on EOC cell lines, pointing out the influence of lactate on PALs' biological effect. Lactate is also directly affected by CAP treatment, displaying a reduction of PARL cytotoxic potential depending on CAP-treated time compared to PAR.

3.2 Materials and Methods

3.2.1 Atmospheric pressure plasma jet

Plasma-activated liquids (PALs) were produced by exposing liquids to a commercial plasma jet (kINPen® IND, Neoplas tools GmbH, Greifswald, Germany, Figure 3.2-1) [11]. The plasma device consists of a hand-held unit that generates plasma under atmospheric conditions, driven by a DC power supply. It is composed of a high-voltage needle electrode embedded in a quartz capillary with a grounded outer electrode. Argon gas (Ar 5.0, Praxair, Spain) is used as a feed gas with a flow rate of

3 L/min. The plasma was operated at 10 mm distance from the nozzle to the surface of the liquid.

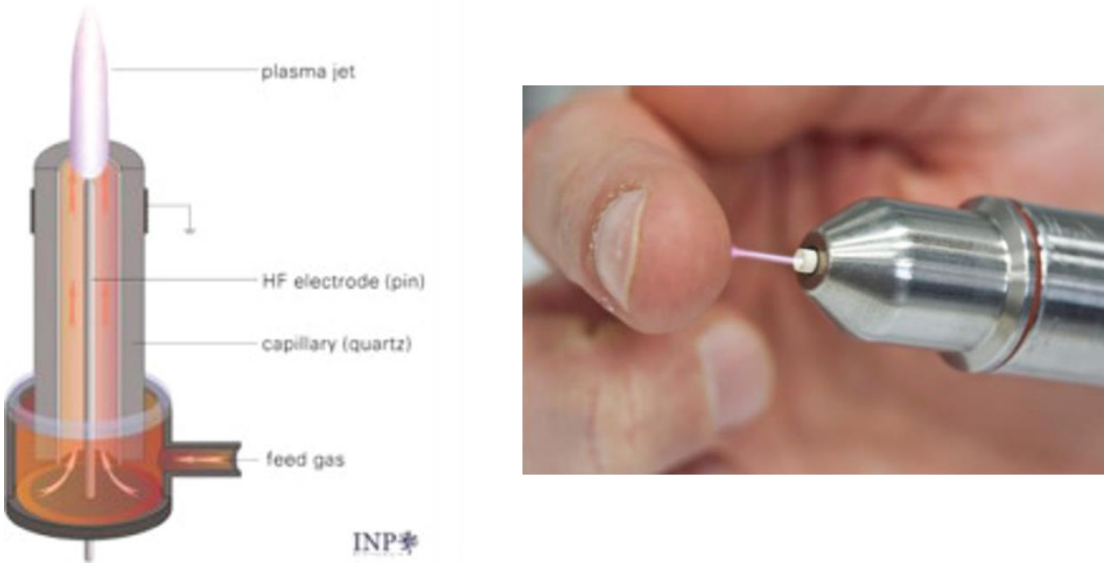

Figure 3.2-1 Picture of the kINPen® plasma jet [12]

3.2.2 Plasma-activated liquids production and characterization

To obtain the plasma-activated Ringer's (PAR) and plasma-activated Ringer's lactate (PARL) solutions, 1 mL of sterile Ringer's saline solution (R; 102.7 mM NaCl, 5.4 mM KCl and 1.8 mM $CaCl_2 \cdot 2H_2O$) or Ringer's lactate solution (RL; exactly same ionic composition of R added with lactate purchased by Fresenius Kabi, Italy) was placed in a 24-well plate and exposed to plasma jet for selected times, from 15 s to 300 s. Subsequently, 10% of heat-inactivated fetal bovine serum (FBS) was added to PAR and PARL to maintain a physiological pH range [2].

In order to isolate the effect of lactate during the plasma treatment, a solution of PAR to which lactate was added after the treatment (PAR+L) was prepared, as a comparison.

The quantification of H_2O_2 and NO_2^- generated during plasma treatment was performed using colorimetric chemical probes before addition of FBS. H_2O_2 detection was carried out using the titanium(IV) oxysulfate method [13]. In presence of hydrogen peroxide, Ti(IV) in sulfuric acid solution generates a yellow complex with absorption maximum at 410 nm. 50 µL of Ti(IV) oxysulfate solution to a 100 µL of PAR or PARL solution were added in a 96-well plate and the absorption spectra

were recorded between 340 and 600 nm. NO_2^- detection was carried out using Griess reagent (composed of 1 % sulphanilamide, 0.1 % N-(1-naphthyl) ethylene diamine, 1.2 % phosphoric acid in ultrapure water). 50 µL of Griess reagent were mixed to 50 µL of plasma-activated solution in a 96-well plate and the absorption spectra were recorded between 400 and 700 nm [14]. Calibration lines were built using standard solutions of hydrogen peroxide and sodium nitrite prepared in the same media used during plasma treatment. The stability of H_2O_2 and NO_2^- after addition of FBS was verified.

Before and after each plasma treatment, the pH of the solutions was evaluated by using MM 41 Crison multimeter. The production of hydroxyl radicals during the plasma treatment was studied using coumarin (COU). COU reacts with free OH radicals to generate the fluorescent product 7-hydroxycoumarin (7-COU-OH). 1 mM solutions of COU in Ringer's and Ringer's lactate were treated with plasma using the conditions described above. After treatment, 400 µL were transferred in a 48-well plate and fluorescence was measured ($\lambda_{ex/em}$ = 360/460 nm) using a Synergy HTX Hybrid Multi Mode Microplate Reader (BioTek Instruments, Inc., USA). All measurements were done at least in triplicate.

3.2.3 High performance liquid chromatography analysis of PARL

High Performance Liquid Chromatography (HPLC) coupled with Diode Array Detector (DAD) was used to detect and quantify the residual lactate in the plasma-activated samples and to verify the formation of oxidation products. The samples were diluted in Ringer's saline when necessary.

HPLC/DAD measurements were done using a Shimadzu Prominence XR instrument with LC-20AD XR pump, DGU-20A5R degassing unit, SIL-20AC HT autosampler and SPD-M20A UV/VIS photodiode array detector equipped with an Agilent Zorbax Sb-AQ analytical column (3.5 um 4.6 x 150 mm). Eluents were phosphate buffer 20 mM pH 1.5 (A) and acetonitrile (B). Elution was isocratic (A:B 99:1), the flow rate was 1 mL min-1, injection volume 20 µL, temperature of the column and detector 35 °C and detection 190-400 nm. Under these conditions, the retention time (r.t.) for pyridine was 3.03 min.

The calibration lines for lactate and pyruvate were obtained by analysing, under the same conditions, standard solutions in Ringer's saline.

The areas of the peaks in the chromatograms were obtained, using the OriginPro 2020 software (version 9.7.0.188, OriginLab Corporation) after proper subtraction of the baseline and deconvolution, when necessary.

3.2.4 Cell lines and culture conditions

Human EOC cell lines SKOV-3, OV-90, OVSAHO and OC314 (ATCC, Manassas, VA, USA) were grown in Roswell Park Memorial Institute 1640 medium (RPMI 1640; GibcoTM, Carlsbad, CA, USA) supplemented with 10 % FBS, 2 mM L-glutamine, 100 U/mL penicillin, 100 µg/mL streptomycin (GibcoTM). The cells were maintained in an incubator with a humidified atmosphere of 5 % CO_2 at 37 °C.

3.2.5 Cell treatment and viability assay

EOC cells were seeded in 96-well plates in complete medium at a density of 3.5 x 10^3 cells/well, except OVSAHO cells which were cultured at 6 x 10^3 cells/well. After 24 hours, cells were treated with 100 µL of freshly produced PARL, PAR, or their corresponding untreated controls for 2 hours. Afterwards, cells were washed in phosphate buffered saline (PBS) solution and cultured in complete medium at 37 °C and 5 % CO_2 (Figure 3.2-2). Cell viability was assayed using WST-1 Assay (Roche, Mannheim, Germany) at 2, 24 and 72 hours after treatment. Treated cell viability was assessed using 18 µL/ml Cell Proliferation Reagent WST-1 in supplemented RPMI (final volume per well 250 µL) and incubated for 1 hour at 37 °C. Afterwards, 100 µL of the supernatant were transferred to another well for absorbance measurement at 440 nm by using Synergy HTX multi-mode microplate reader. The percentage of viability was calculated considering untreated control (UT) at 2 h as 100%.

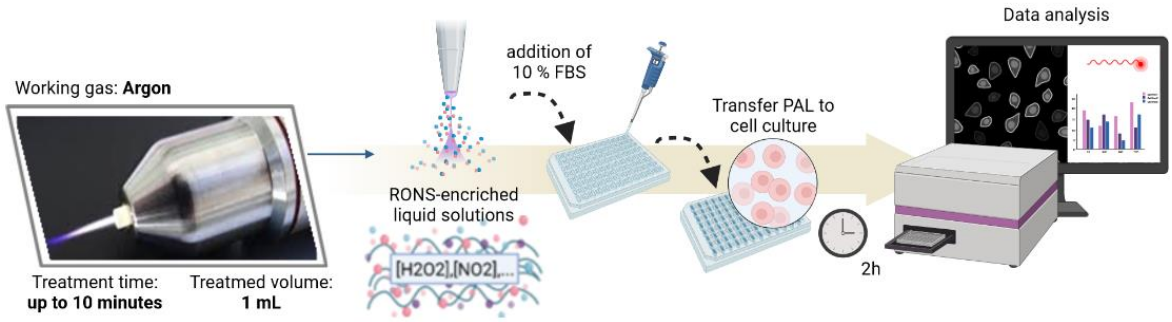

Figure 3.2-2 Workflow of PAL treatments on cell models

3.2.6 Colony formation assay

Colony formation assay was carried out by seeding SKOV-3 and OC314 in 6-well plates at low density (2 x 10^3 cells/well) in complete medium (Figure 3.2-3a, b).

To assess the cell clonogenicity, EOC cells were treated after 24 hours of seeding; to assess the colony proliferative potential, EOC cells were cultured for 6 days, allowing them to form visible colonies, upon which they were treated. The treatments consisted of 2 mL/well of freshly PARL and PAR solution produced at 15 s and 20 s of plasma treatment time; after 2 hours of incubation, cells were washed with PBS and cultured for 6 and 4 days additional at 37 °C and 5 % CO_2, respectively. As control, cells were exposed to 2 mL/well of untreated R or RL, both supplemented with 10 % FBS. The medium was changed every 3 days.

Subsequently, colonies were fixed and stained with 80% crystal violet (CV) solution and 20 % methanol for 20 min, washed 5 times with distilled water. Afterwards, CV was dissolved in 10 % $_{v/v}$ acetic acid and absorbance at 590 nm was measured by using the Microplate Reader.

To assess self-renewing, SKOV-3 and OC314 were seeded in 24-well plates at the density of 2.4 x 10^5 cells/well in complete media (Figure 3.2-3c). After 24 h, cells were treated with 500 µL of freshly produced PAR and PARL at 15 s and 20 s of plasma gas exposure, or their corresponding untreated control. After 2 hours of treatment, cells were washed with PBS and cultured for 3 days. Afterwards, surviving cells were harvested, and 2.000 cells/well were seeded in 6-well plates in complete medium. Colonies were fixed, stained, and analyzed after 6 days, changing the media every 3 days. Colony growth area was quantified by employing ImageJ software. All data were expressed as fold change of the control (UT).

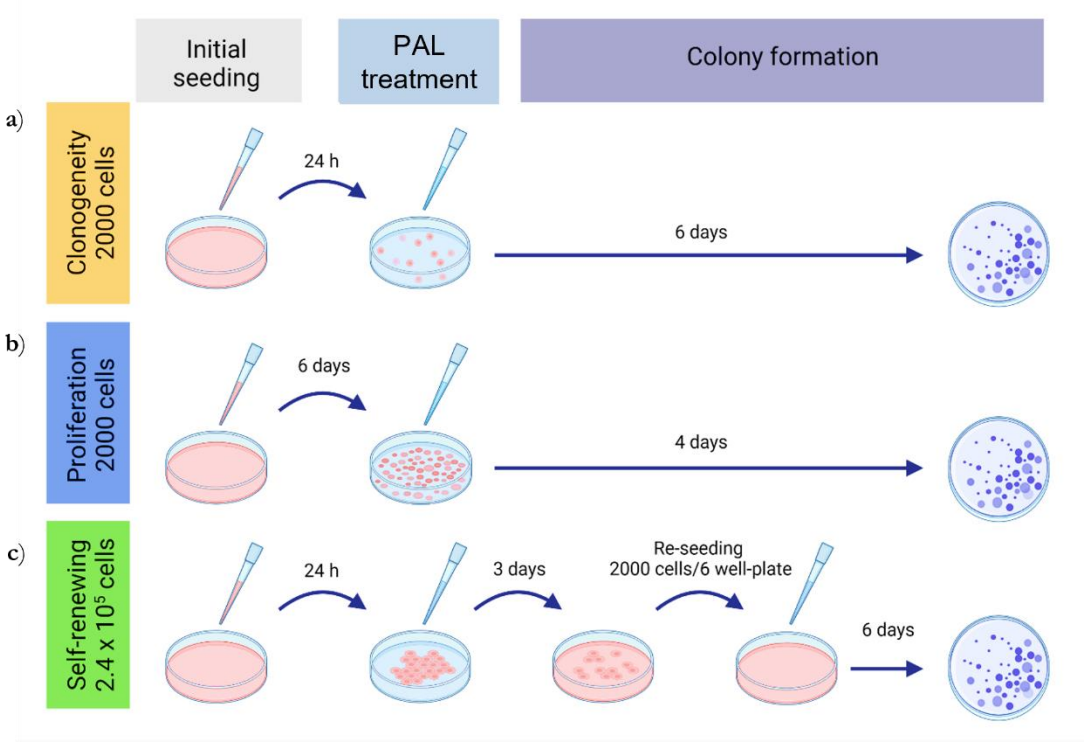

Figure 3.2-3 Protocols followed for the different experiments concerning colony formation.

3.2.7 Statistical Analyses

Statistical analyses were performed using GraphPad Prism software version 8.0. The comparison of means between different groups of numerical variables was performed using two-way ANOVA with Geisser-Greenhouse correction. The results were expressed as the mean ± standard error of the mean (SEM; $n \geq 3$) and statistical significance is specified with asterisks (* $p \leq 0.05$, ** $p \leq 0.001$).

3.3 Results

3.3.1 Chemical features of plasma-activated liquids

To evaluate the influence of the plasma treatment on the reactive species generated in Ringer's saline and Ringer's lactate, the solutions were treated for selected times, from 15 to 300 s, and then analyzed.

H_2O_2 and NO_2^- generated due to the treatment were quantified right after exposure (Figure 3.3-1a, b). In all cases, the concentration of both species increased linearly with the treatment time. By linear fit of the data, it was possible to obtain the generation rate of both species in PAR and PARL (reported in the figure). We obtained the same generation rate, within the experimental error, with and without

the presence of lactate during the treatment, meaning that it does not affect the generation of long-lived reactive species.

Then, we evaluated the production of OH radicals by adding COU in R and RL during the plasma treatment. In solution, COU reacts with OH radicals to generate a highly fluorescent hydroxyl-coumarin product that can be used as an indirect measure of the amount of OH radicals generated by plasma treatment and transferred into the liquid [15,16]. Figure 3.3-1c reports the fluorescence signals, due to the generation of hydroxyl-coumarin, in PAR and PARL as a function of the treatment time. The signals increase linearly with the treatment time in both PAR and PARL. However, a significantly lower signal was recorded in presence of lactate during the treatment.

Figure 3.3-1d reports the evolution of pH in PAR and PARL. Plasma treatment induced a progressive pH decrease from 6.5 to 4.7 in PAR and to 5.9 in PARL. The difference is due to the buffering properties of the lactic acid/lactate pair (pK_a = 3.86). As previously reported [2], the drop of pH can be restored by the addition of 10 % FBS which, in turn, allows to retain a physiological pH of 7.7 ± 0.1, suitable for various biological analyses. Thus, the pH evolution after the addition of 10 % FBS was checked for each plasma treatment time and no variation in physiological pH was observed.

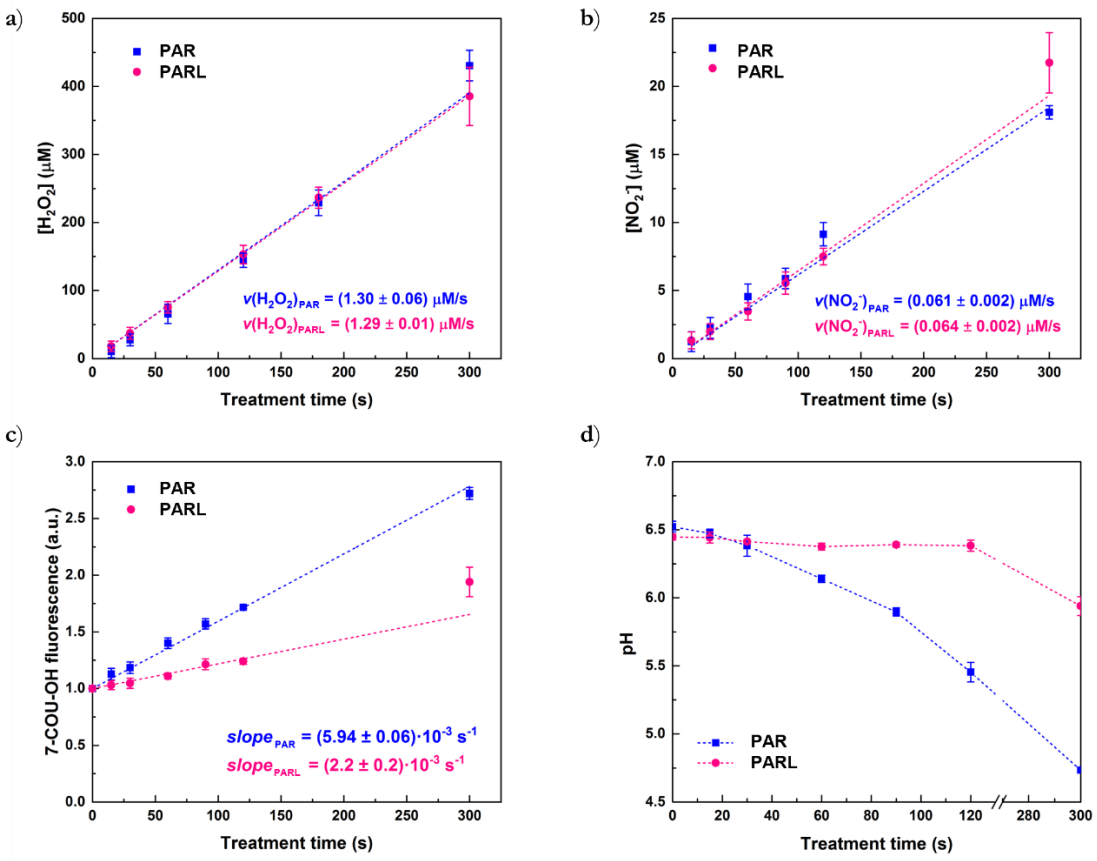

Figure 3.3-1 Concentration of H_2O_2 (a) and NO_2^- (b) in PAR and PARL as a function of treatment time); the dashed lines are the linear interpolations of the experimental data. c) Fluorescence signal due to the generation of 7-COU-OH in PAR and PARL containing 1 mM of coumarin as a function of plasma treatment time; the dashed lines are the linear interpolations of the experimental data. d) pH evolution in PAR and PARL solution at increasing plasma treatment time. Data are presented as mean ± SEM (n = 3).

To assess the impact of plasma treatment on lactate, 0.5 mM lactate solution was added to Ringer's saline treated by plasma at different times and analyzed with HPLC (Figure 3.3-2). In this way, the lactate in the solution and any oxidation product generated during the treatment were separated and detected. The concentration of 0.5 mM was selected as lower than the actual lactate concentration in the other experiments reported in this chapter in order to maximize the effects of the plasma treatment and make them easier to detect and measure. Thus, it can be reasonable to assume that the effects measured at this concentration of lactate are the same as those that happen at higher concentration, just to a different extent. Figure 3a reports the region of chromatograms of untreated RL and 6 min PARL with the peak

of lactate (r.t. 2.47 min). By increasing the plasma treatment time, two new peaks appear at r.t. 2.38 min and 2.63 min, which are due to the formation of oxidation products. More specifically, the comparison between a lactate standard solution and the sample solution led to identifying the peak at 2.46 min as pyruvate. This is in line with nuclear magnetic resonance spectra reported by Hori *et al* [17,18]. The peak areas of lactate and pyruvate were obtained by peak deconvolution of the region between 2.2 and 2.8 min and are reported in Figure 3.3-2b as a function of the plasma treatment time. As expected, the concentration of lactate decreases with a half-life time of (58 ± 7) min. At the same time, the concentration of pyruvate increases until a maximum is reached around 6 min and then it slowly decreases. This means that pyruvate is generated by the oxidation of lactate, but it is then further oxidized by plasma-generated RONS. Some preliminary HPLC experiments on non-diluted PARL led to obtaining the approximate concentration of pyruvate generated during 5-10 min treatment of around 300-400 µM.

Thus, the detectable presence of pyruvate suggests that plasma, with its blend of bio-active species, triggered organic reactions in solution that contribute also to pH dropped and may play an important role in determining a different cellular response to treatment.

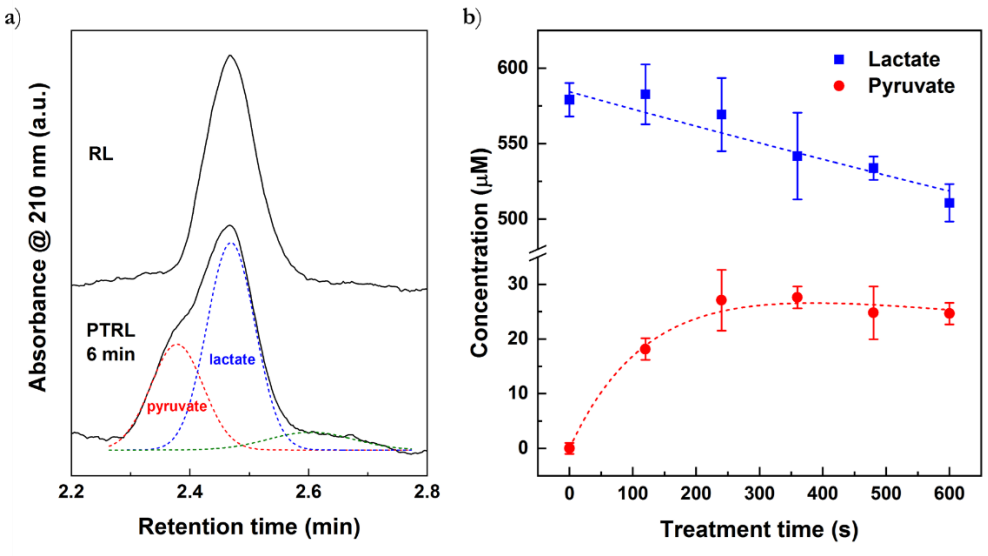

Figure 3.3-2 a) Chromatograms of untreated (RL) and 6 min treated Ringer's lactate (PARL); the dashed lines correspond to the deconvolution of the HPLC signal using 3 Gaussian components. b) Concentration of lactate and pyruvate as a function of the plasma treatment time; the dashed lines are

the interpolation of the experimental data using the exponential function ($C = C_0 e^{-k_1 t}$) and peak function ($C = C_0 k_1 \frac{e^{-k_1 t} - e^{-k_2 t}}{k_2 - k_1}$) for lactate and pyruvate respectively.

3.3.2 PARL and PAR activity on EOC cell viability

The metabolic activity on four EOC cell lines, namely SKOV-3, OV-90, OVSAHO and OC314, was measured employing the WST-1 assay to assess the cytotoxic effect exerted by PARL and PAR. EOC cells were exposed for two hours to PARL, and PAR solutions produced at different plasma-treatment times (from 15 s to 60 s), adding 10 % FBS after treatment, to restore pH and give nutrients to cells (Figure 3.3-3). SKOV-3 and OC314 (Figure 3.3-3a, b) significantly decreased their viability already with 15 s PALs and were similarly affected by PARL and PAR; the cytotoxic effect was fostered after 72 h of treatment displaying an evident plasma treatment-time dependence (Figure 3.7-1a-b, Appendix) and a dramatic decrease in viability over 90% for the conditions at 30 s and 60 s.

On the other hand, OV-90 and OVSAHO (Figure 3.3-3c, d) showed less sensitivity to the treatments, and they appeared to be affected only when they were exposed to liquids treated for long times (30 s and 60 s). However, these conditions were not sufficient to definitely inhibit the cell proliferative capability during the subsequent 72 h, where cells recovered their viability compared to control for OV-90 and showed cytostatic effect at PALs 60 s. OV-90 cells showed a 20 % - 40 % decrease in cell viability at 72 h from PALs treatment, whereas OVSAHO cell line appeared to suffer the exposure to PALs 60 s showing an approximately cytostatic effect during the cultured-time frame (Figure 3.7-1c-d, Appendix).

Although PARL and PAR exerted a similar cytotoxic effect on SKOV-3 and OC314, slightly higher cell viability was detected in PARL than in PAR. More specifically, SKOV-3 showed a survival rate after PARL 15 s and PAR 15 s of 72 % and 38 %, respectively, while for treatment at 30 s it was 5 % for PARL and 3 % for PAR. OC314 showed the same trend with a cell survival of 60 % for PARL 15 s and 33 % for PAR 15 s. The treatment at 30 s had a survival rate of 2 % for PARL and 1.2 % for PAR.

This trend was also confirmed in a 3D scenario, obtained from preliminary confocal microscope images on Collagen SKOV-3 and OC314 3D models (Figure 3.7-2, Appendix).

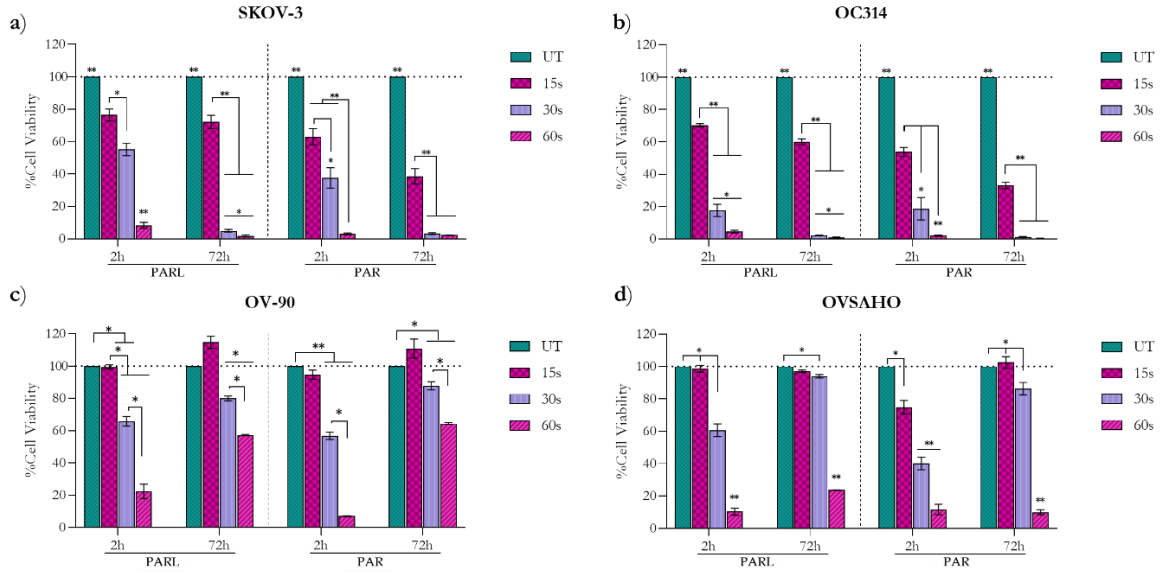

*Figure 3.3-3 Effects of PARL and PAR solution on EOC cell viability. Viability of SKOV-3 (a), OC314 (b), OV-90 (c) and OVSAHO (d) cell cultures treated with PARL and PAR solutions, produced at different plasma-treatment times, at 2 and 72 hours after treatment. Cell viability was normalized to the corresponding control (100) at 2 hours and plotted as fold change relative to the corresponding UT (untreated; RL for PARL treatments and R for PAR treatments) sample, for both time points. Aata are presented as the mean ± SEM (n ≥ 3); * p<0.05 ** p<0.001.*

3.3.3 Effect of PAR+L on EOC cell viability

At this point, we wanted to evaluate how lactate could influence PALs cytotoxicity and whether this is influenced by plasma treatment. Given the higher cytotoxic effects due to PARL and PAR observed in Figure 3.3-3, SKOV-3 and OC314 were selected to understand the possible correlation among plasma treatment, presence of lactate and cell viability (Figure 3.3-4a, b). The lower cytotoxic effect found at 20 s plasma treatment, compared to the 30 s one, retains a cell survival rate of less than 40 % after 72 h exposure to PALs, while the condition at 30 s relies on less than 10 %, abrogating any lactate-induced effect. To understand if the presence of lactate in solution during plasma treatment may influence the cell viability response, a PAR solution was prepared, and 57 mM lactate was added only after plasma treatment

(PAR+L). SKOV-3 and OC314 were exposed to PAR, PARL and PAR+L for 2 h (Figure 3.3-4a, b). Surprisingly, when EOC lines were treated with PAR+L 15 s and 20 s, the cytotoxic effect of PAR on cell viability was significantly reduced, which was evident at 15 s exposure whereby the effect on the EOC growth could be directly compared with the one induced by PARL. In contrast, 20 s plasma treatment showed significant differences between PARL and PAR+L.

More specifically, the presence of lactate in PAR (PAR+L) reduced the PAR cytotoxicity in SKOV-3 by 45 % and 10 % at 15 s and 20 s plasma-treatment times, respectively. In OC314 cells, lactate induced a loss of cytotoxicity of 33 % and 7 % in PAR+L 15 s and PAR+L 20 s, respectively.

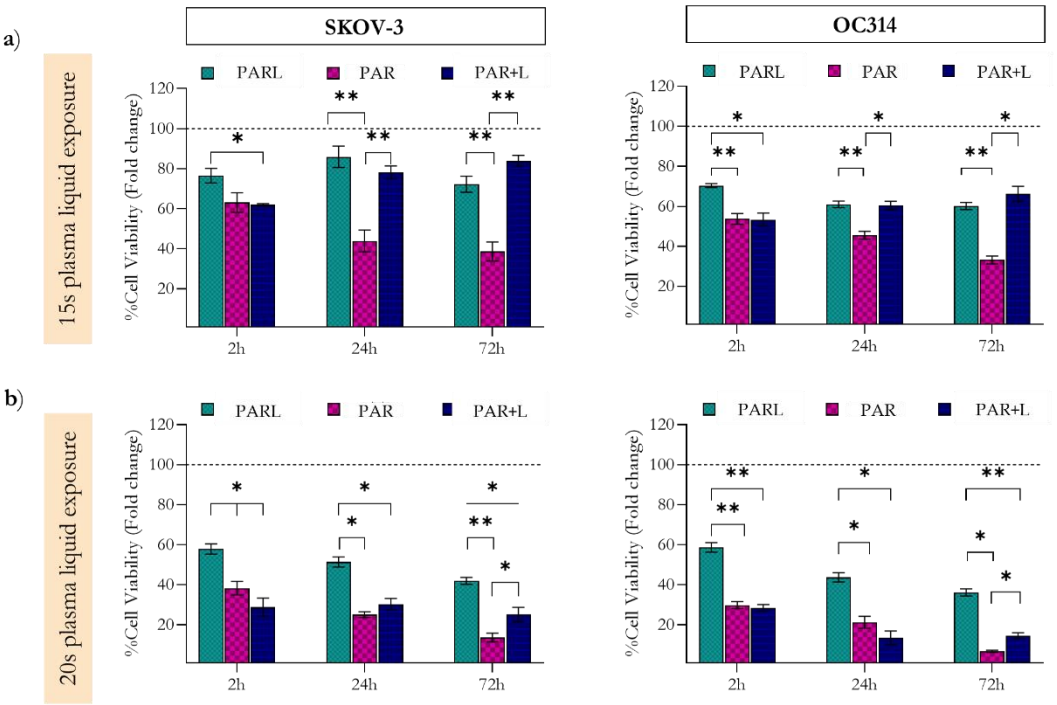

*Figure 3.3-4 Lactate is affected by plasma treatment and reduces the cytotoxicity of PALs. Relative viability of cells treated with PALs produced by exposure to plasma for 15 s (a) and 20 s (b). Cell viability was normalized to the corresponding control at 2 hours and plotted as fold change relative to the corresponding UT (untreated; RL for PARL treatments, R for PAR treatments and R+L for PAR+L) sample, for both time points. Data are presented as the mean ± SEM (n ≥ 3); * p<0.05 ** p<0.001.*

3.3.4 PARL and PAR inhibit EOC tumorigenic potential

At last, we attempted to evaluate if PALs were able to affect the EOC capability to maintain survival and mitotic ability. Indeed, cancer cells are characterized by the ability to generate colonies of a single-cell-derived clonal population and initiate tumorigenesis [19]. Hence, 15 s- and 20 s-treated PAR and PARL solutions were used to assess if they could affect the EOC tumorigenic potential, in terms of clonogenicity and proliferative potential of preformed colonies. As shown in Figure 3.3-5a, both PAR and PARL treatments completely abolished the EOC clonogenicity, in all cases investigated. In addition, when pre-formed colonies were treated with PALs, both EOC colony populations were severely affected by PALs treatments, with respect to the control, and a significant correlation between the clonal growth and the plasma-liquid exposure time was observed (Figure 3.3-5b). Overall, PAR and PARL were able to inhibit the tumorigenic potential and blunted colonies proliferative capability on both EOC cells, in particular with a significant efficacy after 20 s PALs. These data validated a strict correlation between time-liquid exposure to plasma gas and cell response, apparently independent of the kind of liquid employed.

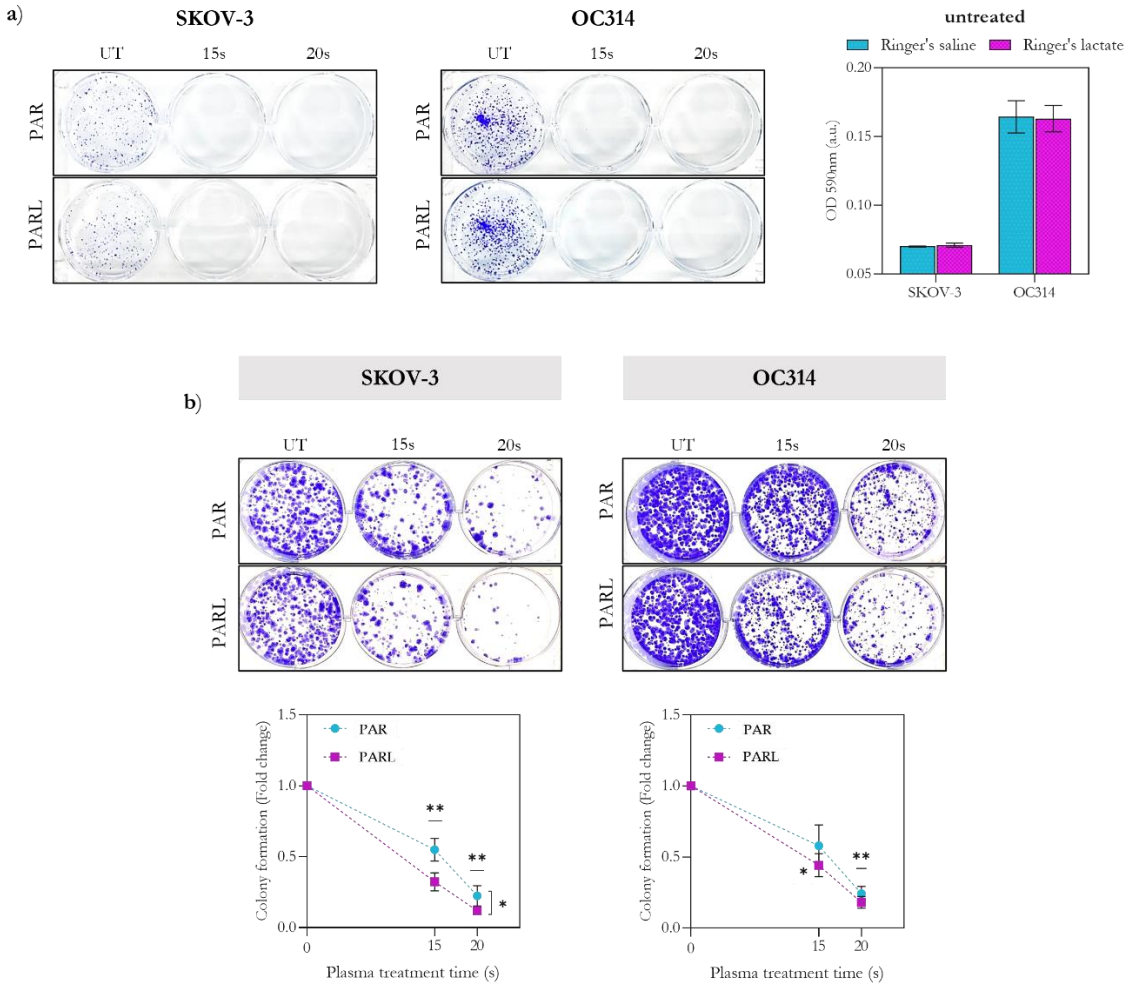

*Figure 3.3-5 PALs inhibit EOC clonogenic potential and blunted colonies proliferative capability. Representative images of 6-well plates containing SKOV-3 and OC314 cells plated at 2.000 cells/well and grown for 6 days (a) and 10 days (b), then stained with crystal violet. Crystal violet absorbed by the cells on each plate was released and absorbance at 590 nm was measured on a spectrophotometer. Bar graph (a) quantifies the growth of each clone in contact with untreated solution (UT). Relative growth curves of treated clones at 10 days were measured (b); absorption measurements were normalized and plotted as fold change relative to the corresponding UT sample. All data are presented as the mean ± SEM ($n \geq 3$); * $p<0.05$ ** $p<0.001$.*

Next, we questioned if PALs treatment may have some influence on EOC aggressiveness, in terms of repopulation of residual tumor cells to form recurrences depending on the self-renewing capacity of cells (Figure 3.3-6). The effect of PAR and PARL solutions was tested by replating a low density of 2 h pre-treated SKOV-3 and OC314, following the procedure described in Figure 3.2-3c. Colony formation

results indicate that neither PAR nor PARL treatments affected the EOC aggressiveness.

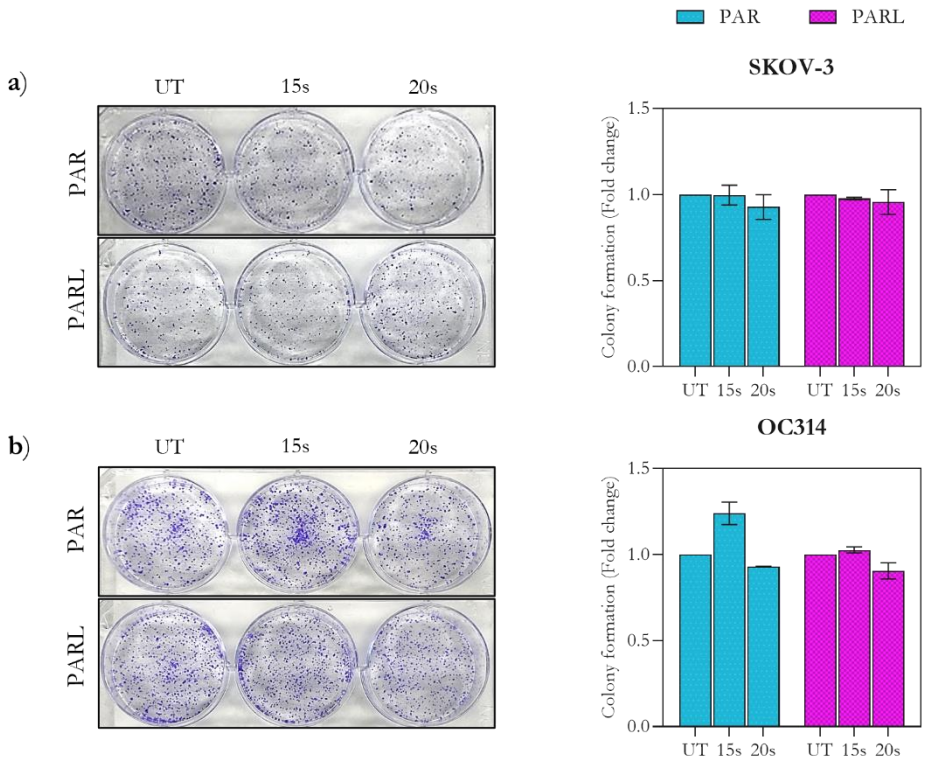

Figure 3.3-6 PALs do not exacerbate the EOC aggressiveness. EOC cells were treated with 15 s and 20 s PAR and PARL for 2 h, then cultured for 3 days. The surviving fraction was harvested, plated at 2.000 cells/well in 6-well plates, and grown for 6 days. The colonies were stained with crystal violet and photographed. Representative images of the colonies formed for SKOV-3 (a) and OC314 (b). Relative bar graph quantifies the area covered by the colonies and expressed as fold change of the control (UT). Data are presented as the mean ± SD (n = 2).

3.4 Discussion

Several studies have reported the anti-tumor activity of different liquids that have been exposed to CAP [2,20,21] against several cancer cell lines, promoting apoptosis and inhibiting proliferation [1,3,17,22–25]. In this work, the effect in EOC cell lines of two clinically relevant solutions, Ringer's saline and Ringer's lactate, exposed to kINPen® IND plasma jet was analyzed. The kINPen® IND plasma source is a certificated medical device, which uses argon to produce plasma. The device has extensively been characterized in literature [11,12] in terms of physical and chemical features of plasma gas and several applications in the field of plasma medicine have

been reported [26–30]. The interaction between plasma, surrounding air and liquid substrates leads to the production of RONS in these liquids [30].

In both PAR and PARL, we measured similar amounts of H_2O_2 and NO_2^-, whose concentrations increase linearly with the treatment time (Figure 3.3-1a, b**)**. Along that, a pH decrease in PALs was observed as a function of treatment time (Figure 3.3-1d**)**, because of the reactions among nitrogen species leading to acidification through the formation of nitric acid [31]. The drop in pH was less evident in PARL since the presence of lactate acts as a buffer by generating a lactate/lactic acid system [32]. The indirect measurement of OH radicals by COU probe (Figure 3.3-1c**)** showed a time-dependent formation of OH into PALs. Notably, the results indicated that the presence of lactate during the treatment influenced the hydroxyl-coumarin signal inducing a slower increase in it, suggesting that lactate acts as a scavenger of OH radicals. Recent studies have reported that CAP treatment induces chemical modifications in RL solution due to the oxidation of lactate to pyruvate by reaction with OH radicals [17,33]. Indeed, the HPLC analysis confirmed that the plasma treatment oxidized lactate to pyruvate in PARL (Figure 3.3-2).

PAR and PARL produced by kINPen were supplemented with 10 % of FBS immediately after plasma treatment, to stabilize the pH and avoid its influences on the cellular response, as previously reported [2]. The PALs dose-response profile on EOC viability was validated, showing a higher cytotoxic effect induced by PAR than PARL, ascribed to the presence of lactate and the production of pyruvate during the plasma treatment. Overall, PARL and PAR were able to exert a dose-response trend related to the plasma-treatment time in EOC cells. Specifically, PALs affected SKOV-3 and OC314 cell viability displaying a time-dependent increase of cytotoxic effect, unlike OV-90 and OVSAHO cell lines which only initially appeared to be affected by PALs, as they apparently recovered their proliferative capability during the subsequent cultured time.

When lactate was added to PAR post-treatment (PAR+L), the cytotoxicity of PAR was significantly reduced (Figure 3.3-4a, b). This effect may be due to the lactate being affected by plasma-produced OH radicals at a later stage. The presence of pyruvate in the PAL could have a cytoprotective effect, attenuating oxidative injury in the cells [9,10,34]. Pyruvate can influence the effectiveness of CAP by protecting cells

from the cytotoxic effects of H_2O_2 through several mechanisms [9]. Indeed, pyruvate can scavenge H_2O_2 at later states through an oxidative decarboxylation reaction, producing CO_2, H_2O, and acetate [10]. This reaction is also important in protecting cells from oxidative stress induced by mitochondria activity, which also contributes to stimulating the cellular antioxidant defence systems to counteract high levels of H_2O_2 [9,35]. On the other hand, it has been suggested that the cytotoxic effects of CAP may also be due to a reduction in antioxidant defences or to the depolarization of the mitochondrial membrane [9,36,37]. Therefore, pyruvate is an important factor to consider in understanding the effectiveness of CAP.

Oxidative stress has a major role in many biological processes, such as proliferation and differentiation, while over a certain intracellular level, ROS are responsible for cytotoxic and cytostatic effects [38]. Clonogenicity is one of the most important characteristic features of cancer cells to guarantee both processes. When the effect of PALs on this cancer hallmark was analyzed, both PAR and PARL effectively led to an abrogation of clonogenic capacity and strong inhibition of colony proliferative capacity in a dose-dependent manner, this could indicate a potential of the treatment to avoid the effect of tumor burden and aggressiveness, as it is the case in relapses [39]. Overall, this study demonstrated that PAR and PARL exert a strong cytotoxic effect on EOC models, and this is attributable not only to a synergy between CAP-generated RONS but also to additional intermediate molecules that are generated and influenced by CAP-dependent reactions that modulate the different cellular responses. Thus, PALs have shown to be effective as new possible therapeutic approaches for EOC treatment, that could contribute to the development of a new personalized cancer medicine if better understood.

3.5 Conclusions

The present study is the first to compare the cytotoxic effect of Ringer’s saline and Ringer's lactate solution exposed to plasma. This was done in particular by evaluating the effects on four different EOC cell lines. We observed that plasma induced lactate conversion to pyruvate. Pyruvate is known as a key ROS scavenger and metabolic intermediate. Despite the presence of pyruvate in PARL, just a minor decrease in its biological activity (cytotoxicity and clonogenic potential) was found.

In light of the results found, both solutions can be considered as equivalent vehicles for plasma-generated RONS, and with potential for transfer to the clinics.

3.6 References

1. Bisag, A. *et al.* Plasma-activated Ringer's Lactate Solution Displays a Selective Cytotoxic Effect on Ovarian Cancer Cells. *Cancers (Basel).* **12**, 476 (2020).
2. Mateu-Sanz, M. *et al.* Cold Plasma-Treated Ringer's Saline: A Weapon to Target Osteosarcoma. *Cancers (Basel).* **12**, 227 (2020).
3. Mateu-Sanz, M., Ginebra, M. P., Tornín, J. & Canal, C. Cold atmospheric plasma enhances doxorubicin selectivity in metastasic bone cancer. *Free Radic. Biol. Med.* **189**, 32–41 (2022).
4. Marino, Paul L.; Sutin, K. M. *The ICU Book, 3rd Edition. Lippincott Williams & Wilkins* (2012).
5. Li, X. *et al.* Lactate metabolism in human health and disease. *Signal Transduct. Target. Ther.* **7**, 305 (2022).
6. Singh, S., Kerndt, C. C. & Davis, D. *Ringer's Lactate*. *StatPearls* (2022).
7. Gladden, L. B. Lactate metabolism: a new paradigm for the third millennium. *J. Physiol.* **558**, 5–30 (2004).
8. Hirschhaeuser, F., Sattler, U. G. A. & Mueller-Klieser, W. Lactate: A Metabolic Key Player in Cancer. *Cancer Res.* **71**, 6921–6925 (2011).
9. Tornin, J. *et al.* Pyruvate Plays a Main Role in the Antitumoral Selectivity of Cold Atmospheric Plasma in Osteosarcoma. *Sci. Rep.* **9**, 10681 (2019).
10. Bergemann, C., Rebl, H., Otto, A., Matschke, S. & Nebe, B. Pyruvate as a cell-protective agent during cold atmospheric plasma treatment in vitro: Impact on basic research for selective killing of tumor cells. *Plasma Process. Polym.* **16**, (2019).
11. Reuter, S., von Woedtke, T. & Weltmann, K.-D. The kINPen—a review on physics and chemistry of the atmospheric pressure plasma jet and its applications. *J. Phys. D. Appl. Phys.* **51**, 233001 (2018).
12. Bekeschus, S., Schmidt, A., Weltmann, K.-D. & von Woedtke, T. The plasma jet kINPen – A powerful tool for wound healing. *Clin. Plasma Med.* **4**, 19–28 (2016).
13. Eisenberg, G. Colorimetric Determination of Hydrogen Peroxide. *Ind. Eng. Chem. Anal. Ed.* **15**, 327–328 (1943).

14. Tornin, J., Labay, C., Tampieri, F., Ginebra, M.-P. & Canal, C. Evaluation of the effects of cold atmospheric plasma and plasma-treated liquids in cancer cell cultures. *Nat. Protoc.* **16**, 2826–2850 (2021).
15. Nosaka, Y. & Nosaka, A. Y. Comment on "Coumarin as a Quantitative Probe for Hydroxyl Radical Formation in Heterogeneous Photocatalysis". *J. Phys. Chem. C* **123**, 20682–20684 (2019).
16. Tampieri, F., Ginebra, M.-P. & Canal, C. Quantification of Plasma-Produced Hydroxyl Radicals in Solution and their Dependence on the pH. *Anal. Chem.* **93**, 3666–3670 (2021).
17. Ito, D. *et al.* Cytotoxicity of plasma-irradiated lactate solution produced under atmospheric airtight conditions and generation of the methyl amino group. *Appl. Phys. Express* **15**, (2022).
18. Tanaka, H. *et al.* Non-thermal atmospheric pressure plasma activates lactate in Ringer's solution for anti-tumor effects. *Sci. Rep.* **6**, 36282 (2016).
19. Rajendran, V. & Jain, M. V. In Vitro Tumorigenic Assay: Colony Forming Assay for Cancer Stem Cells. in 89–95 (2018). doi:10.1007/978-1-4939-7401-6_8.
20. Laroussi, M. Cold Plasma in Medicine and Healthcare: The New Frontier in Low Temperature Plasma Applications. *Front. Phys.* **8**, 1–7 (2020).
21. Freund, E. *et al.* In Vitro Anticancer Efficacy of Six Different Clinically Approved Types of Liquids Exposed to Physical Plasma. *IEEE Trans. Radiat. Plasma Med. Sci.* **3**, 588–596 (2019).
22. Utsumi, F. *et al.* Effect of Indirect Nonequilibrium Atmospheric Pressure Plasma on Anti-Proliferative Activity against Chronic Chemo-Resistant Ovarian Cancer Cells In Vitro and In Vivo. *PLoS One* **8**, e81576 (2013).
23. Matsuzaki, T., Kano, A., Kamiya, T., Hara, H. & Adachi, T. Enhanced ability of plasma-activated lactated Ringer's solution to induce A549 cell injury. *Arch. Biochem. Biophys.* **656**, 19–30 (2018).
24. Sato, Y. *et al.* Effect of Plasma-Activated Lactated Ringer's Solution on Pancreatic Cancer Cells In Vitro and In Vivo. *Ann. Surg. Oncol.* **25**, 299–307 (2018).
25. Adachi, T., Matsuda, Y., Ishii, R., Kamiya, T. & Hara, H. Ability of plasma-

activated acetated Ringer's solution to induce A549 cell injury is enhanced by a pre-treatment with histone deacetylase inhibitors. *J. Clin. Biochem. Nutr.* 1–8 (2020) doi:10.3164/jcbn.19-104.

26. Schuster, M. *et al.* Visible tumor surface response to physical plasma and apoptotic cell kill in head and neck cancer. *J. Cranio-Maxillofacial Surg.* **44**, 1445–1452 (2016).
27. Privat-Maldonado, A. *et al.* ROS from Physical Plasmas: Redox Chemistry for Biomedical Therapy. *Oxid. Med. Cell. Longev.* **2019**, (2019).
28. Bekeschus, S. *et al.* Ex Vivo Exposure of Human Melanoma Tissue to Cold Physical Plasma Elicits Apoptosis and Modulates Inflammation. *Appl. Sci.* **10**, 1971 (2020).
29. Miebach, L. *et al.* Conductivity augments ROS and RNS delivery and tumor toxicity of an argon plasma jet. *Free Radic. Biol. Med.* **180**, 210–219 (2022).
30. Braný, D., Dvorská, D., Halašová, E. & Škovierová, H. Cold Atmospheric Plasma: A Powerful Tool for Modern Medicine. *Int. J. Mol. Sci.* **21**, 2932 (2020).
31. Neretti, G. *et al.* Characterization of a plasma source for biomedical applications by electrical, optical, and chemical measurements. *Plasma Process. Polym.* **15**, 1800105 (2018).
32. Singh, S., Kerndt, C. C. & Davis, D. *Ringer's Lactate*. *StatPearls* (2022).
33. Liu, Y. *et al.* Hydrogen peroxide in lactate solutions irradiated by non-equilibrium atmospheric pressure plasma. *Plasma Sources Sci. Technol.* **30**, (2021).
34. Guarino, V. A., Oldham, W. M., Loscalzo, J. & Zhang, Y. Y. Reaction rate of pyruvate and hydrogen peroxide: assessing antioxidant capacity of pyruvate under biological conditions. *Sci. Rep.* **9**, 1–9 (2019).
35. Kaushik, N. K., Kaushik, N., Park, D. & Choi, E. H. Altered Antioxidant System Stimulates Dielectric Barrier Discharge Plasma-Induced Cell Death for Solid Tumor Cell Treatment. *PLoS One* **9**, e103349 (2014).
36. Ahn, H. J. *et al.* Atmospheric-Pressure Plasma Jet Induces Apoptosis Involving Mitochondria via Generation of Free Radicals. *PLoS One* **6**, e28154 (2011).

37. Panngom, K. *et al.* Preferential killing of human lung cancer cell lines with mitochondrial dysfunction by nonthermal dielectric barrier discharge plasma. *Cell Death Dis.* **4**, e642–e642 (2013).
38. Turrini, E. *et al.* Cold Atmospheric Plasma Induces Apoptosis and Oxidative Stress Pathway Regulation in T-Lymphoblastoid Leukemia Cells. *Oxid. Med. Cell. Longev.* **2017**, 1–13 (2017).
39. Nantasupha, C. *et al.* When dormancy fuels tumour relapse. *Commun. Biol.* **4**, 747 (2021).
40. Tornín, J., Villasante, A., Solé-Martí, X., Ginebra, M. P. & Canal, C. Osteosarcoma tissue-engineered model challenges oxidative stress therapy revealing promoted cancer stem cell properties. *Free Radic. Biol. Med.* **164**, 107–118 (2021).

3.7 Appendix

3.7.1 PARL and PAR activity on EOC cell viability

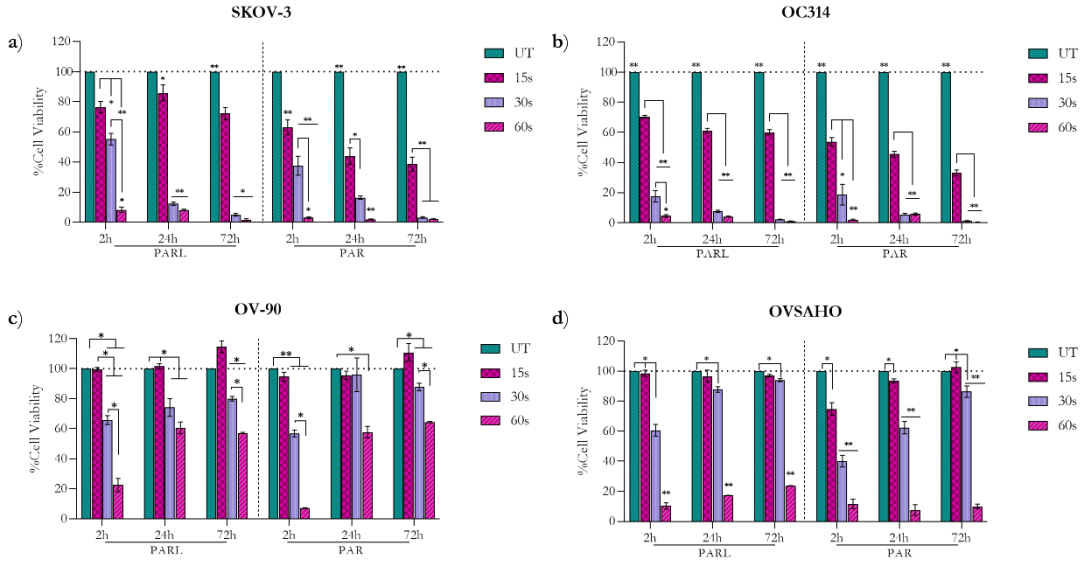

*Figure 3.7-1 Viability of SKOV-3 (a), OC314 (b), OV-90 (c) and OVSAHO (d) cells treated with PARL and PAR solutions. Data are mean ± SEM normalized to the corresponding UT (untreated; RL for PARL treatments and R for PAR treatments) sample. Data are presented as the mean ± SEM ($n \geq 3$); * $p<0.05$ ** $p<0.001$.*

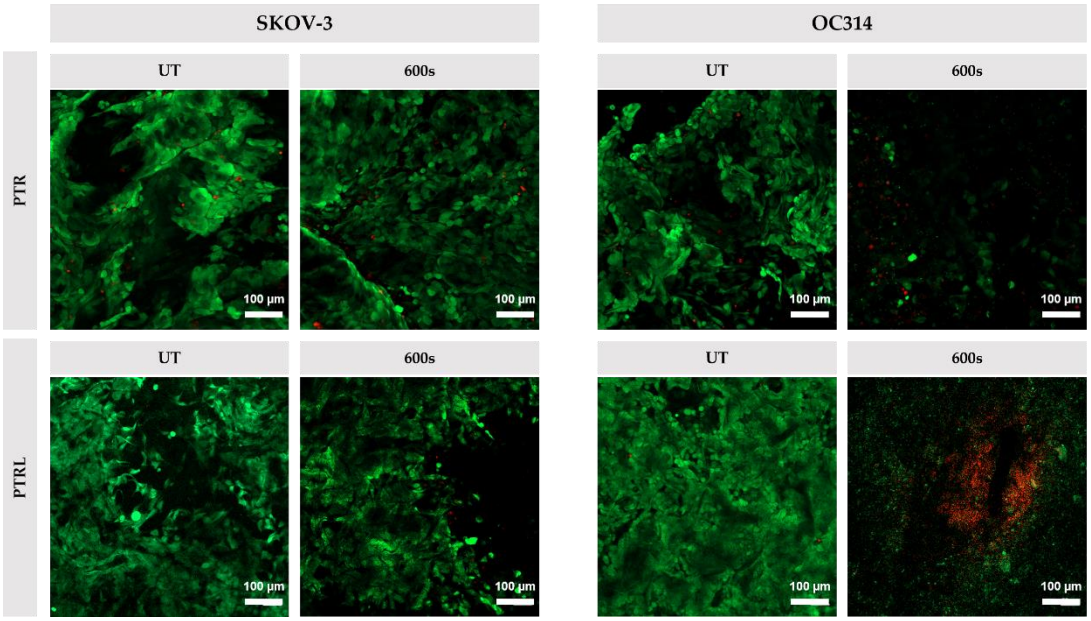

Figure 3.7-2 LIVE/DEAD cell viability images of SKOV-3 and OC314 cells seeded in Collagen Type 1 (COL1) 3D scaffolds. Briefly, COL1 scaffolds were produced following the protocol mentioned in [40], in order to mimic the tumor microenvironment. In this case, the scaffolds were produced without hydroxyapatite nanoparticles (nHA) incorporation. Then, 3 x 10^5 SKOV-3 and OC314 cells respectively were seeded on top of sterile scaffolds, and they were allowed to grow for 6 days, when they were exposed to PAR and PARL untreated (UT) or treated from 240 to 600 s as described in [40]. LIVE/DEAD™ Viability/Cytotoxicity Kit (Invitrogen, #L3224) was performed 3 days after treatment following the manufacturer's protocol and representative images were captured using Zeiss laser scanning microscope. Scale bar = 100 µm.

CHAPTER 4

Summary and Outlook

Plasma medicine involves the use of CAP for therapeutic purposes. It is a dynamic and recently developed field combining multiple scientific and technological disciplines. Since its multidisciplinary nature incorporates engineering, physics, biology and chemistry, a wide range of technologies for improving human health and quality of life have been developed. Moreover, publications and reviews have increased significantly in recent years. CAP devices mostly operate under ambient air conditions or use ambient air as the working gas to generate plasma. This results in the production of reactive oxygen and nitrogen species which are responsible for the specific biological effects of CAP. The composition and amount of RONS in plasma can be influenced by several parameters as well as ambient conditions, and the plasma's interaction with substrates, particularly liquid phases. These can influence the biological performance of CAP devices. However, RONS generated by plasma are similar to those that occur in living organisms and play a role in cellular physiology and biochemistry [1].

Hence, the purpose of this study was to investigate plasma-activated liquids as a potential novel adjuvant intraperitoneal therapy for Epithelial Ovarian Cancer (EOC) treatment. However, the implication of PALs in the clinical field involves understanding the mechanisms underlying the interaction between PALs and the target area, as well as plasma and the liquid-treated substrate. Hence, to safely and effectively use PALs in the clinic it is essential to gain an in-depth understanding of how PALs interact with the cells and biomolecules involved in the treatment process. It is known that one of the main advantages of using CAP in biomedical applications is that RONS are generated locally and only for the duration of the treatment. They can be easily controlled by adjusting plasma parameters, making it a field of applied redox biology useful for understanding CAP effects and their medical applications [1–3]. Indeed, as reported in **section 2.3.1.2** and **section 3.3.1**, it is possible to modulate the production of RONS based on the treatment time, the CAP device employed, and the treated substrate. In response to CAP exposure, cells and tissues can undergo either cell stimulation or death, depending on the exposure conditions such as treatment time. This aligns with the theory of oxidative stress, which differentiates between beneficial (oxidative eustress) and harmful (oxidative distress) stress depending on the level of oxidant exposure (**Section 1.3**, **Figure 1.3-2**) [4]. The balance between these states of

stress will determine the level of exposure of the living system to redox-active species and the ability of cells to adapt. It will determine whether oxidative eustress or distress occurs, ultimately leading to cell recovery or cell death. Additionally, CAP has the potential to be used in cancer treatment, although it is currently in the preclinical research stage. However, it is anticipated to be the next step in clinical plasma application [5]. Identification and analysis of specific reactive oxygen and nitrogen species are both relevant topics in plasma medicine and redox biology, and understanding the cellular mechanisms that alter the sensitivity of cells to the effects of CAP and redox-active species is another similar focus.

The delivery systems of these reactive species, such as cell culture media or saline solution i.e., Ringer's saline or Ringer's lactate solutions, play a crucial role in the anticancer efficacy of PALs. Indeed, cancer cell lines seem to be more susceptible to one PAL, such as Ringer's lactate or Ringer's saline solutions, compared to other PAL, such as culture medium, due to their metabolic profile and the relative availability of certain nutrients and other factors in the different solutions (**section 2.3.2**, **section 3.3.2**, and **section 3.3.3**). Recent studies reported that PALs turned out the most common pathways in cancer [6,7], suggesting that the treatments' effectiveness could actually be ascribed to cancer metabolic heterogeneity [8,9]. Especially, EOC is a highly heterogeneous type of cancer, with different subtypes defined according to the ability to modulate their energy flux relying on the glycolytic or oxidative phosphorylation (OXPHOS) pathway [10–14]. These subtypes can be further categorized as low-OXPHOS or high-OXPHOS, depending on their ability to withstand oxidative stress and sustain cell integrity, respectively [8]. More specifically, in this study, it has been hypothesized that in EOC models PA-RL treatment exerts a more potent cytotoxic effect in those models characterized by lower (SKOV-3) or higher (OC314) metabolic activity (**section 2.3.2**). This suggests that the mechanism of action may be related to the regulation of glucose uptake and the production of reactive oxygen species in these cells. This could pave the way for the development of more targeted and effective treatments for ovarian cancer, in line with the growing focus on personalizing medicine. The study of selectivity in anticancer therapies has been the centre of attention in recent years, as researchers seek to identify molecular differences between cancer and non-cancer cells that can be targeted for treatment. One such difference is

the ability of cancer cells to handle high levels of oxidative stress, due to their active metabolic status, high proliferation rate, and the microenvironmental conditions that contribute to tumor growth [12,15]. CAP has been shown to have selective cytotoxicity on cancer cells compared to non-cancer ones, both *in vitro* and *in vivo* [5]. Thus, this study confirmed that EOC cells expressed higher levels of the antioxidant enzymes as SOD-1 than non-cancer, which were not enough to protect them from PA-RL treatment. While, non-cancer cells displayed the capability to adapt to the PA-RL-induced oxidative burst by increasing SOD-1 levels, suggesting that the levels of enzymes involved in the antioxidant response in cancer cells may not be able to be increased beyond a certain point. This may explain why a certain treatment i.e., PA-RL is more effective in treating ovarian cancer cells than healthy cells (**section 2.3.3**). In conclusion, the field of plasma medicine is a promising and rapidly growing area of biomedical research. It has a wide range of potential applications in treating diseases including cancer. Understanding the redox mechanisms underlying plasma-biological interactions may provide a deeper scientific basis for CAP phenomena and may represent a promising therapeutic option for developing effective and targeted treatments for diseases such as Epithelial Ovarian Cancer. In this context, the ability to modulate the effects of oxidative stress through CAP treatment may open up new paths of research into the "hormesis" phenomenon and the development of personalised treatment plans for patients. However, further research is needed to fully understand the mechanisms and effects of CAP treatment and to establish standard treatment doses and protocols.

References

1. Von Woedtke, T., Schmidt, A., Bekeschus, S., Wende, K. & Weltmann, K. D. Plasma medicine: A field of applied redox biology. *In Vivo (Brooklyn).* **33**, 1011–1026 (2019).
2. Kaushik, N. K. *et al.* Biological and medical applications of plasma-activated media, water and solutions. *Biol. Chem.* **400**, 39–62 (2018).
3. Fridman, A. *Plasma chemistry*. *Plasma Chemistry* vol. 9780521847 (Cambridge University Press, 2008).
4. Privat-Maldonado, A. *et al.* ROS from Physical Plasmas: Redox Chemistry for Biomedical Therapy. *Oxid. Med. Cell. Longev.* **2019**, 1–29 (2019).

5. Tanaka, H. *et al.* Plasma-Treated Solutions (PTS) in Cancer Therapy. *Cancers (Basel).* **13**, 1737 (2021).

6. Tanaka, H. *et al.* Oxidative stress-dependent and -independent death of glioblastoma cells induced by non-thermal plasma-exposed solutions. *Sci. Rep.* **9**, 13657 (2019).

7. Mateu-Sanz, M. *et al.* Cold Plasma-Treated Ringer's Saline: A Weapon to Target Osteosarcoma. *Cancers (Basel).* **12**, 227 (2020).

8. Gentric, G., Mieulet, V. & Mechta-Grigoriou, F. Heterogeneity in Cancer Metabolism: New Concepts in an Old Field. *Antioxid. Redox Signal.* **26**, 462–485 (2017).

9. Wu, Y. *et al.* Targeting oxidative phosphorylation as an approach for the treatment of ovarian cancer. *Front. Oncol.* **12**, (2022).

10. Nantasupha, C., Thonusin, C., Charoenkwan, K., Chattipakorn, S. & Chattipakorn, N. Metabolic reprogramming in epithelial ovarian cancer. *Am. J. Transl. Res.* **13**, 9950–9973 (2021).

11. Gentric, G. *et al.* PML-Regulated Mitochondrial Metabolism Enhances Chemosensitivity in Human Ovarian Cancers. *Cell Metab.* **29**, 156-173.e10 (2019).

12. Vander Heiden, M. G. & DeBerardinis, R. J. Understanding the Intersections between Metabolism and Cancer Biology. *Cell* **168**, 657–669 (2017).

13. Romero-Garcia, S., Lopez-Gonzalez, J. S., B´ez-Viveros, J. L., Aguilar-Cazares, D. & Prado-Garcia, H. Tumor cell metabolism. *Cancer Biol. Ther.* **12**, 939–948 (2011).

14. Ruiz-Iglesias, A. & Mañes, S. The Importance of Mitochondrial Pyruvate Carrier in Cancer Cell Metabolism and Tumorigenesis. *Cancers (Basel).* **13**, 1488 (2021).

15. DeBerardinis, R. J. & Chandel, N. S. Fundamentals of cancer metabolism. *Sci. Adv.* **2**, e1600200 (2016).